

Maximilian Rebhandl, BSc

Analysis and Implementation of non-invasive blood pressure measurement via miniaturised approach

MASTER THESIS

to achieve the university degree of

Diplom-Ingenieur

Master's degree programme: Biomedical Engineering

submitted to

Graz University of Technology

Supervisor

Ao.Univ.-Prof. Dipl.-Ing. Dr.techn. Hermann Scharfetter

Co-Supervisor

Dipl.-Ing. Dr. Jürgen Fortin

Institute of Medical Engineering

Institute Head: Univ.-Prof. Dipl.-Ing. Dr.techn. Rudolf Stollberger

Faculty of Computer Science and Biomedical Engineering

Graz, August 2020

AFFIDAVIT

I declare that I have authored this thesis independently, that I have not used other than the declared sources/resources, and that I have explicitly indicated all material which has been quoted either literally or by content from the sources used. The text document uploaded to TUGRAZonline is identical to the present master's thesis.

Date

Signature

Kurzfassung

Diese Arbeit befasst sich mit der iterativen Entwicklung eines tragbaren nicht-invasiven Blutdruckmesssystems im Projekt CNAP2GO der Firma CNSystems (CNSystems Medizintechnik GmbH, Graz, AT). Zuerst werden geeignete Konzepte zum "proof of principle" entworfen, dann erfolgt die Miniaturisierung zum "wearable device". Mittels Fluidsystem wird in einer Fingermanschette der Druck erhöht und durch Adaption der existierenden CNSystems-Komponenten das Lichtsignal der Pulsplethysmographie gemessen, um die Oszillationen des Lichtsignals als Hüllkurve darzustellen. Die Prototypen zielen auf eine Vergleichbarkeit mit dem aktuell existierenden CNAP System ab, was in einer Messserie bewiesen wurde. Für die feinmechanische Miniaturisierung des Systems als "wearable device" bleiben Herausforderungen für zukünftige Prototypen. Das Endprodukt, das "proof of principle", wurde in dieser Arbeit positiv abgeschlossen.

Schlüsselwörter: Nicht-Invasive Blutdruckmessung, Oszillometrische Einhüllende, CNAP2GO, Tragbares Health-Monitoring, Fluidsysteme

Abstract

This thesis deals with the iterative development of a wearable, non-invasive blood pressure measurement system within the scope of the project CNAP2GO of the company CNSystems (CNSystems Medizintechnik GmbH, Graz, AT). First, suitable concepts for proof of principle are developed, which are then being followed by approaches for miniaturising the wearable device. Using a fluid system, the pressure is increased in a finger cuff. Adapting the existing CNSystems components enables the simultaneous measurement of light signal derived from pulseplethysmography in order to represent the oscillations of the light signal as an oscillometric envelope. The prototypes aim to be comparable with the currently existing CNAP system, as confirmed by measurement series of a further developed prototype. The precise mechanical miniaturisation of the system for the use as a wearable device is the challenge for future prototypes as the end product, the proof of principle, has been successfully completed in this work.

Key Words: Non-Invasive Blood Pressure Measurement, Oscillometric Envelope, CNAP2GO, Wearable Health-Monitoring, Fluid Systems

Contents

| | |
|--|------------|
| Abstract | iii |
| 1. Preamble | 1 |
| 1.1. Motivation | 1 |
| 1.2. Methods of cardiological parameter acquisition | 3 |
| 1.3. CNAP Sensor & VERIFI Algorithm | 7 |
| 1.4. Correlation of photoplethysmography $v(t)$ and cuff pressure $p(t)$ | 9 |
| 1.5. CNAP2GO & Volume Control Technique (VCT) | 10 |
| 1.6. Drive units for CNAP2GO | 17 |
| 1.6.1. Unsealed system | 17 |
| 1.6.2. Sealed system | 19 |
| 1.7. Competitor products for CNAP2GO | 20 |
| 2. Task Definition | 22 |
| 2.1. CNAP2GO | 22 |
| 3. Methods | 23 |
| 3.1. Overview of prototypes | 24 |
| 3.2. Prototype V.0 - "suitability test" | 26 |
| 3.3. Measurement procedure prototype V.0 | 27 |
| 3.4. Prototype V.1 - "first measurement" | 27 |
| 3.5. Measurement procedure prototype V.1 | 30 |
| 3.6. Prototype V.2 - "measurement series" | 31 |
| 3.7. COVID-19 measures | 33 |
| 3.8. Measurement procedure prototype V.2 | 37 |
| 3.9. Prototype V.3 - "miniaturisation approach" | 38 |
| 3.9.1. Computation of the piezo motor | 39 |
| 3.9.2. First setup - prototype V.3 - idealised mounting, 1D | 44 |
| 3.9.3. Second setup - prototype V.3 - full opening, 3D | 46 |
| 3.9.4. Third setup - prototype V.3 - fully embedded, 1D | 47 |
| 3.10. Measurement procedure prototype V.3 | 48 |
| 3.11. Metrological parameterisation | 48 |

| | |
|--|-----------|
| 4. Results | 49 |
| 4.1. Prototype V.0 | 49 |
| 4.2. Prototype V.1 | 51 |
| 4.2.1. Test subject 1 | 51 |
| 4.3. Prototype V.2 | 52 |
| 4.3.1. Test subject 1 | 53 |
| 4.3.2. Boxplots | 59 |
| 4.4. Prototype V.3 | 60 |
| 4.4.1. Results of first setup - V.3 | 60 |
| 4.4.2. Results of second setup - V.3 | 62 |
| 4.4.3. Results of third setup - V.3 | 64 |
| 5. Discussion | 66 |
| 5.1. General discussion | 66 |
| 5.1.1. Fluid component & basic controlling assumptions | 66 |
| 5.1.2. Metrological assumptions | 67 |
| 5.2. Prototype V.0 | 68 |
| 5.2.1. General discussion V.0 | 68 |
| 5.2.2. Discussion of results V.0 | 69 |
| 5.3. Prototype V.1 | 69 |
| 5.3.1. General discussion V.1 | 69 |
| 5.3.2. Discussion of results V.1 | 70 |
| 5.4. Prototype V.2 | 70 |
| 5.4.1. General discussion V.2 | 70 |
| 5.4.2. Discussion of results V.2 | 71 |
| 5.5. Prototype V.3 | 73 |
| 5.5.1. General discussion V.3 | 73 |
| 5.5.2. Discussion of results V.3 | 73 |
| 5.6. Conclusion | 79 |
| Bibliography | 80 |
| A. Additional Components | 84 |

| | |
|---|------------|
| B. Plots | 88 |
| B.1. Prototype V.0 | 88 |
| B.2. Prototype V.1 | 89 |
| B.2.1. Test Subject 1 | 89 |
| B.2.2. Test Subject 2 | 90 |
| B.2.3. Test Subject 3 | 91 |
| B.2.4. Test Subject 4 | 92 |
| B.3. Prototype V.2 | 93 |
| B.3.1. Test Subject 1 | 93 |
| B.3.2. Test Subject 2 | 95 |
| B.3.3. Test Subject 3 | 99 |
| B.3.4. Test Subject 4 | 103 |
| B.3.5. Test Subject 5 | 107 |
| B.3.6. Test Subject 6 | 111 |
| B.3.7. Test Subject 7 | 115 |
| C. Utilised Tools | 119 |
| C.1. CNAP Development Kit | 119 |
| C.2. CNAP SerialGUI & CNS TestInterpreter | 119 |
| C.3. Biopac Measurement System | 120 |

List of Figures

| | |
|--|----|
| 1.1. Causes of death in Austria 2018 | 1 |
| 1.2. Problem of the oscillometric measurement | 4 |
| 1.3. Oscillometric measurement - CNS TaskForce Monitor | 5 |
| 1.4. Difference between oscillometric and invasive arterial measurements | 5 |
| 1.5. CNAP control loop - schematic | 6 |
| 1.6. CNAP control loop - detailed | 8 |
| 1.7. CNAP finger cuff | 8 |
| 1.8. Correlation of light signal and pressure | 10 |
| 1.9. CNAP2GO control loop | 11 |
| 1.10. MAP derived from light signal and pressure signal | 12 |
| 1.11. Influences on the pressure-light curve | 14 |
| 1.12. CNAP2GO filters | 15 |
| 1.13. Pressure fluids | 18 |
| 1.14. Power-to-weight ratios of various actuators | 20 |
| | |
| 3.1. Adapted cuff | 25 |
| 3.2. Prototype V.0 | 26 |
| 3.3. Prototype V.1 | 29 |
| 3.4. Prototype V.2 | 32 |
| 3.5. Measurement setup prototype V.2 | 34 |
| 3.6. PCB piezo motor | 38 |
| 3.7. CNAP2GO design | 39 |
| 3.8. Metric thread according to DIN 13 | 42 |
| 3.9. Cuff systems CNAP2GO and CNAP | 44 |
| 3.10. First setup - prototype V.3 | 45 |
| 3.11. First setup - front view - prototype V.3 | 45 |
| 3.12. Second setup - prototype V.3 | 46 |
| 3.13. Third setup - prototype V.3 | 47 |
| | |
| 4.1. Pressure measurement - index finger - V.0 | 49 |
| 4.2. Pressure signal - index finger - V.0 | 50 |
| 4.3. Point-line diagram - index finger - test subject 1 - V.1 | 51 |

| | |
|---|----|
| 4.4. Point-line diagram - middle finger (R) - test subject 1 - V.2 | 53 |
| 4.5. Point-line diagram - middle finger (L) - test subject 1 - CNAP | 53 |
| 4.6. Point-line diagram with pulses - middle finger (R) - test subject 1 - V.2 | 54 |
| 4.7. Pressure, Oscillations, OE - middle finger (R) - test subject 1 - V.2 | 55 |
| 4.8. Point-line diagram - middle finger (L) - test subject 1 - V.2 | 56 |
| 4.9. Point-line diagram - middle finger (R) - test subject 1 - CNAP | 56 |
| 4.10. Point-line diagram with pulses - middle finger (L) - test subject 1 - V.2 | 57 |
| 4.11. Pressure, Oscillations, OE - middle finger (L) - test subject 1 - V.2 | 58 |
| 4.12. Boxplot MD - V.2 | 59 |
| 4.13. Boxplot KB - V.2 | 59 |
| 4.14. First setup - 11 x 100 steps - V.3 | 60 |
| 4.15. First setup - 23 x 50 steps - V.3 | 61 |
| 4.16. Second setup - human finger - V.3 | 62 |
| 4.17. Second setup - finger dummy PVC - V.3 | 63 |
| 4.18. Second setup - finger dummy silicone - V.3 | 63 |
| 4.19. Third setup - lower pressure region - V.3 | 64 |
| 4.20. Third setup - higher pressure region - V.3 | 65 |
| 5.1. Metrological assumptions | 67 |
| B.1. Pressure measurement - middle finger - V.0 | 88 |
| B.2. Pressure signal - middle finger - V.0 | 88 |
| B.3. Point-line diagram - middle finger - test subject 1 - V.1 | 89 |
| B.4. Point-line diagram - index finger - test subject 2 - V.1 | 90 |
| B.5. Point-line diagram - middle finger test subject 2 - V.1 | 90 |
| B.6. Point-line diagram - index finger - test subject 3 - V.1 | 91 |
| B.7. Point-line diagram - middle finger - test subject 3 - V.1 | 91 |
| B.8. Point-line diagram - index finger - test subject 4 - V.1 | 92 |
| B.9. Point-line diagram - middle finger - test subject 4 - V.1 | 92 |
| B.10. Point-line diagram - index finger(R) - test subject 1 - V.2 | 93 |
| B.11. Point-line diagram - index finger(L) - test subject 1 - CNAP | 93 |
| B.12. Point-line diagram - index finger(L) - test subject 1 - V.2 | 94 |
| B.13. Point-line diagram - index finger(R) - test subject 1 - CNAP | 94 |

| | |
|--|-----|
| B.14.Point-line diagram - index finger(R) - test subject 2 - V.2 | 95 |
| B.15.Point-line diagram - index finger(L) - test subject 2 - CNAP | 95 |
| B.16.Point-line diagram - index finger(L) - test subject 2 - V.2 | 96 |
| B.17.Point-line diagram - index finger(R) - test subject 2 - CNAP | 96 |
| B.18.Point-line diagram - middle finger(R) - test subject 2 - V.2 | 97 |
| B.19.Point-line diagram - middle finger(L) - test subject 2 - CNAP | 97 |
| B.20.Point-line diagram - middle finger(L) - test subject 2 - V.2 | 98 |
| B.21.Point-line diagram - middle finger(R) - test subject 2 - CNAP | 98 |
| B.22.Point-line diagram - index finger(R) - test subject 3 - V.2 | 99 |
| B.23.Point-line diagram - index finger(L) - test subject 3 - CNAP | 99 |
| B.24.Point-line diagram - index finger(L) - test subject 3 - V.2 | 100 |
| B.25.Point-line diagram - index finger(R) - test subject 3 - CNAP | 100 |
| B.26.Point-line diagram - middle finger(R) - test subject 3 - V.2 | 101 |
| B.27.Point-line diagram - middle finger(L) - test subject 3 - CNAP | 101 |
| B.28.Point-line diagram - middle finger(L) - test subject 3 - V.2 | 102 |
| B.29.Point-line diagram - middle finger(R) - test subject 3 - CNAP | 102 |
| B.30.Point-line diagram - index finger(R) - test subject 4 - V.2 | 103 |
| B.31.Point-line diagram - index finger(L) - test subject 4 - CNAP | 103 |
| B.32.Point-line diagram - index finger(L) - test subject 4 - V.2 | 104 |
| B.33.Point-line diagram - index finger(R) - test subject 4 - CNAP | 104 |
| B.34.Point-line diagram - middle finger(R) - test subject 4 - V.2 | 105 |
| B.35.Point-line diagram - middle finger(L) - test subject 4 - CNAP | 105 |
| B.36.Point-line diagram - middle finger of(L) - test subject 4 - V.2 | 106 |
| B.37.Point-line diagram - middle finger(R) - test subject 4 - CNAP | 106 |
| B.38.Point-line diagram - index finger(R) - test subject 5 - V.2 | 107 |
| B.39.Point-line diagram - index finger(L) - test subject 5 - CNAP | 107 |
| B.40.Point-line diagram - index finger(R) - test subject 5 - CNAP | 108 |
| B.41.Point-line diagram - middle finger(R) - test subject 5 - V.2 | 109 |
| B.42.Point-line diagram - middle finger(L) - test subject 5 - CNAP | 109 |
| B.43.Point-line diagram - middle finger(L) - test subject 5 - V.2 | 110 |
| B.44.Point-line diagram - middle finger(R) - test subject 5 - CNAP | 110 |
| B.45.Point-line diagram - index finger(R) - test subject 6 - V.2 | 111 |

| | |
|--|-----|
| B.46.Point-line diagram - index finger(L) - test subject 6 - CNAP | 111 |
| B.47.Point-line diagram - index finger(L) - test subject 6 - V.2 | 112 |
| B.48.Point-line diagram - index finger(R) - test subject 6 - CNAP | 112 |
| B.49.Point-line diagram - middle finger(R) - test subject 6 - V.2 | 113 |
| B.50.Point-line diagram - middle finger(L) - test subject 6 - CNAP | 113 |
| B.51.Point-line diagram - middle finger(L) - test subject 6 - V.2 | 114 |
| B.52.Point-line diagram - middle finger(R) - test subject 6 - CNAP | 114 |
| B.53.Point-line diagram - index finger(R) - test subject 7 - V.2 | 115 |
| B.54.Point-line diagram - index finger(L) - test subject 7 - CNAP | 115 |
| B.55.Point-line diagram - index finger(L) - test subject 7 - V.2 | 116 |
| B.56.Point-line diagram - index finger(R) - test subject 7 - CNAP | 116 |
| B.57.Point-line diagram - middle finger(R) - test subject 7 - V.2 | 117 |
| B.58.Point-line diagram - middle finger(L) - test subject 7 - CNAP | 117 |
| B.59.Point-line diagram - middle finger(L) - test subject 7 - V.2 | 118 |
| B.60.Point-line diagram - middle finger(R) - test subject 7 - CNAP | 118 |

List of Tables

| | |
|---|----|
| 1.1. Classification of Hypertension | 2 |
| 3.1. Setting of the Biopac System | 25 |
| 3.2. Test Subject Data - V.1 | 29 |
| 3.3. Flow Rate of Syringe Pump | 31 |
| 3.4. Measurement Series CNAP2GO | 34 |
| 3.5. Test Subject Physical Data - V.2 | 35 |
| 3.6. Test Subject Finger Data - V.2 | 36 |
| 3.7. Computation - V.3 | 41 |
| 3.8. Computation of Torque - V.3 | 43 |
| 4.1. Results of Prototype V.1 | 52 |
| 5.1. Recomputation of Prototype V.3 | 77 |
| A.1. Components of Biopac System | 84 |
| A.2. Additional Components - V.0 | 84 |
| A.3. Additional Components - V.1 | 85 |
| A.4. Additional Components - V.2 | 86 |
| A.5. Additional Components for CNAP Classic - V.2 | 86 |
| A.6. Additional Components - V.3 | 87 |
| A.7. Piezo Motor Data - V.3 | 87 |

List of Abbreviations

| | |
|-------------|---|
| ABP | Arterial Blood Pressure |
| ADC | Analog-to-Digital Converter |
| CNS | CNSystems Medizintechnik GmbH |
| CO | Cardiac Output |
| DBP | Diastolic Blood Pressure |
| ECG | Electrocardiography |
| ESC | European Society of Cardiology |
| FEM | Finite Element Method |
| IPG | Impedance Plethysmography |
| ISW | Institute for Fluid Mechanics and Heat Transfer |
| KB | Width of the Oscillometric Envelope |
| MAP | Mean Arterial Pressure |
| MD | Mean Pressure of the Oscillometric Envelope |
| MEMS | Microelectromechanical Systems |
| NIBP | Non-Invasive Blood Pressure |
| OE | Oscillometric Envelope |
| PAT | Pulse Arrival Time |
| PPG | Photoplethysmography |
| PPV | Pulse Pressure Variation |
| PTT | Pulse Transit Time |
| SBP | Systolic Blood Pressure |
| SD | Standard Deviation |
| SDR | Standardised Death Rate |
| SVR | Systemic Vascular Resistance |
| SVV | Stroke Volume Variation |
| VCT | Volume Control Technique |
| VUT | Vascular Unloading Technique |

1. Preamble

1.1. Motivation

The most prevalent cause of death in the year 2018 in Austria were diseases of the circulatory system. Out of 83 975 individuals, 38.9% died because of pathology of the circulatory system, whereas more than half of these cases of deaths occurred after the age of 80. Within this particular age group, every second death was caused by circulatory issues. In the average adulthood (40 – 79 years of age), one quarter of the deceased individuals died due to diseases of the circulatory systems, the percentage of causes of death due to circulatory issues for adolescents and young adults (10 – 40 years of age) is 7.4% [1]. Figure 1.1 depicts the graphic progression of the percentage distribution of deceased individuals in 2018 dependent on the age group.

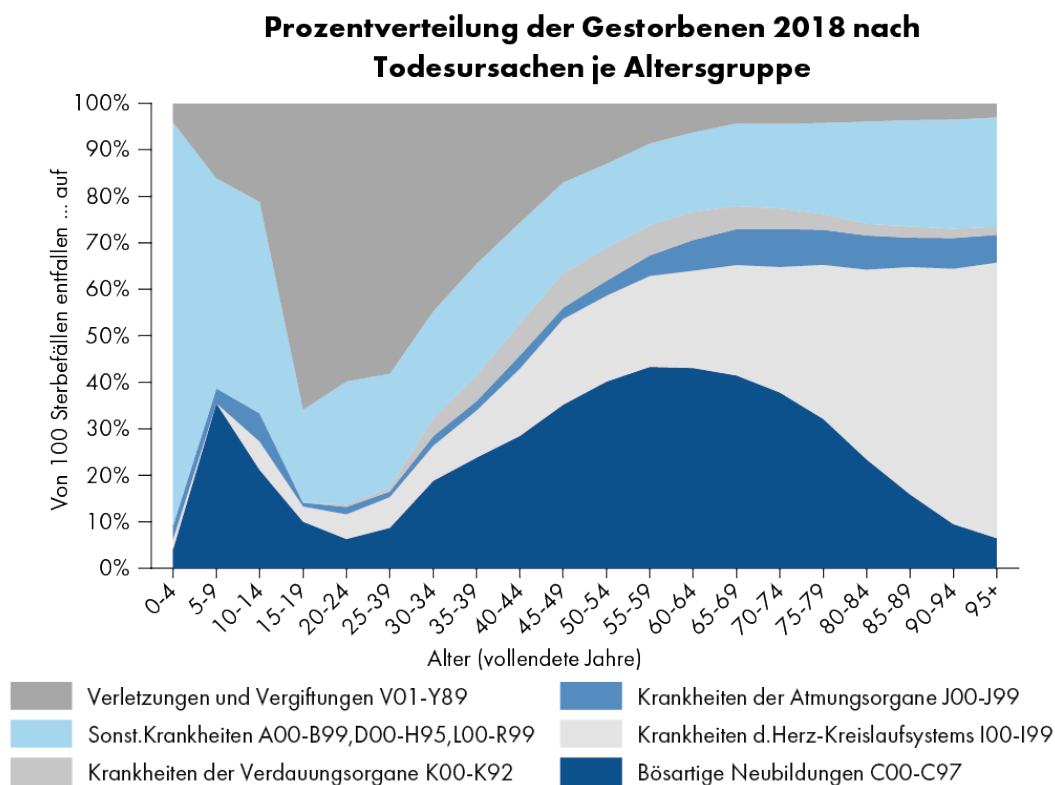


Figure 1.1.: Causes of death in Austria in the year 2018 - light gray colour: cardiovascular diseases I00-I99. Percentage distribution of deceased individuals dependent on the age group cited from [1].

On a larger scale, by means of analysing the figures within the European Union, "eurostat" (European Commission - Eurostat, Luxemburg, Luxemburg) provides an overview on the statistics of causes of deaths for the year 2016. The Standardised Death Rate (SDR) enables - as the weighted average of the age-specific death rates of a determined population - a superior representation of death causes within a certain time frame and an enhanced comparison between member states of the European Union. Thus, this SDR is computed by the World Health Organization (WHO) on the basis of a european standardised population per 100.000 inhabitants [2]. The average of the SDR within the EU-28 member states (Great Britain still included) was 358.3 for cardiovascular diseases and 118.8 for heart diseases (ischemic heart diseases). Worldwide, 14% of all causes of death are attributed to the diagnosis "Hypertension" [3]. The European Society of Cardiology (ESC) defines hypertension as systolic blood pressure (SBP) values ≥ 140 mmHg and diastolic blood pressure (DBP) values ≥ 90 mmHg. As a condition for this definition, these categories of blood pressures are defined by measuring the blood pressure on a sitting individual in a clinical environment according to the gold standard: the Riva-Rocci and Korotkoff method by means of a mercury sphygmomanometer [4]. In table 1.1, the detailed classification of hypertension is shown.

| Category | Systolic (mmHg) | | Diastolic (mmHg) |
|--------------------------------|-----------------|--------|------------------|
| optimal | <120 | and | <80 |
| normal | 120 – 129 | and/or | 80 – 84 |
| high normal | 130 – 139 | and/or | 85 – 89 |
| Grade 1 Hypertension | 140 – 159 | and/or | 90 – 99 |
| Grade 2 Hypertension | 160 – 179 | and/or | 100 – 109 |
| Grade 3 Hypertension | ≥ 180 | and/or | ≥ 110 |
| isolated systolic Hypertension | ≥ 140 | and | ≤ 90 |

Table 1.1.: Classification of Hypertension. Detailed categories of hypertension with systolic and diastolic tolerances - cited from [5]

High blood pressure, cholesterol, diabetes and smoking are the most important factors for diseases of the circulatory system. The combination of these factors proportionally increases the cardiovascular risk of each individual.

In Austria, blood pressure measurements were carried out in 56 centres (general practitioners, outpatient departments, pharmacies & fitness studios) in 2017 as part of the "May Measurement Month" of the International Society of Hypertension. More than half of the people tested had blood pressure values of $\geq 140/90$ mmHg [6]. Based on the data presented, effective and correct blood pressure management (standardised diagnostic strategies, prevention, clarification, etc.) is an important and frequent problem for many doctors. The monitoring of blood pressure changes, physiological rhythms, as well as pulse waves provides important information in various medical fields such as anaesthesia, intensive care, cardiology, neurology & internal medicine. Hypertensive or hypotonic phases indicate disturbances in the cardiovascular system such as heart defects, shock, loss of blood volume, aneurysms or haemorrhages. Therefore, various methods are used to measure the relevant cardiological parameters.

1.2. Methods of cardiological parameter acquisition

In this subchapter, the following different methods of measuring cardiological parameters are discussed:

1. Invasive blood pressure measurement by arterial cannulation
(arterial line as gold standard)
2. Riva-Rocci and Korotkoff method (gold standard)
3. Oscillometric Measurement
4. Vascular Unloading Technique and CNAP (CNSystems Medizintechnik GmbH, Graz, Austria)

Invasive blood pressure measurement by means of arterial puncturing enables intravascular blood pressure measurement and blood gas analysis and is defined as gold standard in anesthesiology. "There is almost universal agreement that "true" blood pressure is best determined using a reliable, calibrated transducer directly in an artery [7]." An aggravated risk for complication is synchronised to the invasivity of this method, whereas temporary occlusion of the radial artery poses the most common pathology with a percentage of 19.7%. Haematomas, bleeding, local infections, sepsis and pseudoaneurysms are other possible pathologies of invasive blood pressure measurement [8].

The ease of application of the Riva-Rocci and Korotkoff method served as the main factor for the establishment as gold standard for non-invasive blood pressure measurement. However, this intermittent method cannot provide information on a continuous beat-to-beat level.

The oscillometric method is a widely used method with applications ranging from home use to intensive care. Automated algorithms calculate the Oscillometric Envelope (OE) - the envelope curve of the measured oscillations - and estimate the systolic and diastolic blood pressure. Ideally, the Mean Arterial Pressure (MAP) is at the maximum of the oscillometric envelope: Due to regulatory requirements, this value is not displayed, provided that the Riva-Rocci method was used as reference measurement [9]. As can be seen in figure 1.2, the problem with this measurement method arises due to changes in blood pressure and arrhythmias in the seconds range, whereas the typical bias is 5 ± 8 mmHg. Time sequential successive measurements produce different results due to sinus arrhythmias - measurement 1 is only a few seconds before measurement 2.

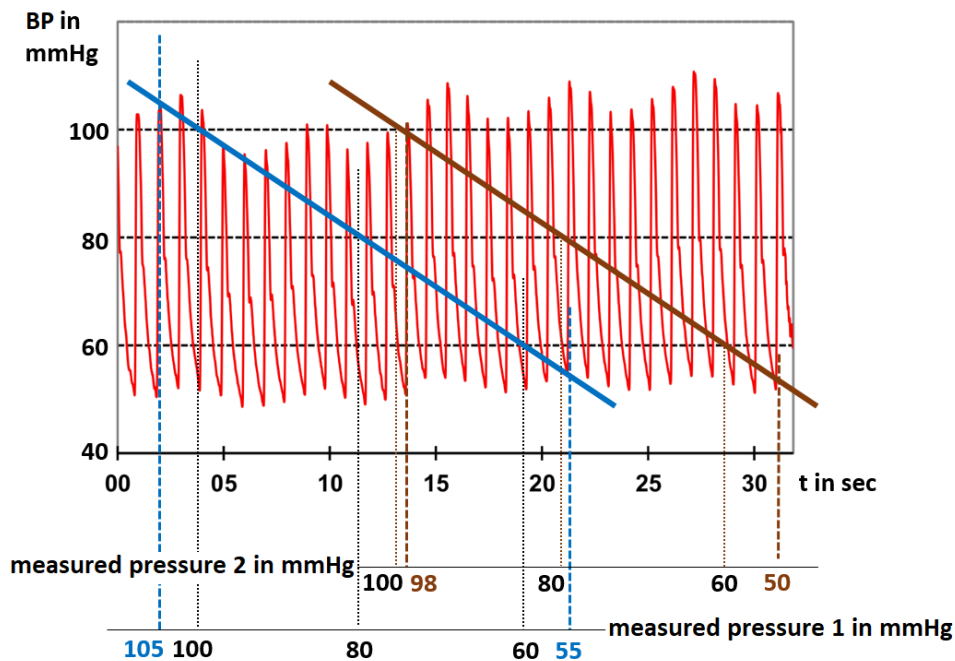


Figure 1.2.: Oscillometric Method & Auscultatory Method. Measurement problem due to the time shift of the blood pressure measurement curve.

In figure 1.3 a result of the oscillometric measurement method, conducted with the CNSystems TaskForce Monitor (an all-in-one device for continuous recording of haemodynamics developed by CNSystems; see www.cnsystems.com last accessed on 03.08.2020), is depicted as modified scan. The positions marked in blue represent systolic blood pressure, diastolic blood pressure and mean blood pressure.

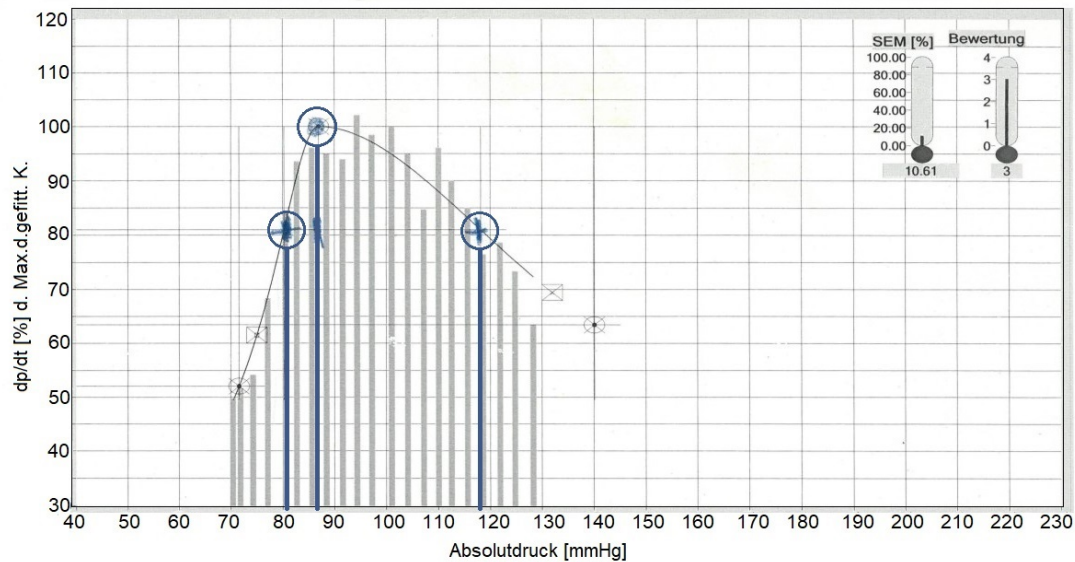


Figure 1.3.: Oscillometric measurement. Real oscillometric envelope recorded with a CNSystems TaskForce Monitor.

Although both methods are considered the gold standard in cardiological examination, they show strong differences in measurement results depending on absolute blood pressure [10]. The results of 24.225 patients under anaesthesia monitoring show elevated non-invasive blood pressure values (NIBP) at low absolute blood pressure and lower values at elevated absolute blood pressure - evident in figure 1.4.

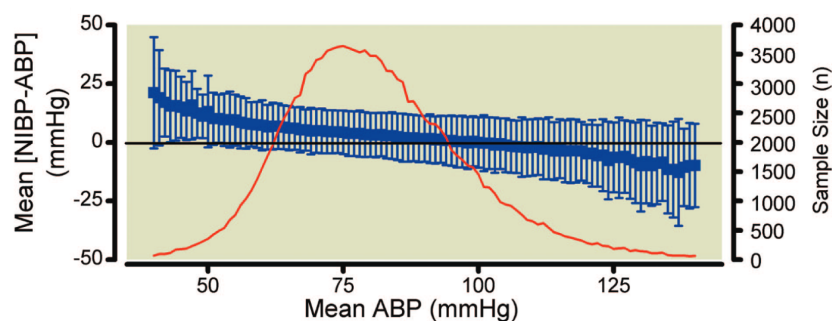


Figure 1.4.: Difference between oscillometric measurement (NIBP) and invasive arterial blood pressure (ABP). Averaged standard deviation (\pm SD) of NIBP and ABP, as well as total sample size of data pairs for each ABP value - cited from [10].

The Peñáz principle - also known as the Vascular Unloading Principle - combines the principle of plethysmography (measuring the change in arterial blood volume, but not blood pressure) with the application of counter-pressure in a finger cuff. Maintaining a constant value of the blood volume signal, the cuff pressure is then equal to the pressure in the artery. Thus, the arterial wall is "unloaded" and the arterial blood volume is kept at a constant diameter [11]. Vasomotor aspects, venous congestion, haematocrit and tissue fluid squeezing are the most important disturbances of this measurement method. The CNAP System copes with this problem by means of cascading various adaptive controllers and using a specific algorithm called "VERIFI" (Vasomotoric Elimination and Reconstructed Identification of the Initial set-point) (shown in figure 1.5 as well as in the subsequent chapter). For calibration purposes, the blood pressure values (systolic, diastolic and mean blood pressure) are recorded with an upper arm cuff at the arteria brachialis. Then, changes of blood pressure are determined by the VERIFI-Algorithm, whereas physiological rhythms and pulse wave changes are recognised with the Vascular Unloading Technique (VUT) [12, 13].

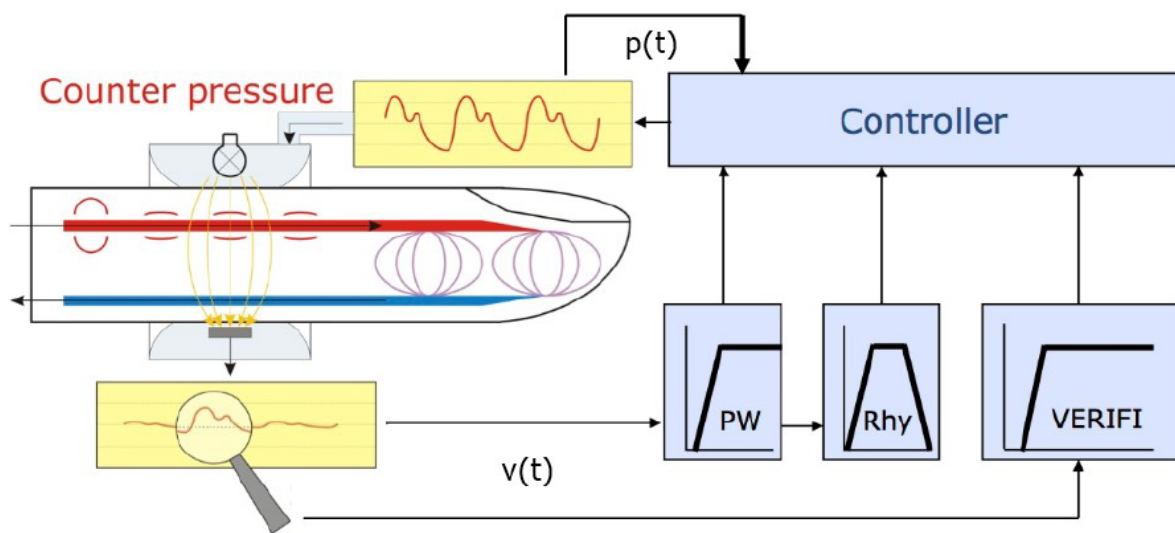


Figure 1.5.: CNAP control loop - schematic. Combination of VUT and VERIFI algorithm cited and modified from [13].

1.3. CNAP Sensor & VERIFI Algorithm

The CNAP principle combines the concept of the VUT, the calibration mechanism (NIBP) and the VERIFI-Algorithm [13]. The VUT is keeping the blood volume in the finger artery constant at a certain set-point by applying pulsatile counter-pressure (double-finger cuff - "CNAP Classic Cuff"). The aim of the VERIFI-Algorithm is the extension of the control system of the VUT, due to the aforementioned problematic nature of the vasomotoric activity. Thus, the applied set-point - also referred to as inflection point of the s-shaped pressure-light curve, which is described in the subsequent section - shall be tracked. After calibration, the pulsatile pressure changes in the finger cuff are then precisely corresponding to the genuine arterial pressure.

Figure 1.6 depicts a schematic representation of the CNAP control mechanisms. The measured plethysmographic signal $v(t)$ is filtered and then sent to several adaptive controllers. The highpass-filtered signal $v_{\text{Pulse}}(t)$ ("Pulse Filter") is used in a PID-controller ($\text{VUT}_{\text{Pulse}}$) for the correct mapping of each measured blood pressure wave. A so-called beat-to-beat detection enables the calculation of the integral of each blood pressure wave. As the value of the computed integral differs from 0, the counter-pressure in the finger cuff is increased or decreased via the control loop (depending on the sign of the integral value). The bandpass-filtered signal $v_{\text{Rhythm}}(t)$ ("Rhythm Filter") is used for respiratory rhythms ("Traube-Hering-Mayer Waves") in a second PID-Controller ($\text{PID}_{\text{Rhythm}}$). This controller is associated with the VERIFI-Algorithm (filtered signal $v_{\text{VERIFI}}(t)$) as follows: All frequencies of $v(t)$ below a cut-off frequency $f_{\text{VLF}} (\approx 0.02 \text{ Hz})$ are eliminated, due to the influence of the vasomotoric activity of the arterial walls on these signals. Thus, in order to correctly generate specific blood pressure trends, VERIFI reconstructs these low-frequency signals adaptively, using a beat-to-beat detection of the residual pulses of the signal $v(t)$. VERIFI then matches the characteristics of the chronological new pulses with the precedent pulses, as well as the initial set-point at the outset of the measurement. Therefore, the set-point of the second controller, that tracks slow blood pressure changes, is computed [13].

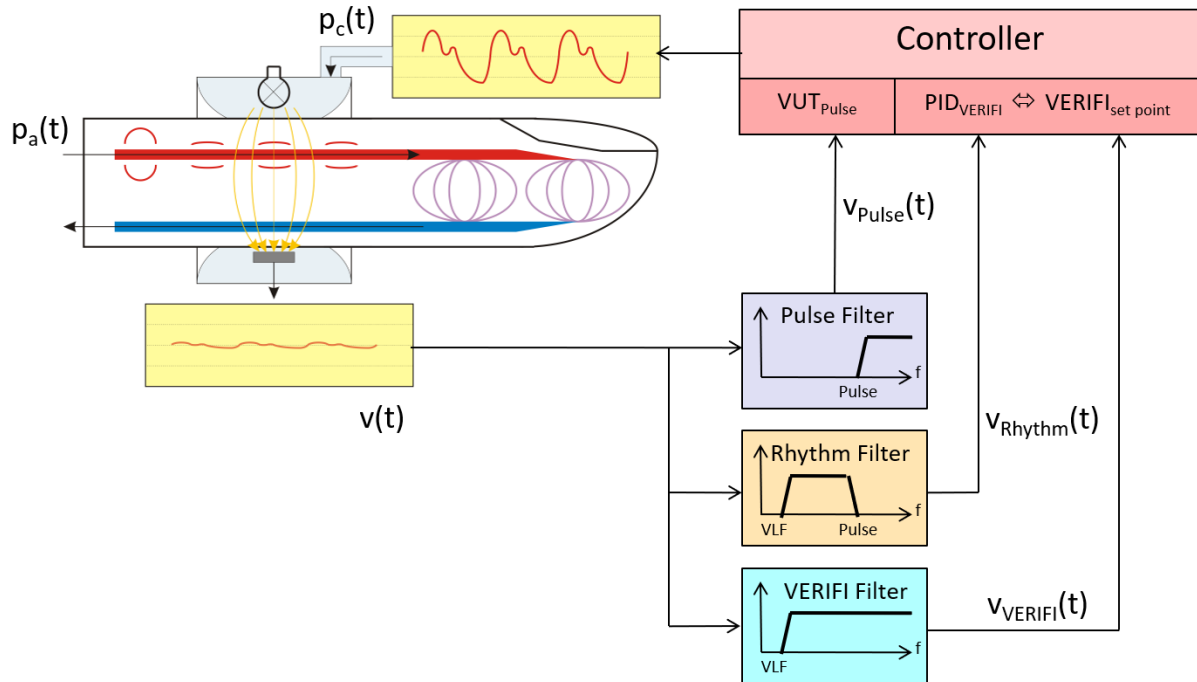


Figure 1.6.: CNAP control loop - detailed. Combination of VUT and VERIFI-Algorithm cited from [13].

The reusable double-finger sensor is shown in figure 1.7. It is attached onto two adjacent fingers by a simple "slip-on" movement all the way to the fingerroots and does not need any further fastening. The infrared sensors, electronics and inflatable pressure chambers are embedded on the inside of the cuff.



Figure 1.7.: CNAP finger cuff - cited from "www.cnsystems.com"; last accessed on 03.08.2020.

1.4. Correlation of photoplethysmography $v(t)$ and cuff pressure $p(t)$

A sigmoidal/s-shaped correlation between the Photoplethysmography-Signal (PPG) and the pressure signal $p(t)$ can be established. At the maximum of oscillation - the inflection point of the curve/peak value of the oscillations of the light signal - the counter-pressure in the finger cuff corresponds to the mean intra-arterial pressure p_{mean} . Therefore, the envelope curve of the local oscillation maxima (OE) can be constructed. The s-shaped transfer function is dependent on the vasomotoric parameters: Constriction of the arteries results in an increase of the minimal $v(t)$ -signal due to the lower light absorption of the finger. This signal $v(t)$ can be described simplified by the subsequent mathematical model 1.1 cited from [14]:

$$v(t) = \begin{cases} V_{\min} + (V_0 - V_{\min}) \cdot e^{\frac{c_{\max}}{V_0 - V_{\min}} \cdot (p_c - p_a)} & \text{for } p_c < p_a \\ V_{\max} - (V_{\max} - V_0) \cdot e^{-\frac{c_{\max}}{V_{\max} - V_0} \cdot (p_c - p_a)} & \text{for } p_c > p_a \\ V_0 & \text{for } p_c = p_a \end{cases} \quad (1.1)$$

Figure 1.8 serves as a more detailed illustration of the aforementioned parameters in equation 1.2. V_{\min} , V_{\max} and V_0 correspond to the according intensity of the light signal at the correlating cuff pressure, p_c and p_a represent finger cuff pressure and intra-arterial pressure, c_{\max} is the maximum slope of the s-curve, which corresponds to the maximum amplitude of the light signal oscillations. The slope k can be obtained according to equation 1.2:

$$k = \frac{dv}{dp} = \begin{cases} c_{\max} \cdot e^{\frac{c_{\max}}{V_0 - V_{\min}} \cdot (p_c - p_a)} & \text{for } p_c < p_a \\ c_{\max} \cdot e^{-\frac{c_{\max}}{V_{\max} - V_0} \cdot (p_c - p_a)} & \text{for } p_c > p_a \\ c_{\max} & \text{for } p_c = p_a \end{cases} \quad (1.2)$$

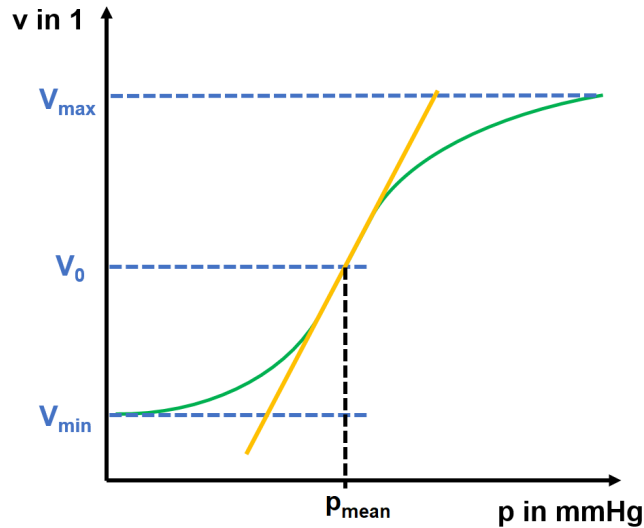


Figure 1.8.: Pressure-light diagram. Correlation between the recorded light signal and the intral-arterial pressure.

1.5. CNAP2GO & Volume Control Technique (VCT)

The project "CNAP2GO" of CNSystems Medizintechnik GmbH aims to develop a wearable device, that determines mean arterial blood pressure non-invasively and energy efficiently by means of a novel approach. This novel Volume Control Technique (VCT) can be utilised and integrated within small-scale wearable sensors such as a ring on the finger. Softwareprototypes, compatible with the existing CNAP Hardware, have been developed and tested in comparison to the invasive blood pressure measurement method (46 patients; during surgery). The blood pressure signal obtained by CNAP2GO can then be applied for the derivation of Cardiac Output (CO) and further haemodynamic variables [15].

The control loop of the novel VCT is depicted in Fig. 1.9. If the first PID-controller for controlling $v_{\text{Pulse}}(t)$ is deactivated, the counter-pressure of the finger cuff $p_c(t)$ loses its pulsatile behavior and corresponds to the mean arterial pressure. Furthermore, the pulse signal $v(t)$ is displayed inverted, because of the mitigation of the light signal in the finger during systole due to increased blood volume. Despite $v(t)$ now depicting the pulse signal, the bandpass-filtered signal $v_{\text{Rhythm}}(t)$ is maintained as small as possible by the second controller ($\text{PID}_{\text{Rhythm}}$) and used in combination with the VCT-Algorithm ($v_{\text{vct}}(t)$, computation of the integral of the blood pressure wave) to control the pressure $p_c(t)$.

For the purpose of the generation of the pulsatile pressure signal, $v(t)$ is filtered by a high-pass and then - as $v_{\text{Pulse}}(t)$ - multiplied with a constant k (at "vascular unloaded" state), that is derived from an initial oscillometric calibration measurement at the start of the CNAP2GO measurement. It is necessary to filter the signal $v(t)$, because the DC-component in the signal does not correspond to the real mean arterial pressure. Thus, the pressure signal $p_c(t)$ - which corresponds to the real mean arterial pressure in the vascular unloaded state - is added to the scaled signal $v_{\text{Pulse}}(t)$ for the computation of the pulsatile blood pressure signal $p_{\text{C2G}}(t)$. However, the vital part of the control mechanism is the integral part of the control (summation of the pulse integrals see eq. 1.3 and 1.4) for the reconstruction of the blood pressure information with sufficient accuracy [15].

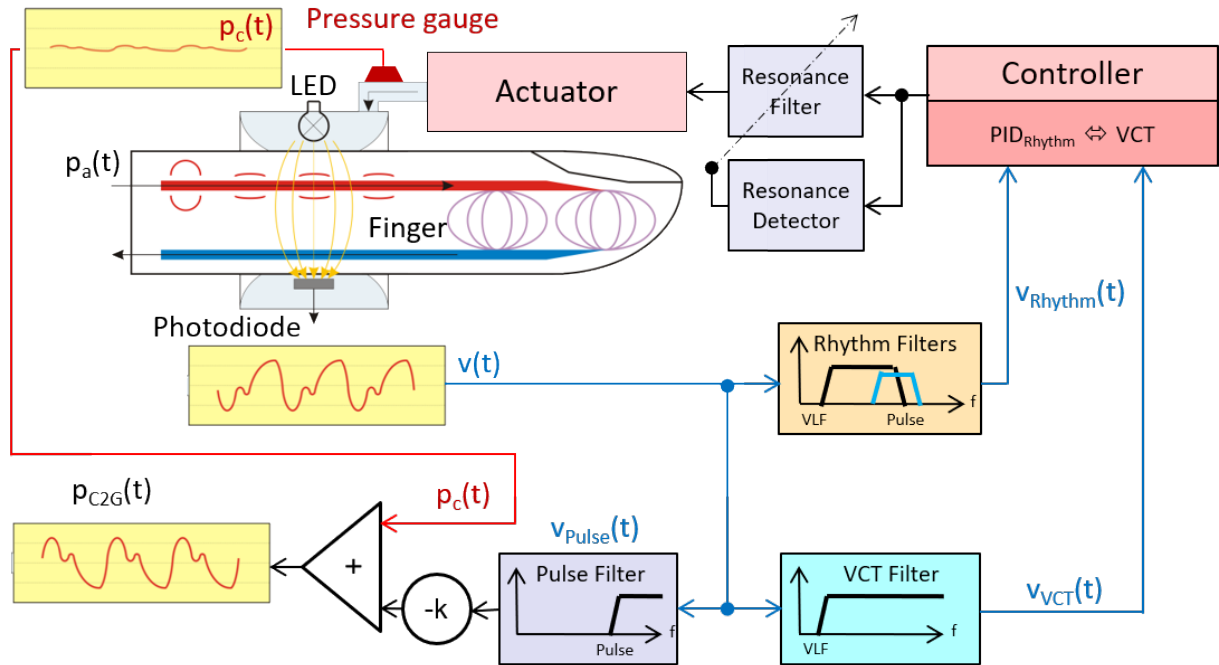


Figure 1.9.: Control Loop CNAP2GO. Measurement of the blood pressure by controlling the pressure via the VCT-Algorithm - cited from [15].

In order to obtain the initial set-point of the MAP, the pressure in the finger cuff is increased as shown in Fig. 1.10 and the corresponding PPG pulse amplitudes $v_{\text{Pulse}}(t)$ are recorded. This s-shaped pressure-light curve - as discussed in the previous chapter 1.4. - is limited at the top (pressure above the SBP) and at the bottom (no deformation of the finger due to too low cuff pressure). The upper asymptote corresponds to the maximum detectable light signal, if the blood volume in the finger has been displaced entirely and no pulses are demonstrable anymore. The lower asymptote corresponds to $p_c(t) = 0$.

Therefore, the amplitudes of the signal $v_{\text{Pulse}}(t)$ are now used in combination with the corresponding pressure signals to generate the Oscillometric Envelope (OE), whereas the maximum of the OE matches the MAP. These light amplitudes are determined via the PPG-signal by means of measuring the light strokes (differences of maximum and minimum light signal within a pulse) - condition for the correct computation of these amplitudes is an accurate PPG-signal and therefore high-quality sensors. This corresponding pressure (MAP) is applied as initial finger cuff pressure $p_c(t)$ and saved as set-point p_0 with the corresponding pulse signal v_0 for the continuous control mechanism [15].

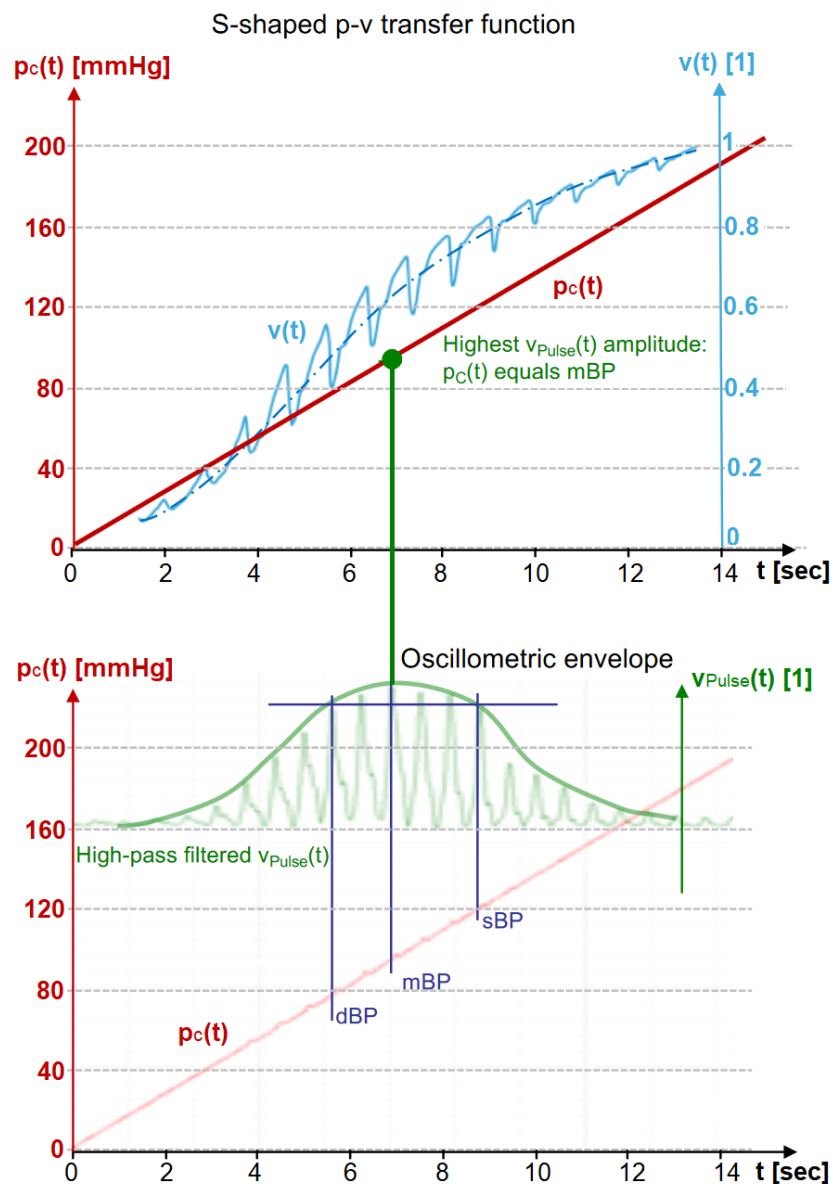


Figure 1.10.: Pressure and light signal in dependency of the measurement time. At the maximum light stroke v_0 (difference of maximum & minimum light signal during a pulse), the applied cuff pressure corresponds to the MAP. Additional illustration of the OE - modified from [15].

The continuous measurement of the MAP (= tracking of the inflection point) requires the consideration of vasomotoric aspects as well as the associated blood pressure changes. These respective changes of the s-shaped pressure-light curve are shown in figure 1.11.

The upper graph a) depicts optimal and suboptimal signals at the respectively applied cuff pressure, whereas higher pressure than the MAP results in "spiky" pulses with lower light amplitude and lower pressure than the MAP results in "fat" pulses with likewise smaller light amplitude.

The middle graph b) depicts the influence of the vasomotoric aspects with the example of vasoconstriction, by means of an upward shift of the lower asymptote, due to the reduction of the blood volume in the finger during vasoconstriction. Thus, a lower set-point than the inflection point - and therefore a "fatter" pulse shape - is generated (vice versa for vasodilatation: the set-point is increased, the pulse shape is "spikier").

The lower graph c) depicts the changes of the controlled cuff pressure after every beat. The CNAP2GO controller is responsible for maintaining the following condition for stabilised control of the blood volume: The initial set-point p_0 and the resulting pressure $p_c(t)$ have to be controlled and adjusted for every heart beat, that the integral value of the respective blood pressure wave equals zero. An increase of the MAP shifts the set-point in direction of the lower asymptote of the pressure-light curve (shift of the curve to the right), the integral value of the respective beat is negative and the new set-point is increased by the control mechanism. Vasodilatation shifts the sigmoidal pressure-light curve to the left, thus, decreasing the set-point due to the VCT.

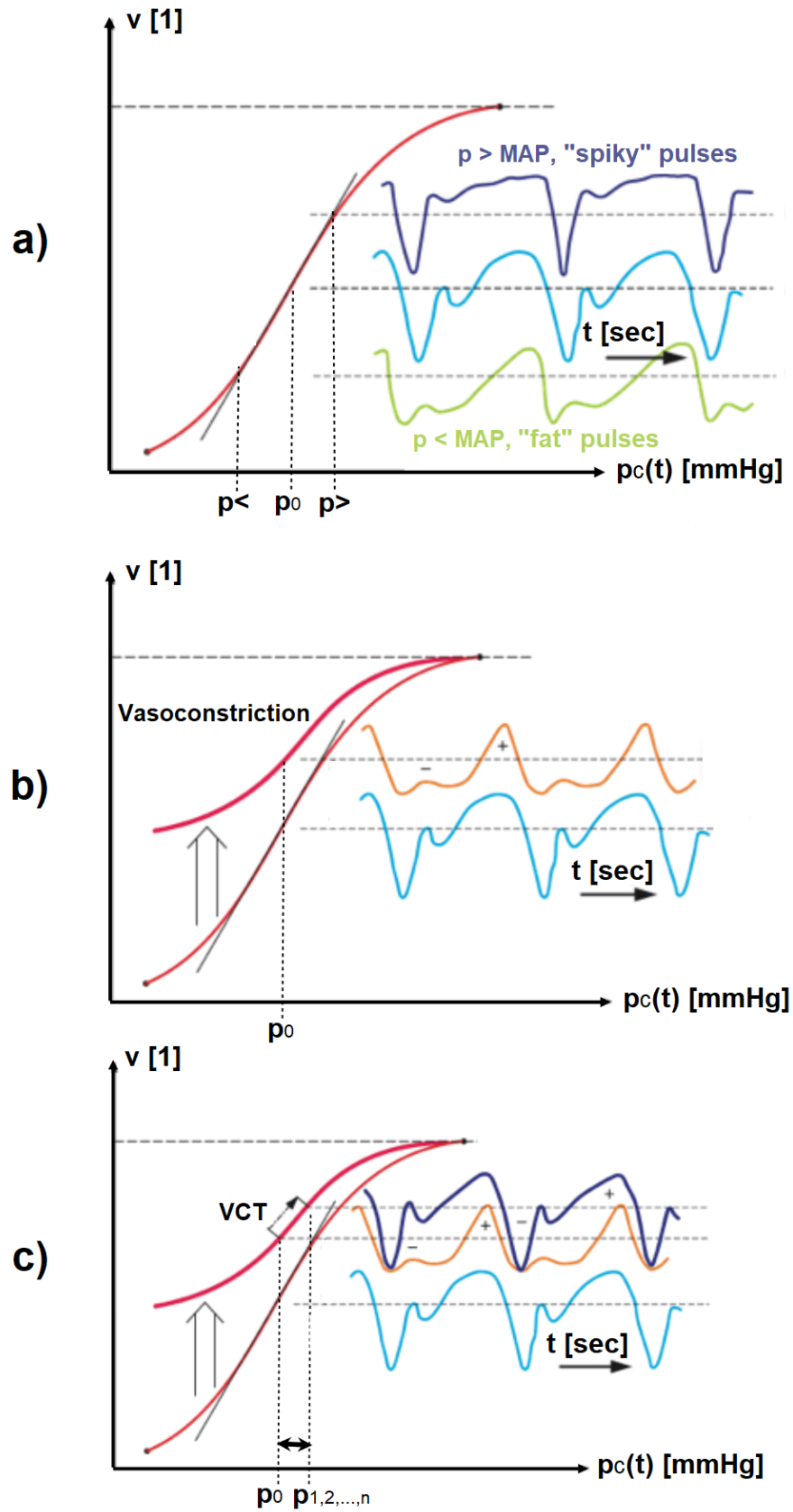


Figure 1.11.: Variation of the s-shaped pressure-light curve. a) Influence of the pressure changes, b) Vasomotor effects, c) Controlling the cuff pressure per beat - modified from [15].

A stable and continuous long-term measurement of the MAP with correction of the vasomotoric influences can be achieved by means of the VCT. Tracking and Controlling rapid changes of the MAP and physiological blood pressure changes, is done by adjusting $p_c(t)$ and simultaneously maintaining $v_{\text{Rhythm}}(t)$ as low as possible. An increase of blood pressure results in an increase of blood volume in the finger and consequently in a decrease of $v(t)$. The control loop generates the negative feedback: As the blood pressure rises, $p_c(t)$ is increased simultaneously in order to keep the blood volume in the finger constant. In addition to this control task, the signal $v_{\text{dRhythm}}(f)$ is computed to address pronounced blood pressure changes (e.g. vasalva manoeuvres, hyperventilation, etc.). The pulsatile frequencies are suppressed by a bandpass filtering mechanism - in order to follow the CNAP2GO principle. Figure 1.12 depicts both amplitude and phase responses of the control signals. The blue marked bandpass (v_{dRhythm}) represents the blue filter shown in the "Rhythm Filters" in figure 1.9. The green marked bandpass represents the black filter in the "Rhythm Filters" ($v_{\text{Rhythm}}(t)$). Both bandpasses are always active and both signals are fed into the controller - as stated in the subsequent control equations 1.5 - 1.7. Additionally, the graph illustrates which part of the blood pressure rhythms (DC-components, Rhythms and Pulses) is addressed by the corresponding signals [15].

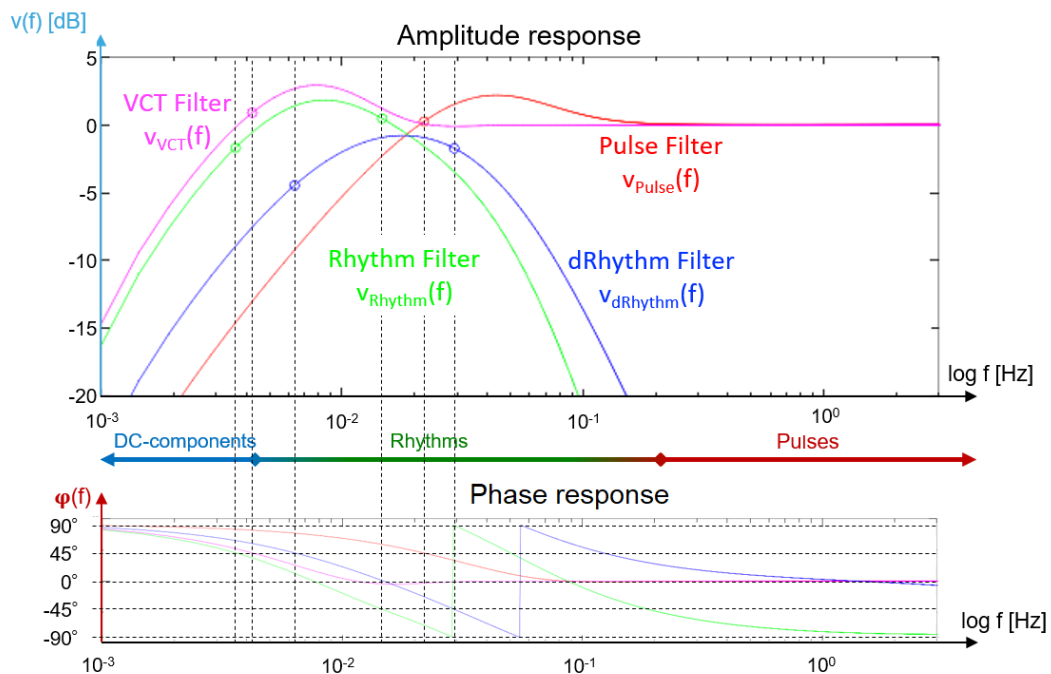


Figure 1.12.: Amplitude and phase response of the CNAP2GO signals. $v_{\text{VCT}}(f)$, $v_{\text{Rhythm}}(f)$, $v_{\text{dRhythm}}(f)$ and $v_{\text{Pulse}}(f)$ illustrated with the corresponding blood pressure ranges (DC-Components, Rhythms & Pulses) - modified from [15].

The control equations of the VCT-Algorithm are described subsequently (see [15]). This beat-based VCT uses the preceding heart beat for the computation of the integral value and triggers the adjustment of the set-point P_n , shown in equation 1.3:

$$P_n = P_0 - c_{BI} \cdot \sum_0^n \bar{V}_n - c_{BP} \cdot \bar{V}_n \quad (1.3)$$

P_0 is the initial set-point (see p.12), c_{BI} and c_{BP} are constants, used for the beat-based integral- and proportional control. The integral per beat \bar{V}_n (pulse-based averaging) is computed in equation 1.4, t_b represents the time of the beat detection and PI represents the pulse interval from t_{b-1} to t_b . The resulting value is one of the important parameters for the control system (VCT) and necessary for the aforementioned summing of pulses (i.e. storing the pulse information for continuous blood pressure monitoring):

$$\bar{V}_n = \frac{1}{PI} \cdot \int_{t_{b-1}}^{t_b} v_{VCT}(t) dt \quad (1.4)$$

The control system equations for the CNAP2GO System (1.5 - 1.6) are depicted below. The coefficients c_P, c_I and c_D are the control constants of the control system, that keep $p_c(t)$ at the inflection point of the s-shaped pressure-light curve.

$$y_{PD} = c_P \cdot v_{Rhythm} + c_D \cdot v_{dRhythm} \quad (1.5)$$

$$y_I = c_I \cdot \sum_0^n y_{PD} \quad (1.6)$$

The final CNAP2GO pressure can then be obtained from the previous equations 1.3, 1.5 and 1.6. This specific pressure $p_c(t)$ in equation 1.7 is then identical to the MAP.

$$p_C(t) = P_n - y_I - y_{PD} \quad (1.7)$$

1.6. Drive units for CNAP2GO

The key findings of the clinical study (see [15]) - conducted on 46 patients - regarding miniaturisation are:

1. Drive component with a maximum speed of 25 - 30 mmHg/s
2. Maximum applicable pressure of 250 mmHg

Two different concepts implementing an adaption of the existing finger cuff (CNAP Classic Cuff) are analysed as drive systems for CNAP2GO. In the following, both variants are explained. They can be distinguished in the underlying approach as "unsealed" and "sealed" system.

1.6.1. Unsealed system

The "unsealed" system uses the conveying of a fluid into the adapted CNAP2GO cuff in order to apply the required pressure onto the finger. This concept aims at the use of hydraulic drive systems such as pumps and hydraulic circuits, with the advantages of the simple generation of the linear movement as well as the superior suitability for the use in controlled drives for automated equipment [16].

The identification of a suitable hydraulic fluid, serving as a construction element for power transmission, is vital. In comparison to standard hydraulic systems, the role of the pressure fluid in the CNAP2GO System is altered, as no additional lubrication of sliding / rolling contacts (no lubricating film necessary for high loads) or heat dissipation (no heat development when measuring blood pressure) is required. In general, pressure fluids can be classified according to Fig. 1.13. Additionally, these fluids are assessed by viscosity and compressibility, whereas temperature dependence has no decisive influence in the CNAP2GO application.

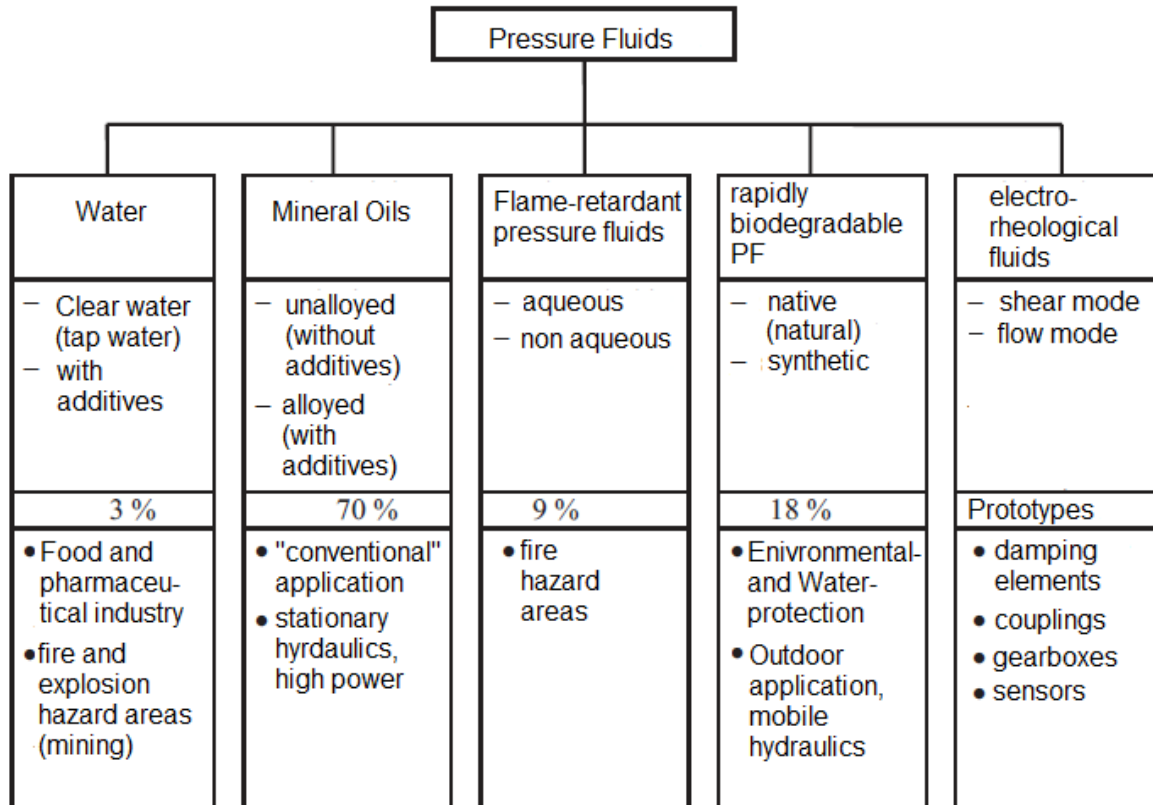


Figure 1.13.: Classification of pressure fluids - translated from [16].

The use of water as a pressure fluid has the advantages of availability, environmental compatibility, non-flammability, product compatibility as well as an economical advantage. As an application, hydraulic systems in food processing combine the power transmitting properties of water as a pressure medium with the possibility of cleaning the machine system. The compression modulus, which is increased by a factor of 2 compared to mineral oil, improves hydraulic control due to the increased rigidity. Furthermore, the almost temperature-independent viscosity is also an advantage [16]. The important parameters in the "unsealed" system are the controlled flow rate (speed of the system) and the required maximum pressure limit. Further design aspects in the hydraulic concept are venting of the system, storage of the pressure fluid (fluid reservoir) and line design. Miniature pumps such as an eccentric diaphragm pump (Schwarzer Precision GmbH, Essen, Germany) or piezo pump (BMT Fluid Control Solutions GmbH, Frankfurt am Main, Germany) are possible pump drive types for the concept.

1.6.2. Sealed system

The application of the required pressure in the approach of the "sealed" system is carried out externally onto the adapted, fluid-filled, sealed CNAP2GO cuff and therefore on the finger. This concept aims at the use of motors or linear actuators as drive unit, in order to use the linear movement to increase the pressure from the exterior. The integration of precision mechanics and microelectronics (integrated circuits, microelectromechanical pressure sensors (MEMS)) allows the miniaturisation of the system. The key advantages of DC motors as drive unit are the adjustability and controllability of the speed as control variable over a wide supply voltage range as well as the operation with direct current (batteries).

The electromechanical design of the brushless DC motor is used in the stepper motor to control various holding positions or angles of rotation from a stator with several controllable windings in combination with a permanent magnet as a rotor. Especially in so-called hybrid technology, the rotor consists of a permanent magnet, that is magnetised in the axial direction with specially toothed pole shoes to achieve relatively high power and a self-holding torque in the de-energised state. Positive aspects of stepper motor control are direct compatibility with integrated circuits and a maintenance-free, cost-effective drive concept [17].

The main disadvantage of electromechanical actuators is the high proportion of "moving mechanics", the inertia of the components and undesired tribology as well as the total weight. Therefore, the design of piezoelectric actuators using the reciprocal piezoelectric effect is a suitable concept for miniaturisation. In figure 1.14 the power-to-weight ratios of different actuator concepts are given in Watts per kg. These concepts refer to actuators which are preferably used for small to medium actuating power and perform translatory movements, thus the graph does not allow a statement regarding scalability or dependence on the size. The advantages of the static, currentless holding torque, as well as the low power consumption combined with high actuating forces and shortest actuating times, are used, for example, for injection valves in the automotive industry.

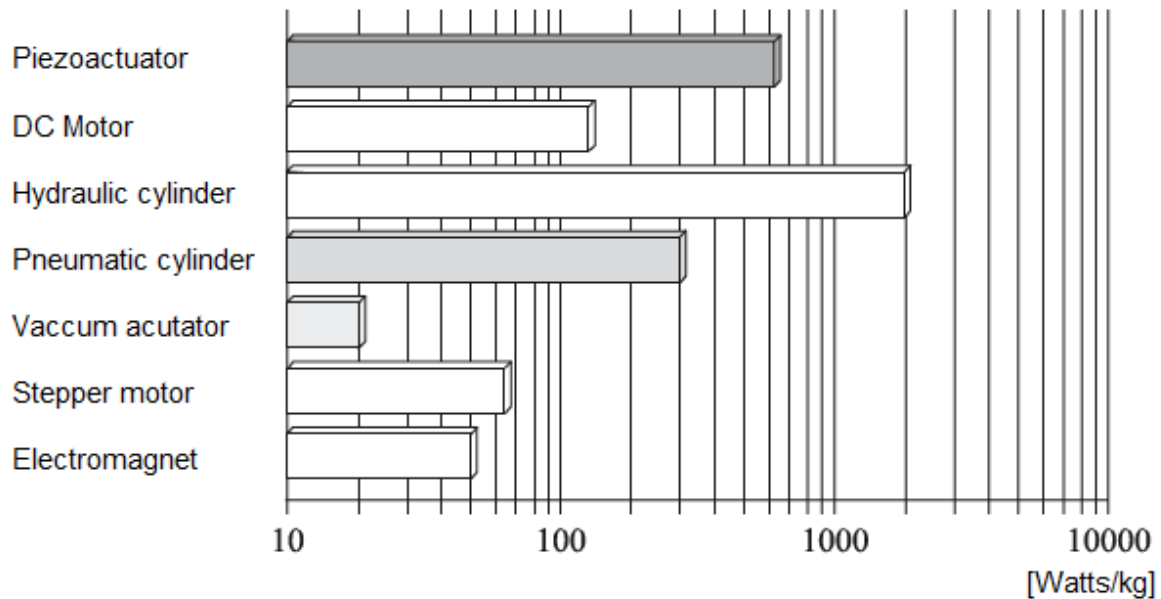


Figure 1.14.: Power-to-weight ratios of various actuators in Watts/kg - translated from [17].

1.7. Competitor products for CNAP2GO

In this subchapter, possible alternative concepts as well as competitor products are explained, which aim at the non-invasive blood pressure measurement and adhere to the ISO Standard 81060-2 (Standard for intermittent non-invasive sphygmomanometers): difference of mean value $5 \pm$ standard deviation 8 mmHg. The most accurate and precise results of blood pressure measurement are obtained by approaches that determine the Pulse-Transit-Time (PTT) or the Pulse-Arrival-Time (PAT) via a proximal and a distal sensor, and combine these results with additional information from the PPG and/or Electrocardiography (ECG) [18, 19]. These approaches were tested under both static and dynamic conditions, whereas the approach in [18] was not verified for hypertensive patients or pathologies, but the approach in [19] was verified with a total sample size of 33 individuals (including 14 hypertensive individuals). Another concept is the usage of dual sensors such as Impedance Plethysmography (IPG) and PPG at both proximal and distal measuring points for obtaining the PTT, which also achieves meaningful results [20, 21]. The first approach of Nabeel et.al. [20] was tested on 35 young and healthy volunteers (normotensive) after exercising - no pathological conditions were tested. The second approach of Nabeel et.al. [21] was tested on 83 subjects, whereas 43 individuals were hypertensive and over 75% of the tested individuals were under medication.

Designed as a bracelet, this combination of impedance measurement and PPG indicates an accuracy of 0.01 ± 8.1 SBP and -0.06 ± 5.5 mmHg DBP, whereas the tested subjects were 15 healthy individuals without any history of cardiovascular disease [22]. Novel technological concepts for measuring with a smartphone may combine PPG and force transducer signals. Following an initial calibration phase, the blood pressure is measured with values at 3.3 ± 8.1 SBP and 5.6 ± 7.7 mmHg DBP [23]. This approach was tested on 35 healthy adults, but it was not tested under pathological conditions.

The metrological difficulty for a correct, continuous blood pressure measurement is due to the influences of the cardiovascular, respiratory and autonomous nervous system (and the vasomotoric activity associated with it) [15]. Thus, the researched alternative concepts using blood pressure estimation by means of the PTT in combination with PPG are united by the problem of the consideration of the vasomotoric aspects: Assuming that the blood vessels close due to a body reaction (Vasoconstriction), blood pressure increases and although pulse pressure also increases, the PTT decreases due to the vascular resistance. This erroneously leads to a measured lower blood pressure. Artificial Intelligence Approaches, as for instance used in the competitor product Aktiia (Aktiia SA, Neuchâtel, Switzerland) [24, 25], try to compensate this error.

Commercial products such as

1. "Aktiia" (Aktiia Inc., New York, US / Aktiia SA, Neuchâtel, Switzerland) - FDA Approval and CE Marking pending
2. "Visi Mobile" (Sotera Wireless Inc., San Diego, USA) with FDA Approval
3. "InstaBP" (Samsung R&D Institute, Bangalore, India) - App according to manufacturer not suitable for diagnostic purposes
4. "Somnotouch-NIBP" (SOMNOmedics GmbH, Randersacker, Germany) - Validation according to International Protocol of the ESH, Clinical Trial
5. "Empatica E4" (Empatica Inc., Boston, USA) - CE Marking (Klasse 2a)

are a selection of relevant competitor products for CNAP2GO and make use of PPG sensor technology for the determination of blood pressure.

2. Task Definition

2.1. CNAP2GO

In the course of the project CNAP2GO of CNSystems Medizintechnik GmbH and the associated publication “A novel art of continuous non-invasive blood pressure measurement“ [15], a miniaturised Prototype shall be designed and developed iteratively.

First, the existing CNAP System and its components shall be analysed in terms of adaptability. As a medium for the application of the required finger cuff pressure, a preferably incompressible fluid shall be used. The aim of this work are various prototypes that implement the measurement of the blood pressure by integrating hardware & software and adapt the existing CNAP components. Measurements are to be carried out using these developed prototypes (if applicable: test plans and measurement series) and the findings and results shall be compared to the existing CNAP system. The mathematical parameters described in the subsequent chapter ”Methods” shall be used as comparison parameters in order to demonstrate representativity and reproducibility of the measurement results.

The prototypes of the iterations shall represent concept trials and integrate controllable drive units for the generation of a test series as a further step. ”Proof of principle” shall be achieved by an advanced prototype, whereas the utilisation of the CNAP Algorithm can be neglected in this step. Energy considerations shall be the relevant factor in the context of miniaturisation of the measurement system. Furthermore, the discussion of applicable alternative concepts/alternative drive systems in respect of price, speed, energy consumption and - most importantly - pressure application is required.

3. Methods

Analogically to the NIBP at the upper arm, the existing finger cuff of the CNAP system is using air as pressure medium. Pressure signal and light signal are the relevant parameters for the measurement of the oscillometric envelope. However, the utilisation of a fluid is most reasonable for the miniaturisation. The compression of air and therefore, the associated size of the required components (compressor system with pressure reservoir) as well as the energy consumption of the compressor system proves to be inadequate. In order to measure the oscillometric envelope, the pressure on the finger must be applied from 0 to 200 mmHg with a slope of 5 mmHg per 3 seconds (at a heart rate of 80 min⁻¹). The mean arterial pressure can be computed simplified as shown in equation 3.1:

$$\text{MAP} = \text{Diastole} + \frac{1}{3} \cdot (\text{Systole} - \text{Diastole}) \text{ in mmHg} \quad (3.1)$$

Combining the information of table 1.1 and the aforementioned equation 3.1 permits the determination of "worst case" values for hypertensive individuals. The calculated MAP for hypertensive individuals with Grade 3 Hypertension with a systolic pressure of 190 mmHg and a diastolic pressure of 120 mmHg is 143 mmHg. Thus, for the purpose of measuring the values from 1.1, the pressure value of 200 mmHg is defined as maximum pressure value including orthostatic tolerance.

Based on the requirement for the pressure medium, experts of the "Institute for Fluid Mechanics and Heat Transfer (ISW)" of the University of Technology Graz were consulted. The key findings of this expert opinion are stated below:

1. Utilisation of a syringe pump/a linear actuator for the application of the pressure medium into the cuff
2. For above-mentioned slow pressure changes, fluid flow characteristics such as turbulences can be neglected
3. Utilisation of distilled water as pressure medium is more practical and appropriate than utilisation of hydraulic oils (contamination, reusability of compontens during iterative prototype construction)

3.1. Overview of prototypes

An overview of the iteratively developed prototypes is listed below. Every designed version builds on the findings, results and components of the preceding variants.

1. Prototype V.0

... manual approach for investigation of metrological influential factors of the fluid & the pressure curve - "suitability test"

2. Prototype V.1

... manual approach in combination with the CNAP components for the simultaneous measurement of the light signal - "first measurement"

3. Prototype V.2

... motorised approach via syringe pump in combination with the CNAP components for the simultaneous measurement of the light signal - "second measurement / measurement series"

4. Prototype V.3

... motorised approach via piezo motor and pressure application - "approach for miniaturisation"

The subsequent prototypes were utilizing a pressure measurement system from Biopac (Biopac Systems Inc., Goleta, USA) and the according software AcqKnowledge. In addition, for the simultaneous recording of the light signal, prototypes V.1 and V.2 combined the Biopac System and the CNAP System. The Biopac components can be seen in table A.1 in the appendix. The Biopac blood pressure transducer TSD104A was calibrated according to the internal CNSystems calibration protocol by means of a pressure manometer DPI 800P (AKS-Messtechnik GmbH, Gelhausen, Germany). Its output characteristic is $5 \mu\text{V}/\text{mmHg}$, thus, 200 mmHg correspond to 1 mV output voltage [26]. At a gain factor of 1000 (see table 3.1) this results in an output characteristic of 1V per 200 mmHg or 5 mV/mmHg. The differential amplifier DAC100C of Biopac was configured according to the settings shown in table 3.1:

| Settings DAC100C | |
|-----------------------|--------|
| Gain Factor | 1000 |
| 10 Hz Low Pass Filter | Off |
| Low Pass Filter | 300 Hz |
| High Pass Filter | DC |

Table 3.1.: Setting of the Biopac differential amplifier DAC100C

The connections of the complete fluid system - consisting of syringe, pressure sensor and cuff - had to be as short as possible in order to avert elastic phenomena (deformations), pressure fluctuations, pressure losses and turbulent flow. For connecting a Luer-Lock valve the adapted cuff of the CNAP system had to be disconnected from the standardised air supply line. Figure 3.1 illustrates the cuff, adapted for the fluid system and fixed at rest. The black strap and the purple housing in the figure represent the connected pressure sensor.



Figure 3.1.: Adapted cuff for the fluid system with connected pressure sensor (black strap).

3.2. Prototype V.0 - "suitability test"

The first, rudimentary setup was designed as suitability test of the chosen approach as well as for the detection of metrologically relevant factors. For the purpose of a functional test, these first measurements only apply pressure to the finger. Additional components used for this setup are listed in the Appendix A.2.

First, the measurement system had to be filled with distilled water via the syringe. Then the small amount of residual air in the connection lines, in the cuff and in the pressure sensor was retracted from the system into the syringe by applying negative pressure and aligning the setup vertically (syringe on top - residual air ascends close to syringe outlet). Thus, the filling of the overall measurement system was sufficiently guaranteed, because the residual air in the syringe could no longer leak into the system due to the syringe geometry (outlet nozzle of syringe arranged eccentrically). After starting the AcqKnowledge software, the distilled water was conveyed into the cuff from the syringe through the pressure sensor by screwing the trapezoid thread of the mechanical screw clamp. This increased the pressure in the overall system. The continuous rotation of the screw clamp was the crucial factor for achieving incremental pressure steps and regular pressure stages. The setup of the measurement system "syringe - sensor - cuff" is depicted in Fig. 3.2.



Figure 3.2.: Prototype V.0: Mechanical actuator - syringe - pressure sensor - cuff. Suitability test of the selected approach.

3.3. Measurement procedure prototype V.0

1. Start of measurement software AcqKnowledge
2. Filling of the syringe with distilled water
3. Connection of the syringe to the system
4. Filling of the measurement system
5. "Venting" the system via negative pressure generation (as mentioned before; residual air sucked into syringe)
6. Start of the measurement
7. Continuous increase of pressure - Simulation of the step function (5 mmHg / 3 seconds)

The resulting pressure curves from the AcqKnowledge software are displayed in the section "Prototype V.0" of the next chapter "Results". Measurements were taken respectively of the index finger and the middle finger of the left hand of a test subject.

3.4. Prototype V.1 - "first measurement"

This first iteration furthermore made use of the mechanical actuator for the application of pressure in the cuff and onto the finger. In addition to the Biopac system, the components listed in table A.3 in the appendix were used. The CNSystems Development Kit (CNS DevKit) in combination with the CNSystems cuff controller allow the measurement of blood pressure and other relevant cardiovascular parameters. CNSystems SerialGUI (CNS SerialGUI) and CNSystems TestInterpreter (CNS TestInterpreter) are software modules for controlling the CNS DevKit. Communication takes place via a USB interface with a specific data protocol. Prototype V.1 applied and measured the light signal via the DevKit, whilst simultaneously recording the cuff pressure via the Biopac system. This setup was adapted, in order to obtain improved results: relaxed support of the hand and cuff in horizontal position via fixation, connection and fixation of syringe and cuff controller for reduction of the movement of individual components. The remaining air after filling was extracted from the system in the same way as in the prototype V.0 (see p.26).

A script code was implemented on the CNS TestInterpreter for controlling the cuff via the CNS DevKit, for the purpose to record the light signal during the measurement procedure. At the starting point of the measurement, the CNS TestInterpreter set an intervention, in order to enable time synchronisation of pressure signal and light signal in the subsequent data evaluation. Similarly, at the beginning of the pressure measurement, a so-called "event" was generated automatically by the AcqKnowledge Software. This "event" had to be inserted into the dataset and then exported after completion of the measurement procedure. Both systems used a sampling frequency of 100 Hz.

The evaluated data were pseudonymised, synchronised, formatted and evaluated using WinPy - respectively Spyder with Python 3.7.6.. The CNS DevKit generated a pdp-file for each measurement, which then had to be converted into a hdf-file for data evaluation of the light signal. The pressure signal was exported as csv-file and could therefore be used immediately for data analysis. An important factor for the data evaluation was the beat detection. A CNS internal dll-file was used within the evaluation to detect the maximum and minimum light signal and the according difference of light intensity at a certain measurement time point. Synchronizing the mean pressure from one systolic beat time to the subsequent systolic beat time with the according light stroke (= difference of maximal light signal and minimal light signal for a beat) created the desired output format - the Oscillometric Envelope (OE). A 5-step "Moving-Average-Procedure" was utilised to generate the mean of 5 light strokes and 5 corresponding pressure values - here the two preceding and the two following data points around the current point were used for averaging. This resulted in more decisive representations of the oscillometric envelope as point-line diagram without higher frequency components (outliers). The mathematical characterisation criteria (see 3.11) were applied, enabling evaluation of the different approaches. The evaluated data and plots are shown in the results under "Prototype V.1".

In figure 3.3 the setup of prototype V.1 is displayed. The red screw clamp served as an actuator for the pressure increase. The cuff controller and the syringe were attached to each other via a black ribbon. The cuff itself was fixated in horizontal position via a second screw clamp, thereby keeping movements of the individual components as limited as possible.

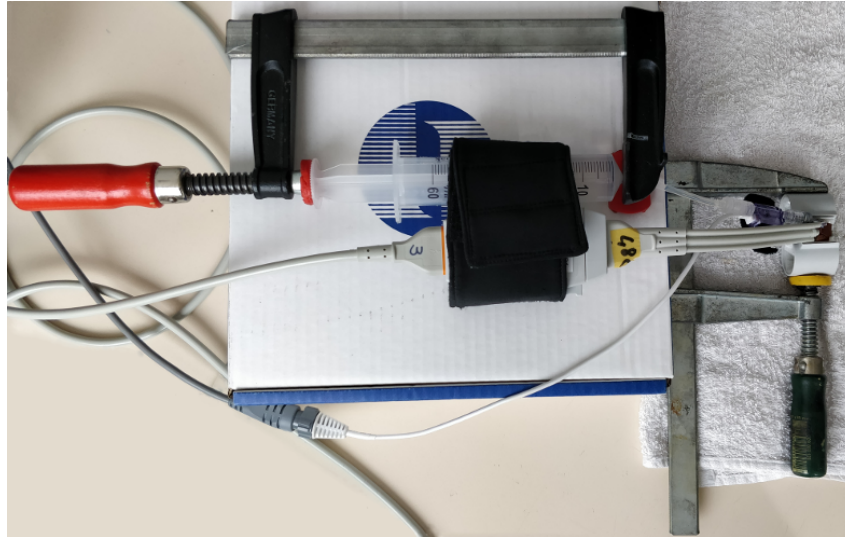


Figure 3.3.: Prototype V.1: Mechanical actuator - syringe with cuff controller - pressure sensor - fixated cuff. First measurement series with 4 test subjects.

This prototype was tested on 4 sitting subjects - on the index and middle finger of the left hand, respectively. Table 3.2 shows the relevant data of the 4 test subjects.

| | Sex | Age | Size in cm | Weight in kg |
|------------------|------------|------------|-----------------------|-------------------------|
| Subject 1 | m | 32 | 189 | 88 |
| Subject 2 | f | 40 | 170 | 67 |
| Subject 3 | m | 45 | 185 | 77 |
| Subject 4 | f | 37 | 168 | 58 |
| Range | | 32 - 45 | 168 - 189 | 58 - 88 |

| | Perim. Index(L) in cm | Ø Index(L) in cm | Perim. Middle(L) in cm | Ø Middle(L) in cm |
|------------------|----------------------------------|-----------------------------|-----------------------------------|------------------------------|
| Subject 1 | 6.1 | 1.9 | 6.1 | 1.9 |
| Subject 2 | 5.7 | 1.8 | 5.7 | 1.8 |
| Subject 3 | 6.1 | 1.9 | 6.4 | 2.0 |
| Subject 4 | 5.6 | 1.8 | 5.9 | 1.9 |
| Range | 5.6 - 6.1 | 1.8 - 1.9 | 5.7 - 6.4 | 1.8 - 2.0 |

Table 3.2.: Pseudonymised test subject data of prototype V.1 - sex, age, size, weight as well as perimeter and diameter of the left index and middle finger

3.5. Measurement procedure prototype V.1

1. Start of measurement software AcqKnowledge
2. Start of SerialGUI and TestInterpreter, Loading of TestInterpreter Script
3. Connection of the syringe to the system
4. Filling of the measurement system (as mentioned before; see p.26)
5. "Venting" the system via negative pressure generation (as mentioned before; residual air sucked into syringe; see p.26)
6. Start of the measurement
 - a) Inserting finger into cuff
 - b) Start of the light signal measurement via TestInterpreter
 - c) Start of the pressure signal measurement via AcqKnowledge – automated generation of an "event" at the starting point for time synchronisation. Note: Manual insertion into the journal of the AcqKnowledge file after termination of the measurement.
 - d) Continuous increase of pressure from 0 to 200 mmHg – Simulation of the step function ($\Delta = 5$ mmHg)
7. Stop of measurement
 - a) Reduction of pressure to 0 mmHg
 - b) Stop AcqKnowledge measurement – finger had to stay in the cuff for correct stopping of the light signal measurement
 - c) Stop TestInterpreter – via confirmation of warning message
8. Storing of measurement results
 - a) Saving of AcqKnowledge event
 - b) Export of AcqKnowledge file
 - c) *.pdp-files conversion into *.hdf-files
9. Data evaluation via Python

3.6. Prototype V.2 - "measurement series"

For the second iteration, a motorised syringe pump was used as actuator. This iteration was considered as the concept for the "proof of principle". In addition to the Biopac system, the components listed in table A.4 in the appendix were used. For conducting the measurements, the remaining air after filling was extracted from the system in the same way as in the prototype V.0 (see p.26). The key data of the utilised syringe pump (manufacturer, description) are listed in the appendix A.4. The maximum conveying speed is 99.9 ml/h. Therefore, an empirical determination of the required fluid flow rate was conducted, enabling the continuous increase of pressure in the system.

For this purpose, the cuff was filled (with already inserted middle finger). The overall volume (10 ml) as well as the additional volume (3 ml) for increasing the pressure from 0 to 200 mmHg were measured. Table 3.3 depicts the additional delta volume of the syringe, the measured pressure and the pressure difference to the previous pressure step. After the insertion of the finger, the pressure value was 5 mmHg (= Offset), which had to be taken into account for the computations. The increase of pressure was assumed to be continuously 5 mmHg per 3 seconds (1.67 mmHg/s). In equation 3.2, the empirical computation of the fluid flow rate in ml/h is shown, whereas the value of the numerator represents 1 ml volume difference.

$$\text{Flow Rate in ml/h} = \frac{1}{\frac{\text{Pressure Difference in mmHg/ml}}{1,67 \text{ mmHg/s}}} \cdot 3600 \quad (3.2)$$

| Additional Volume in ml | Measured | | Computed |
|----------------------------|---------------------|-----------------------------------|-------------------------------|
| | Pressure in mmHg | Pressure Difference in mmHg/ml | Required Flow Rate in ml/h |
| 0 | 5 | | - |
| 1 | 25 | 20 | 300 |
| 2 | 65 | 40 | 150 |
| 3 | 200 | 135 | 45 |

Table 3.3.: Pressure and volume data for computing the flow rate for prototype V.2

An important conclusion due to the non-linear pressure behaviour with linear increase of the fluid volume was the adaptation of the flow rate to the current pressure in the cuff. Thus, for the pressure steps from 0 to 65 mmHg the maximum flow rate of 99.9 ml/h was applied, recording at least 3 seconds of data per 5 mmHg step. For the pressure steps above 65 mmHg, the flow rate had to be decreased to 45 ml/h, as a means to continuously enable slow pressure increases.

Figure 3.4 shows the prototype V.2. Syringe and syringe pump formed the unit of control. Shortest possible connection lines led to the adapted cuff via the Biopac pressure sensor. The recorded light signal was sent to the CNS Development Kit (left side of the figure) via the CNS cuff controller.

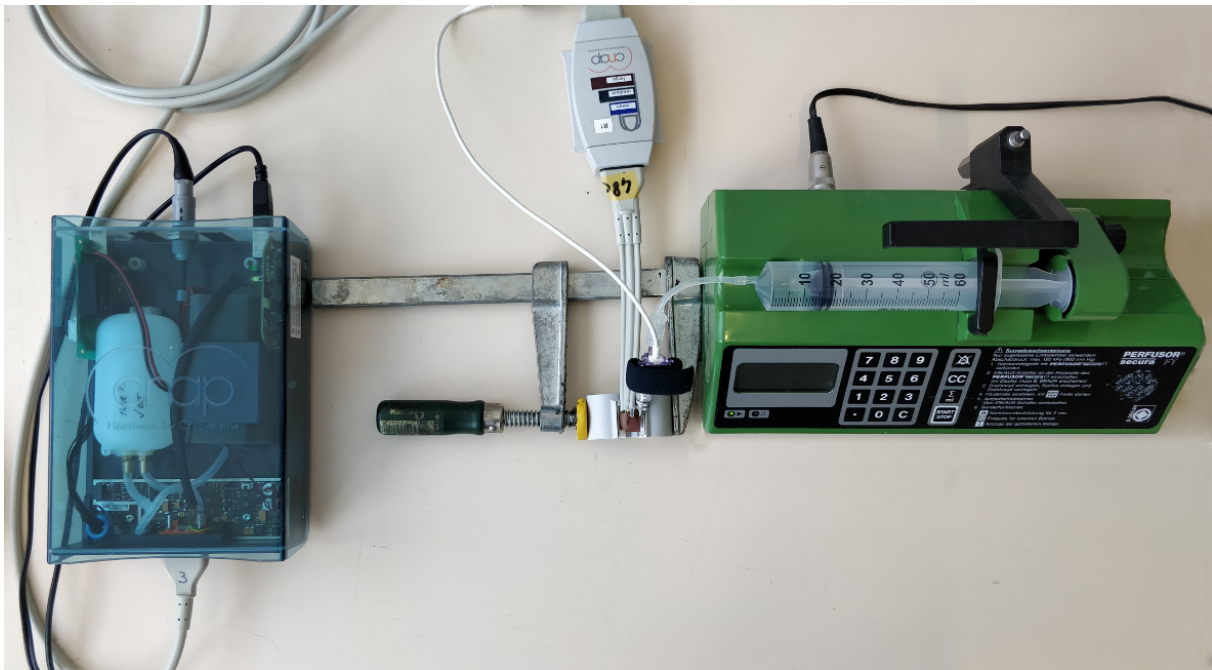


Figure 3.4.: Prototype V.2: Syringe and syringe pump as unit of control - pressure sensor - fixated cuff. The light signal was sent via the cuff controller to the DevKit.

For this prototype - and the "proof of principle" - a comparison with the existing CNAP system as reference measurement was sought. The further required components for the classical CNAP measurement are listed in table A.5 in the appendix.

The setup for the measurement series is shown in figure 3.5 with the CNAP2GO approach and the CNAP system. As explanatory addition, table 3.4 lists all required components. This measurement was conducted with a sample size of 7 test subjects, sitting with the finger size "medium" according to the CNAP system. Both index and middle finger on both hands were measured, resulting in the following configurations:

1. CNAP Classic index finger left / CNAP2GO index finger right
2. CNAP Classic middle finger left / CNAP2GO middle finger right
3. CNAP Classic index finger right / CNAP2GO index finger left
4. CNAP Classic middle finger right / CNAP2GO middle finger left

3.7. COVID-19 measures

Due to the acute emergency situation of the COVID-19 pandemic, strict safety precautions have been established based on given hygiene standards. The measures included:

1. Disinfection of all surfaces and sensors before and after each measurement
2. Disinfection of the fingers before and after each measurement
3. Wearing of mouth-nose protection of all persons involved
4. Safety distances of at least 1 m had to be maintained at all times
 - a) This measure was supported by the measurement setup, because the test subject and the test operator were separated in 2 different areas upon entering the measurement laboratory. In Fig. 3.5 this spatial separation is illustrated.
5. Opening of the windows to allow circulation of fresh air if possible
6. If the test person felt pain during the measurement, the measurement had to be stopped immediately



Figure 3.5.: Measurement setup for the comparative measurement of CNAP2GO (prototype V.2) and the CNAP classic system with aforementioned COVID-19 safety measures.

| Position | Description |
|----------|--|
| 1 | Testperson Side |
| 2 | CNAP Sensor with Biopac Transducer for CNAP2GO |
| 3 | Syringe Pump Braun Perfusor segura FT |
| 4 | CNAP Sensor for CNAP Classic |
| 5 | DevKit for CNAP Classic |
| 6 | DevKit for CNAP2GO (Prototype V.2) |
| 7 | Testoperator Side |

Table 3.4.: Components of the comparative measurement series: CNAP2GO and CNAP

The steps taken after the measurement of prototype V.1 were also applied for this measurement series for prototype V.2. The evaluation in Python was enhanced, so that both parallel measurements (CNAP2GO and CNAP Classic) were comparable. The sampling frequency of the AcqKnowledge software was reduced to 10 Hz, in order to decrease CPU-load and decrease the file size. Point-line diagrams were produced, which are shown in the results under prototype V.2. Furthermore, for improved representation of the principle, decisive pressure points and the correlating pulse signal were plotted. As an additional diagram, the chronological sequence of the applied pressure, the oscillations of the light signal as well as the OE were generated in further plots (see results). Within these plots, the pressure signal was low-pass filtered using a 4th order Butterworth Filter with a cut-off frequency of 0.01 Hz. The oscillations of the light signal were high-pass filtered with a 10th order Butterworth Filter with a cut-off frequency of 0.5 Hz.

Table 3.5 and 3.6 show the relevant pseudonymised data of the 7 test subjects - sex, age, size, weight as well as perimeter and diameter of both index and middle finger.

| | Sex | Age | Size in cm | Weight in kg |
|------------------|------------|------------|-----------------------|-------------------------|
| Subject 1 | m | 38 | 186 | 81 |
| Subject 2 | m | 41 | 173 | 104 |
| Subject 3 | w | 34 | 161 | 79 |
| Subject 4 | m | 52 | 188 | 130 |
| Subject 5 | w | 37 | 165 | 65 |
| Subject 6 | m | 26 | 174 | 72 |
| Subject 7 | m | 32 | 189 | 88 |
| Range | | 26 - 52 | 161 - 189 | 65 - 130 |

Table 3.5.: Pseudonymised test subject data of prototype V.2 - sex, age, size and weight

| | Perim. I(L) in cm | Ø I(L) in cm | Perim. I(R) in cm | Ø I(R) in cm |
|------------------|------------------------------------|-------------------------------|------------------------------------|-------------------------------|
| Subject 1 | 6.5 | 2.1 | 6.8 | 2.2 |
| Subject 2 | 7.2 | 2.3 | 7.9 | 2.5 |
| Subject 3 | 6.1 | 1.9 | 6.2 | 2.0 |
| Subject 4 | 7.1 | 2.3 | 7.3 | 2.3 |
| Subject 5 | 6.0 | 1.9 | 6.1 | 1.9 |
| Subject 6 | 6.0 | 1.9 | 6.0 | 1.9 |
| Subject 7 | 6.1 | 1.9 | 6.2 | 2.0 |
| Range | 6.0 - 7.2 | 1.9 - 2.3 | 6.0 - 7.9 | 1.9 - 2.5 |

| | Perim. M(L) in cm | Ø M(L) in cm | Perim. M(R) in cm | Ø M(R) in cm |
|------------------|------------------------------------|-------------------------------|------------------------------------|-------------------------------|
| Subject 1 | 6.7 | 2.1 | 6.9 | 2.2 |
| Subject 2 | 7.9 | 2.5 | 7.9 | 2.5 |
| Subject 3 | 6.0 | 1.9 | 6.0 | 1.9 |
| Subject 4 | 7.2 | 2.3 | 7.3 | 2.3 |
| Subject 5 | 6.0 | 1.9 | 6.1 | 1.9 |
| Subject 6 | 6.0 | 1.9 | 6.0 | 1.9 |
| Subject 7 | 6.1 | 1.9 | 6.1 | 1.9 |
| Range | 6.0 - 7.9 | 1.9 - 2.5 | 6.0 - 7.9 | 1.9 - 2.5 |

Table 3.6.: Pseudonymised test subject data of prototype V.2 - perimeters (Perim.) and diameters of the left (L) and right (R) index (I) and middle finger (M)

3.8. Measurement procedure prototype V.2

1. Start of measurement software AcqKnowledge
2. Start of SerialGUI and TestInterpreter, Loading of TestInterpreter Script
3. Filling of the syringe
4. Fixation of the cuff, to reduce movement artefacts
5. Connection of the syringe with the system (cuff, connection lines, Biopac pressure sensor) and filling of the system with "venting" the system via negative pressure generation (as mentioned before; residual air sucked into syringe; see p.26)
6. Insertion of the syringe into the syringe pump, pressure adjustment to 0 mmHg in the AcqKnowledge software via adjusting the syringe pump wheel
7. Setup of the CNAP Systems for comparative measurement
8. Start of measurement
 - a) Start of the light signal measurement via TestInterpreter
 - b) Start of the pressure signal measurement via AcqKnowledge – automated generation of an "event" at the starting point for time synchronisation. Note: Manual insertion into the journal of the AcqKnowledge file after termination of the measurement.
 - c) Continuous increase of pressure from 0 to 200 mmHg
 - i. Setting the flow rate according to the computation (99.9 ml/h until 65 mmHg, followed by 45 ml/h until 200 mmHg)
9. Stop of measurement
 - a) Reduction of pressure to 0 mmHg
 - b) Stop AcqKnowledge measurement – finger had to stay in the cuff for correct stopping of the light signal measurement
 - c) Stop TestInterpreter – via confirmation of warning message
10. Storing of measurement results
 - a) Saving of AcqKnowledge event
 - b) Export of AcqKnowledge file
 - c) *.pdp-files conversion into *.hdf-files
11. Data evaluation via Python

3.9. Prototype V.3 - "miniaturisation approach"

The third iteration (prototype V.3) aimed for a concept for the miniaturisation of the system. A piezo motor (PCBMotor ApS, Hillerød, Denmark) was used as drive unit. A further setup was implemented and test measurements were made. Various cuff systems were tested in sub-iterations and the corresponding pressure curves were generated and analysed. The precision mechanical construction consisted of the piezo motor as drive unit and the Biopac TSD104A as pressure sensor. Using prototype V.3, the aim was to apply the required pressure to a "sealed" system as mentioned in the chapter "Preamble". The piezo motor has a threaded spindle with a M3 x 0.35 mm thread (see Fig. 3.6), a 4 mm thread stroke and applied the pressure from outside via a metallic pressure surface onto various cuff systems.



Figure 3.6.: PCB piezo motor: 30 mm motor with 200 step encoder, position sensor and controller - modified from "www.pcbmotor.com"; last accessed 03.08.2020.

The motor was controlled via the software terminal Termite (ITB CompuPhase, Bussum, NL) a configurable RS232 terminal, which is free for personal and commercial use. The piezo motor enabled a positioning movement of 200 microsteps per revolution, the achieved step speed varied for each motor load (and motor voltage). Thus, the motor enabled a thread stroke of 0.35 mm per revolution or 200 microsteps. The step designations "A x B" in the subsequent chapter "Results" shall be interpreted so that A is the total number of steps and B is the number of microsteps of the motor per number of steps A. Exact data (description, power and geometric data) of the motor are listed in the appendix in tables A.6 and A.7. The analysis of the implementability, speed and power consumption in order to compare the motor with other drive technologies was the main goal of this design.

3.9.1. Computation of the piezo motor

The aim for the CNAP2GO concept using a piezo motor is to apply the pressure of 200 mmHg, respectively 0.26 N/mm^2 , via a single fluid bladder (one compartment for the pressure medium) placed on the upper side of the finger. The figure 3.7 serves for a better illustration of the concept and as a supporting explanation for the following calculations.

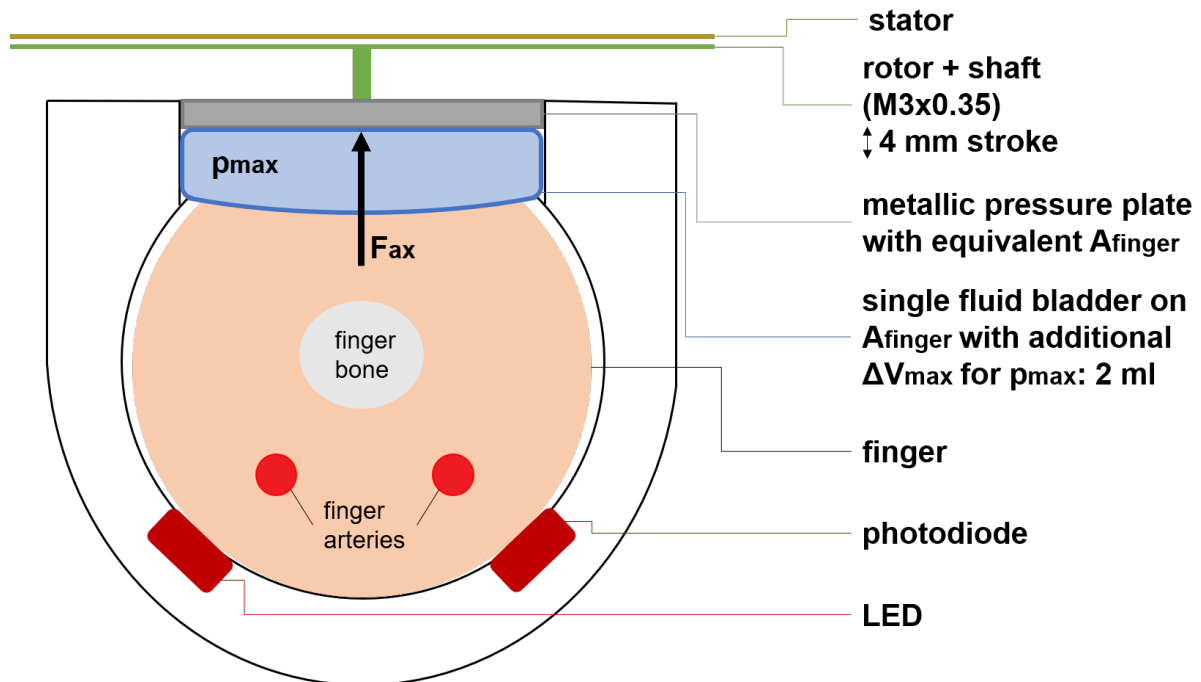


Figure 3.7.: CNAP2GO design. Piezo motor placed above the single fluid bladder applying pressure via a metallic pressure plate. p_{\max} is 200 mmHg, the additional volume ΔV_{\max} is 2 ml, A_{finger} is the pressured finger area and F_{ax} is the calculated axial force.

The maximum required force F_{ax} ideally corresponds to the axial force on the motor and results from the maximum required pressure p_{\max} and the finger area A_{finger} .

$$F_{\text{ax}} = p_{\max} \cdot A_{\text{finger}} \quad (3.3)$$

The volume difference ΔV that is required per mmHg pressure increase is computed from the additionally required maximum pressure volume ΔV_{\max} and the maximum pressure p_{\max} . The assumption for this calculation is: There are no displacement effects, i.e. volume that leads to deformation at undesired locations. The additionally required maximum pressure volume ΔV_{\max} was determined by increasing the pressure to the maximum pressure p_{\max} in a single fluid bladder via conveying of distilled water.

$$\frac{\Delta V}{\text{mmHg}} = \frac{\Delta V_{\max}}{p_{\max}} \quad (3.4)$$

The length difference ΔL respectively the stroke per mmHg results from the volume difference and the pressure area. The required speed for a pressure increase of 1.67 mmHg/s (5 mmHg slope per 3 seconds) is computed from this length difference.

$$\frac{\Delta L}{\text{mmHg}} = \frac{\Delta V}{\text{mmHg} \cdot A_{\text{finger}}} \quad (3.5)$$

The aforementioned speed of the motor is computed in mm/s (v_{ML}) as well as rev/s (v_{MR}) using length difference and thread pitch P .

$$v_{\text{ML}} = 1.67 \frac{\text{mmHg}}{\text{s}} \cdot \frac{\Delta L}{\text{mmHg}} \quad (3.6)$$

$$v_{\text{MR}} = \frac{v_{\text{ML}}}{P} \quad (3.7)$$

The maximum achievable pressure p_e for 4 mm stroke H is also calculated using the length difference.

$$p_e = \frac{H}{\frac{\Delta L}{\text{mmHg}}} \quad (3.8)$$

In conclusion, table 3.7 includes measured and computed data from the aforementioned calculations.

| Computation - V.3 | | |
|---|--------------|-----------------|
| Measured | | |
| Description | Value | Unit |
| Maximum pressure p_{\max} | 200 | mmHg |
| Width of the finger | 20 | mm |
| Height of the finger | 20 | mm |
| Finger area A_{finger} | 400 | mm ² |
| Additional volume ΔV_{\max} (0 - 200 mmHg) | 2 | ml |
| Thread pitch P | 0.35 | mm |
| Stroke of the motor H | 4 | mm |
| Speed of the motor (acc. to feedback of PCB Motors) | 0.22 | mm/s |
| Computed | | |
| Description | Value | Unit |
| Maximum finger force F_{ax} | 10.7 | N |
| Volume difference ΔV per mmHg | 0.01 | ml/mmHg |
| Length difference ΔL per mmHg | 0.025 | mm/mmHg |
| Required speed v_{ML} for 1.67 mmHg/s | 0.042 | mm/s |
| Required speed v_{MR} for 1.67 mmHg/s | 0.12 | rev/s |
| Maximum achievable pressure p_e | 160 | mmHg |

Table 3.7.: Computation of the parameters for prototype V.3

Furthermore, a calculation of the required torque was conducted according to "Roloff Matek Maschinenelemente" [27] (shown in table 3.8 and equations 3.9 to 3.12). Figure 3.8 from [28] shows the geometry of the metric thread according to DIN 13.

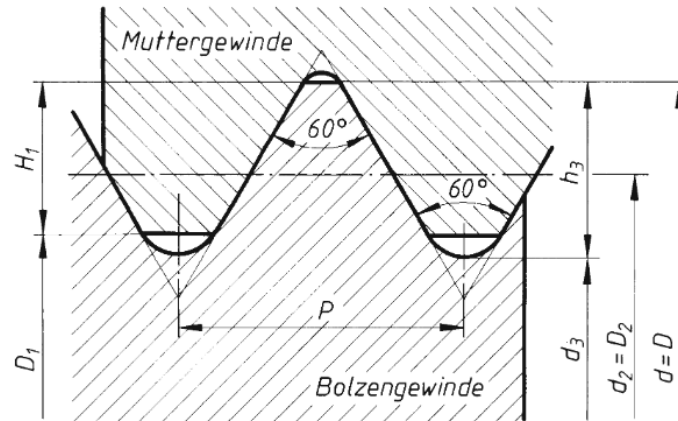


Figure 3.8.: Geometry of the metric thread according to DIN 13 with pitch P and pitch diameter d_2 as calculation parameters - cited from [28]

The pitch angle α is calculated from thread pitch P and pitch diameter d_2 :

$$\alpha = \arctan\left(\frac{P}{d_2 \cdot \Pi}\right) \quad (3.9)$$

The effective friction angle ρ follows from the friction coefficient μ :

$$\rho = \arctan(\mu \cdot 1.07) \quad (3.10)$$

The torque M_T is calculated from pitch diameter d_2 , axial force F_{ax} , pitch angle α and effective friction angle ρ :

$$M_T = \frac{d_2}{2} \cdot F_{ax} \cdot \tan(\rho + \alpha) \quad (3.11)$$

The torque with consideration of the friction M_{TR} on the coupling surface between the threaded spindle (head diameter d_k) and the metallic pressure plate is calculated according to [27] as follows:

$$M_{TR} = F_{ax} \cdot \left(0.159 \cdot P + \mu \cdot \left(0.577 \cdot d_2 + \frac{d_k}{2}\right)\right) \quad (3.12)$$

Computation of Torque - V.3
Measured

| Description | Value | Unit |
|--|--------------|-------------|
| Thread type metric | M3 | |
| Thread pitch P | 0.35 | mm |
| Pitch diameter d_2 | 2.675 | mm |
| Head diameter d_k | 3 | mm |
| Friction coefficient (steel - steel) μ | 0.15 | |

Computed

| Description | Value | Unit |
|--|--------------|-------------|
| Pitch angle α | 2.38 | ° |
| Effective friction angle ρ | 9.12 | ° |
| Torque M_T | 2.91 | Nmm |
| Torque (with surface coupling friction) M_{TR} | 5.48 | Nmm |

Table 3.8.: Computation of the torque for prototype V.3

According to the previous calculation, the selected piezo motor fulfils both the required torque M_{TR} and the required speed v_{MR} . In appendix A.7 the stalling torque M_{LL} of 10 Nmm and the idle speed v_{LL} of 1 rev/s of the motor are listed for comparison.

3.9.2. First setup - prototype V.3 - idealised mounting, 1D

In figures 3.10 and 3.11 the first setup of the prototype is depicted. The square cuff was placed in a polymethylmethacrylate (PMMA, colloq. plexiglass) housing, embedded on all sides and filled with distilled water to achieve an ideal, one-dimensional power transmission system. The CNAP2GO system shall - in contrast to the CNAP Classic system - not implement a 3D-cuff geometry with three compartments for the pressure medium, but a 1D-system with one compartment for the pressure medium. This arrangement is schematically shown in Fig. 3.9. Various pressure curves were generated by controlling the motor via Termite, first in continuous operation and then in step operation. With this setup, only the calculation was analysed, an additional light measurement to generate the OE was not possible. Before the measurement, the contact surfaces and the threaded spindle were oiled to minimise friction losses. The remaining air after filling was extracted from the system ("Venting") in the same way as in the prototype V.0 (see p.26).

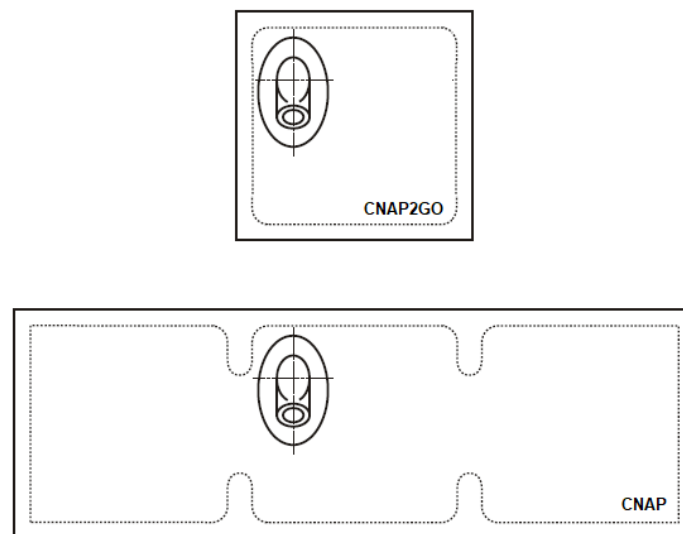


Figure 3.9.: Cuff systems CNAP2GO and CNAP. Above: 1D system of CNAP2GO; Below: 3D system of CNAP Classic.

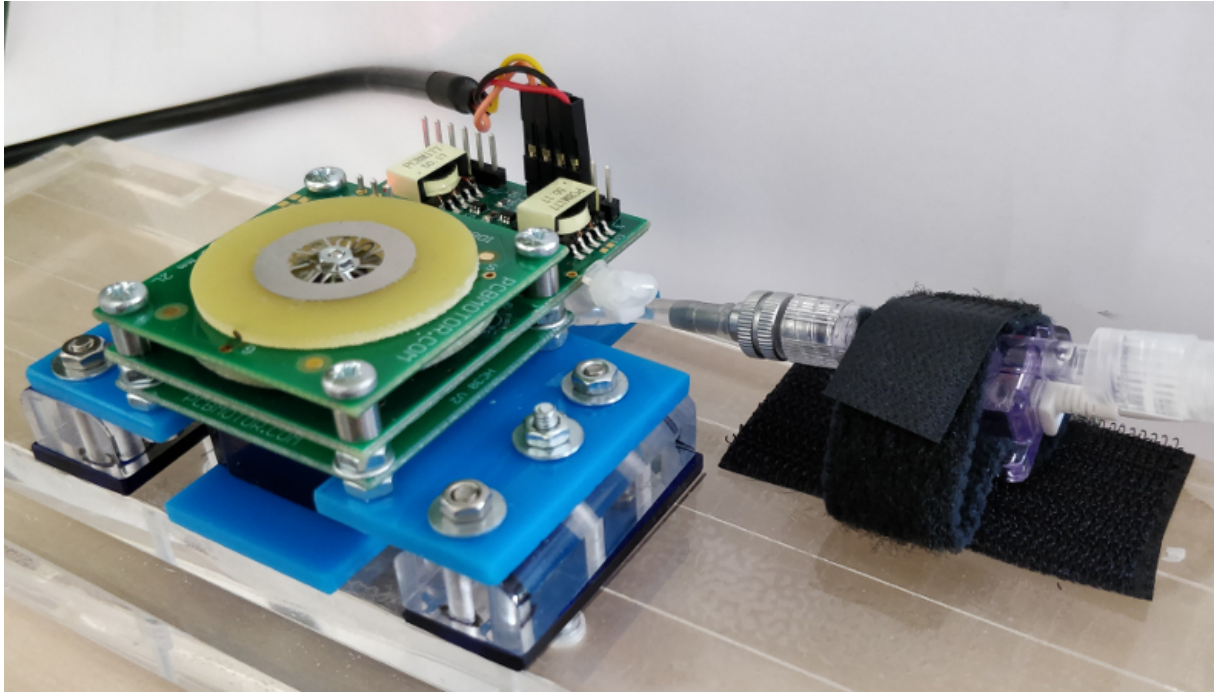


Figure 3.10.: Prototype V.3: First Setup. Left: piezo motor with housing for cuff (darkblue), Right: pressure sensor TSD104A.

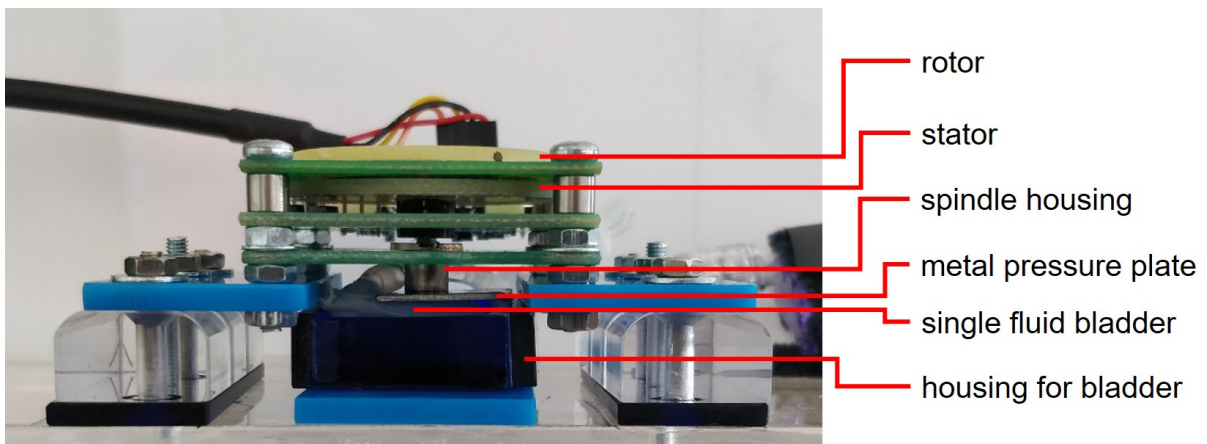


Figure 3.11.: Prototype V.3: First Setup - Front View. Piezo motor with threaded spindle mounted above housing and cuff.

3.9.3. Second setup - prototype V.3 - full opening, 3D

Figure 3.12 shows the front view of the second setup. A classic CNAP cuff system with 3 compartments was used, which is embedded over the entire inner sheath of the housing. The housing was modified so that pressure could be applied onto the finger via the metallic pressure surface by rotating the threaded spindle. The adaption of the cuff housing - depicted in Fig. 3.12 - was the full opening of the top side of the housing. In addition, two finger dummies were tested with this setup, one made of silicone (soft) and one made of polyvinyl chloride (PVC, hard). Those were analysed with regard to differences in the pressure curve to the human finger. Friction losses were also minimised by lubrication with oil. The remaining air after filling was extracted from the system ("Venting") in the same way as in the prototype V.0 (see p.26). The resulting findings from the stepping operation of the motor are shown in the subsequent chapter "Results", which are further analysed in the chapter "Discussion".

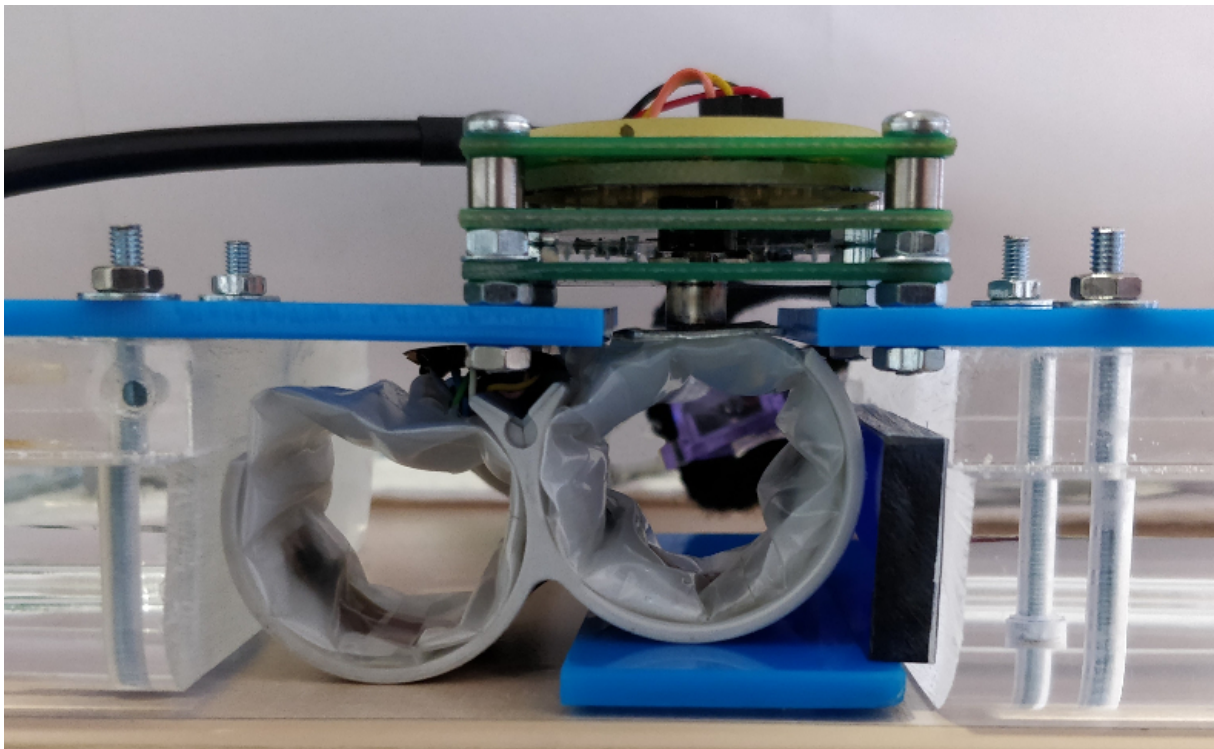


Figure 3.12.: Prototype V.3: Second Setup - Front View. Piezo motor with threaded spindle mounted above CNAP classic cuff.

3.9.4. Third setup - prototype V.3 - fully embedded, 1D

The third setup with the piezo motor is shown in figure 3.13. For schematic illustration, a silicone finger is insterted, which was replaced by a human finger for the measurement. The findings of the previous setups 1 and 2 were taken into account and this setup was adjusted accordingly. The CNAP classic cuff was modified again, but only adjusted geometrically so that the motor spindle could be placed over the metallic pressure surface while still maintaining the mechanical stability of the housing. Before the measurement, the contact surfaces and the threaded spindle were again oiled to minimise friction losses. The remaining air after filling was extracted from the system ("Venting") in the same way as in the prototype V.0 (see p.26). The pressure curves measured by continuous control are shown in the results and are analysed in the chapter "Discussion".

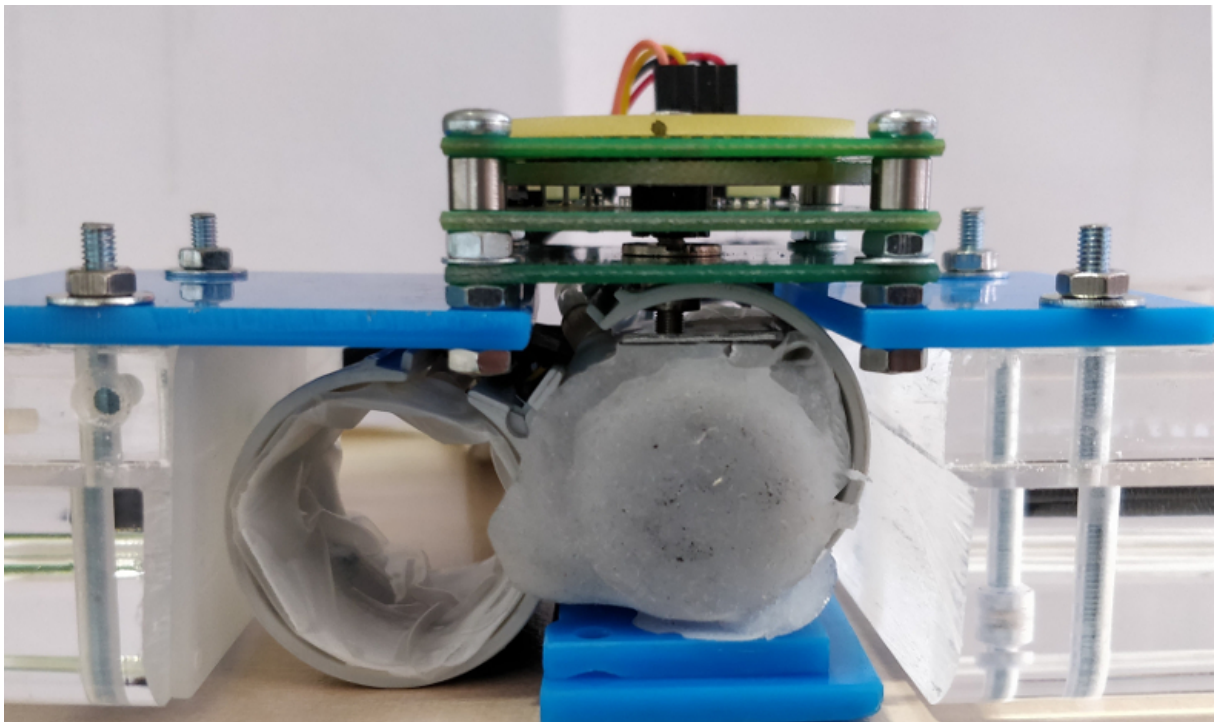


Figure 3.13.: Prototype V.3: Third Setup - Front View. Piezo motor with threaded spindle mounted above CNAP classic cuff.

3.10. Measurement procedure prototype V.3

1. Start of measurement software AcqKnowledge
2. Filling of the syringe with distilled water
3. Connection of the syringe to the system
4. Filling of the measurement system
5. "Venting" the system via negative pressure generation (as mentioned before; residual air sucked into syringe; see p.26)
6. Start of measurement
7. Continuous increase of pressure – simulation of the step function (5 mmHg / 3 beats) via controlling the step motor by the Termite software

3.11. Metrological parameterisation

In order to compare the prototypes with the current CNAP system, the parameters described below were used. The value of the MAP around 120 mmHg, as well as pressure-light curves that are morphologically as narrow as possible, are optimal for the measurement performance described in the theory of the Vascular Control Technique [15], because higher MAP values distort the pressures due to cuff design. The mathematical parameters used for metrological verification are defined analogously to the Gaussian distribution parameters and enable better assessment of the pressure-light curves regarding morphology. For this purpose, the first point where the value of the light signal is greater than 90% of the light signal maximum is to be determined on the left (point X1) and right sides (point X2). The Width of the Oscillometric Envelope (KB) is defined as the difference of pressure values of both points X2 and X1, the Mean Pressure of the Oscillometric Envelope (MD) is defined as mean pressure value in the interval of X1 to X2. For the classical NIBP measurement, 8 mmHg standard deviation is defined according to ISO 81060-2 (standard for intermittent non-invasive sphygmomanometers). Therefore the requirement for good measurement systems for the VCT-Algorithm is a plateau as narrow as possible, the KB-value should not exceed a maximum of 30 mmHg. This is approximately 4 times the standard deviation (\cong confidence interval). Further explanations for metrological parameterisation can be found in the chapter "Discussion".

4. Results

Exemplary plots of the prototypes and final results as boxplots are documented below. The entirety of all plots created can be seen in the appendix. These are also analysed in the chapter "Discussion" with regard to metrological parameters.

4.1. Prototype V.0

Figures 4.1 and 4.2 show the results of the pressure measurement of the first prototype V.0 with a manual approach. The graphs have been exported from the measurement software AcqKnowledge. They show the applied pressure on the finger in mmHg in relation to the absolute measurement time in seconds.

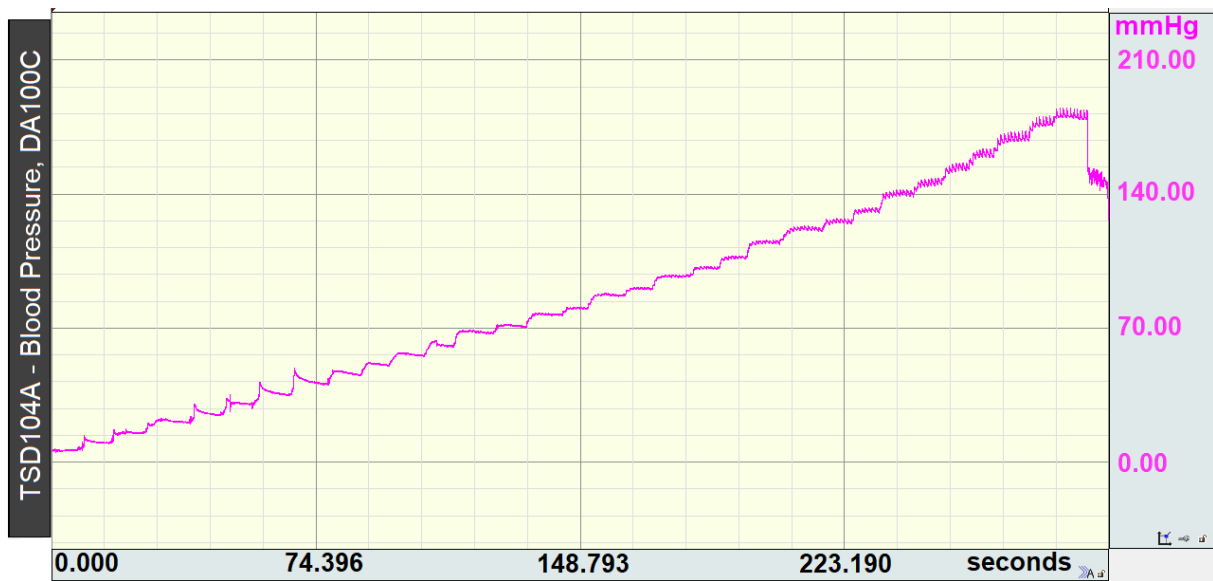


Figure 4.1.: Prototype V.0. Pressure measurement on the index finger of the test subject, fs = 100 Hz.

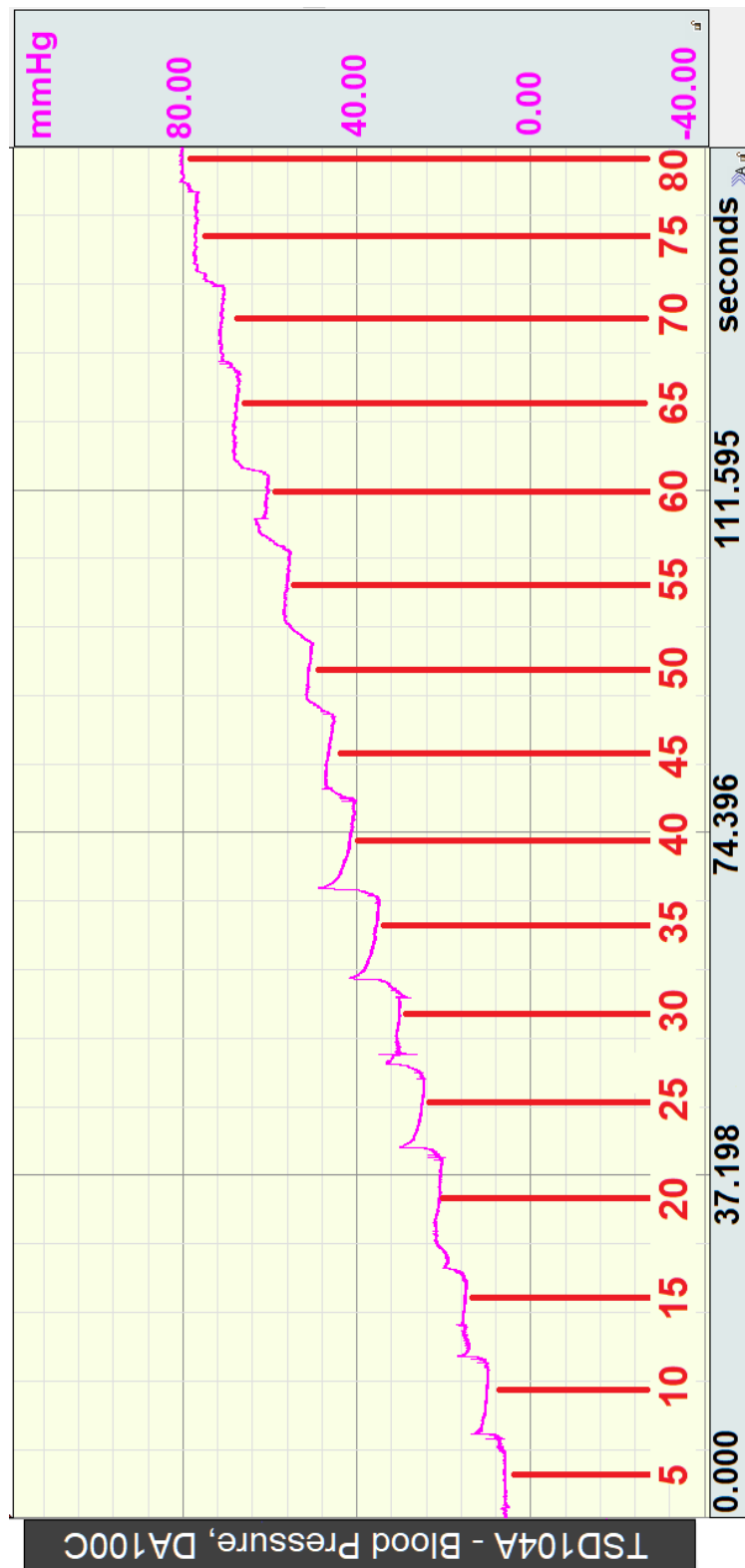


Figure 4.2.: Prototype V.0. Exemplary range between 5 and 80 mmHg, 5 mmHg pressure steps per pressure level, $f_s = 100$ Hz.

4.2. Prototype V.1

For the prototype V.1, the averaged point-line diagram for the OE measured on the index finger of the test subject 1 is shown as example (see Fig. 4.3). The light signal of the oscillations is shown in relation to the finger cuff pressure. The entirety of all the plots produced can be seen in the appendix and is also used for discussion. The parameters explained in the chapter "Methods" KB and MD are depicted as black line (KB) and marked centre (MD) of the black line.

4.2.1. Test subject 1

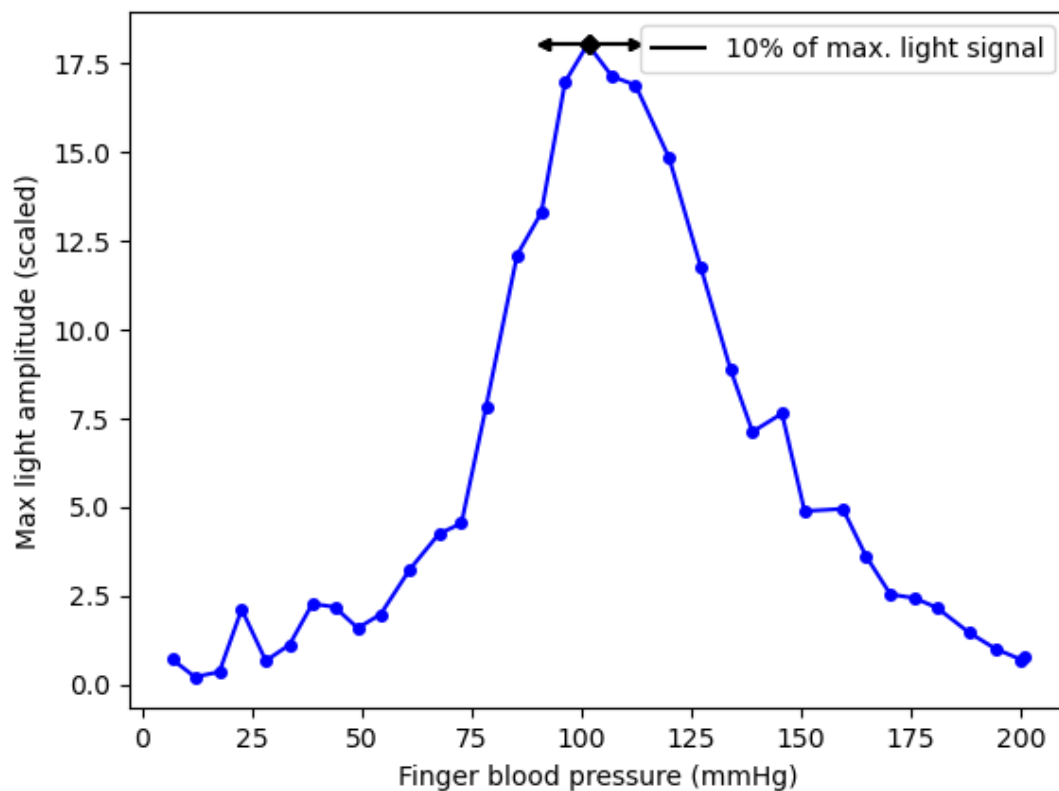


Figure 4.3.: Prototype V.1. Oscillometric envelope as averaged point-line diagram; recorded on the index finger of test subject 1, $f_s = 100$ Hz.

The following table 4.1 shows the results for MD and KB of the first prototype V.1 and calculates median and lower and upper quartile of the total measured values.

| | Index Finger | | Middle Finger | |
|------------------|----------------------|----------------------|----------------------|----------------------|
| | MD in mmHg | KB in mmHg | MD in mmHg | KB in mmHg |
| Subject 1 | 101.9 | 20.9 | 108.5 | 17.7 |
| Subject 2 | 120.2 | 17.8 | 118.2 | 13.0 |
| Subject 3 | 97.4 | 20.9 | 112.8 | 10.9 |
| Subject 4 | 119.4 | 16.0 | 131.3 | 16.1 |

| Total | | |
|-----------------------|----------------------|----------------------|
| | MD in mmHg | KB in mmHg |
| Median | 115.5 | 16.9 |
| Upper Quartile | 103.5 | 13.7 |
| Lower Quartile | 119.6 | 20.1 |

Table 4.1.: Measured values for MD and KB for the prototype V.1.

4.3. Prototype V.2

The full results of the comparative measurement of the prototype V.2 are given in the appendix. Figures 4.6, 4.7, 4.10 and 4.11 are provided for a better visual representation of the physiological phenomena ("fat", "normal" & "spiky" pulses) and for argumentation purposes (General view: pressure curve, oscillations, oscillometric envelope). Those are not visible for all measurements in the appendix. Here, selected measurement results of a test subject are shown, which allow representative comparisons between CNAP and CNAP2GO. Furthermore, the statistical parameters are shown in mmHg: CNAP2GO mean value "MD" and CNAP2GO width "KB". These parameters are shown as black line (KB) and marked centre of the black line (MD).

4.3.1. Test subject 1

Middle finger (left hand: CNAP, right hand: prototype V.2)

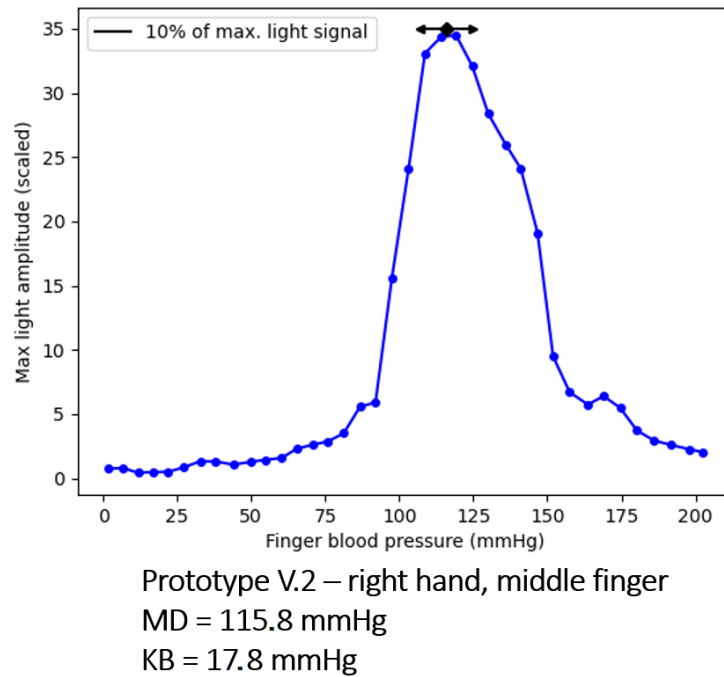


Figure 4.4.: Prototype V.2. Oscillometric envelope as averaged point-line diagram; recorded on the right middle finger of test subject 1, $f_s = 10$ Hz.

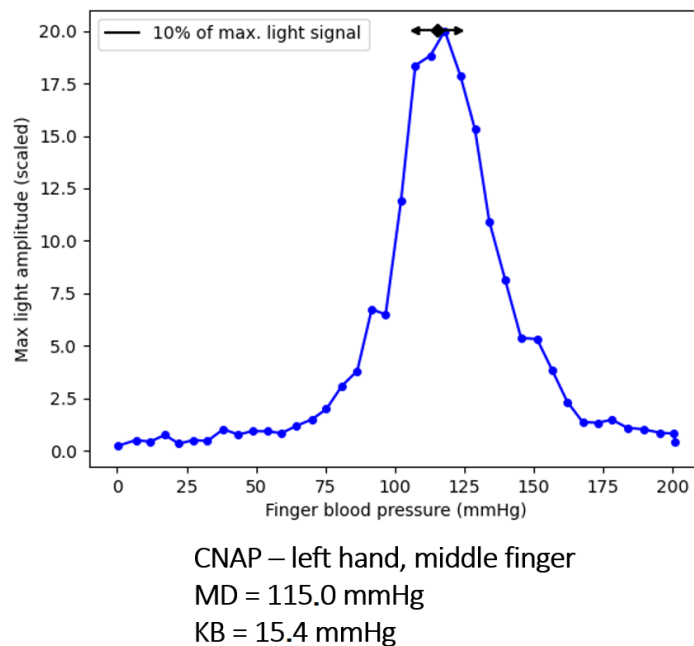


Figure 4.5.: CNAP. Oscillometric envelope as averaged point-line diagram; recorded on the left middle finger of test subject 1, $f_s = 10$ Hz.

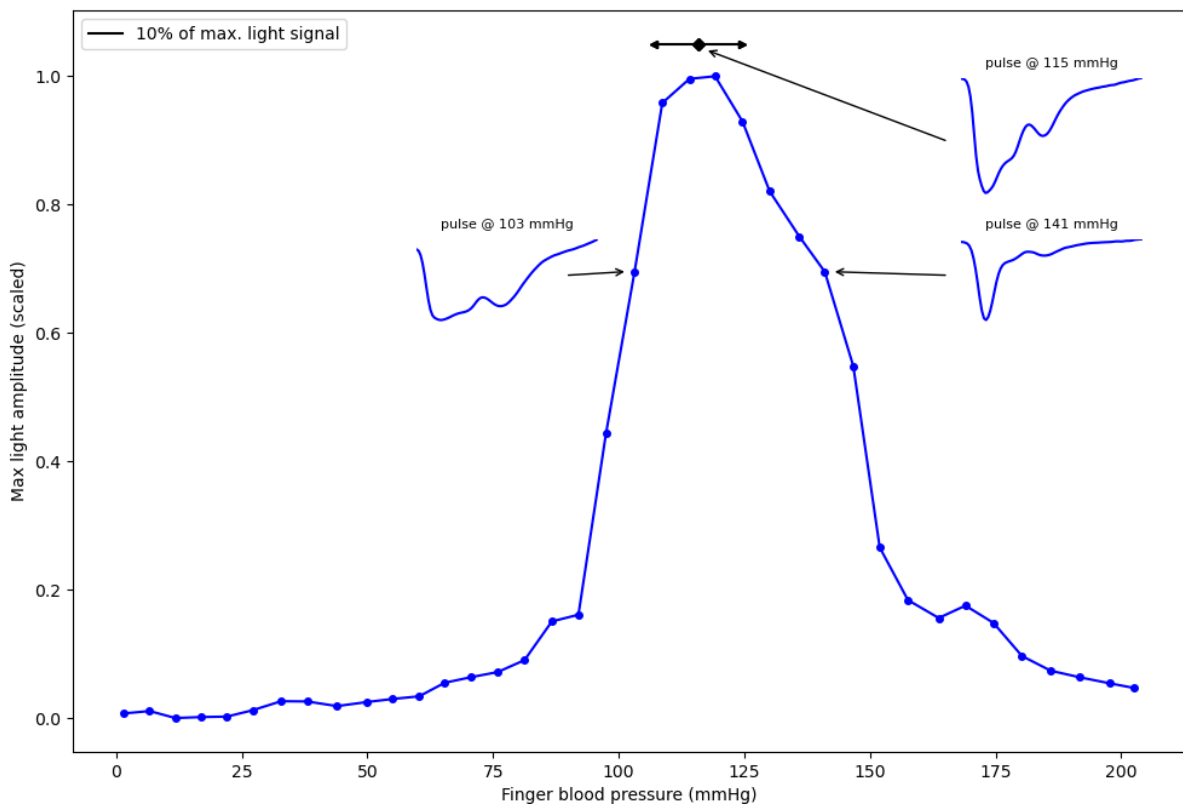


Figure 4.6.: Prototype V.2. Oscillometric envelope as averaged point-line diagram with pulse signal at decisive pressure values; recorded on the right middle finger of test subject 1, $f_s = 10$ Hz.

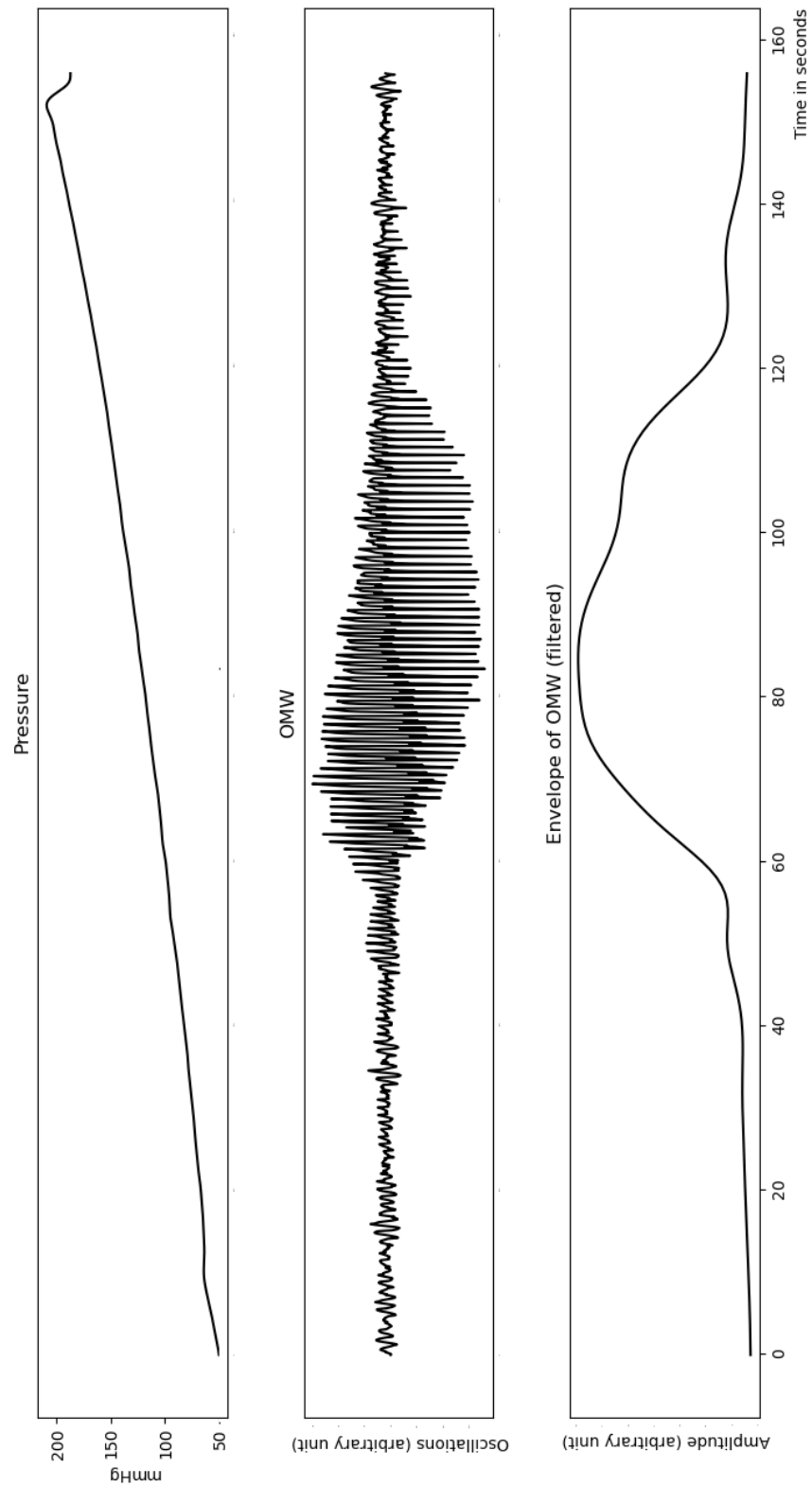
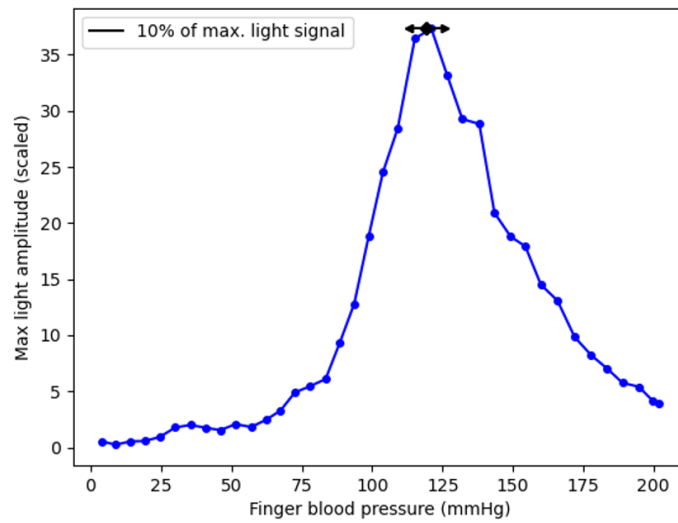


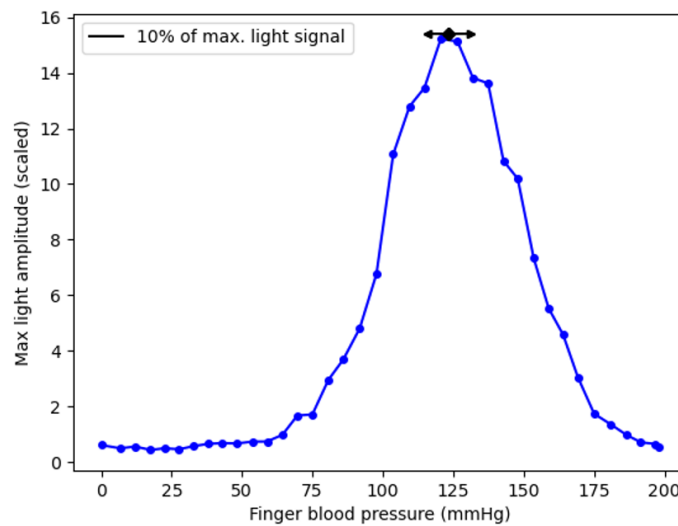
Figure 4.7.: Prototype V.2. Applied pressure, oscillations and oscillometric envelope as averaged point-line diagram; recorded on the right middle finger of test subject 1.

Middle finger (right hand: CNAP, left hand: prototype V.2)



Prototype V.2 – left hand, middle finger
 MD = 119.4 mmHg
 KB = 12.6 mmHg

Figure 4.8.: Prototype V.2. Oscillometric envelope as averaged point-line diagram; recorded on the left middle finger of test subject 1, $f_s = 10$ Hz.



CNAP – right hand, middle finger
 MD = 123.4 mmHg
 KB = 15.4 mmHg

Figure 4.9.: CNAP. Oscillometric envelope as averaged point-line diagram; recorded on the right middle finger of test subject 1, $f_s = 10$ Hz.

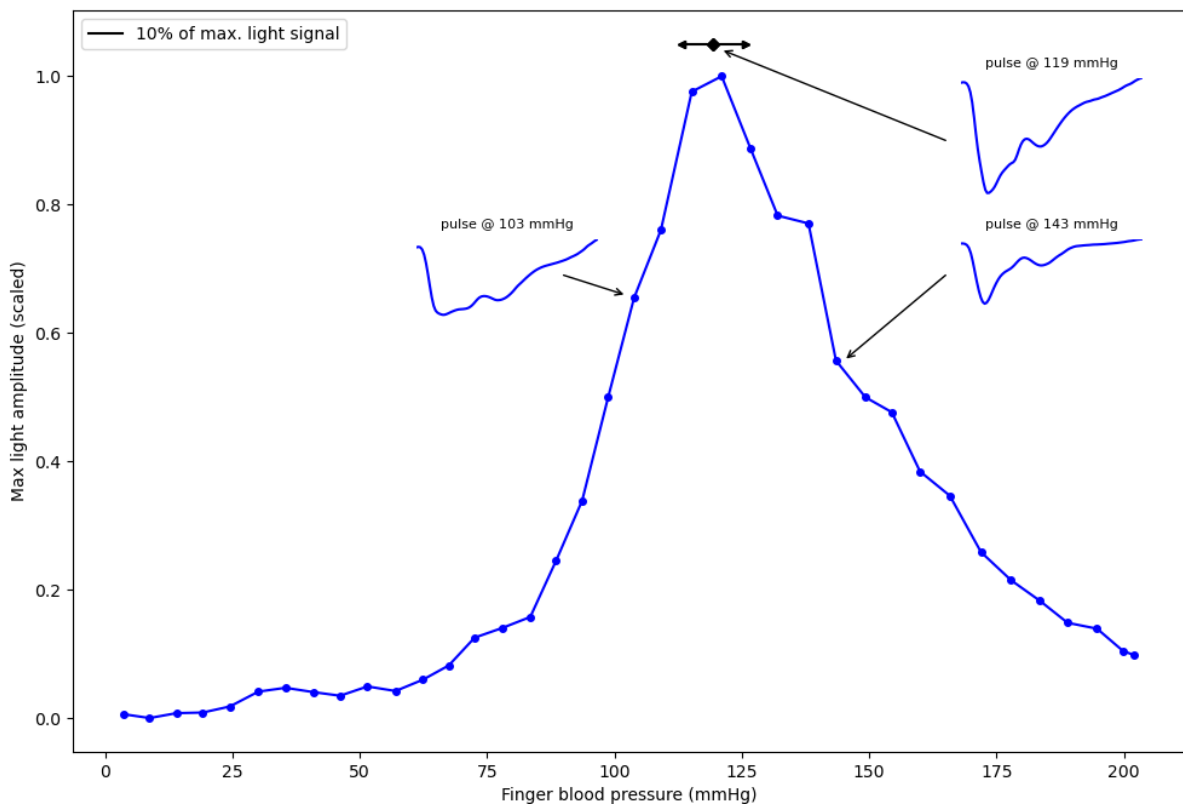


Figure 4.10.: Prototype V.2. Oscillometric envelope as averaged point-line diagram with pulse signal at decisive pressure values; recorded on the left middle finger of test subject 1, $f_s = 10$ Hz.

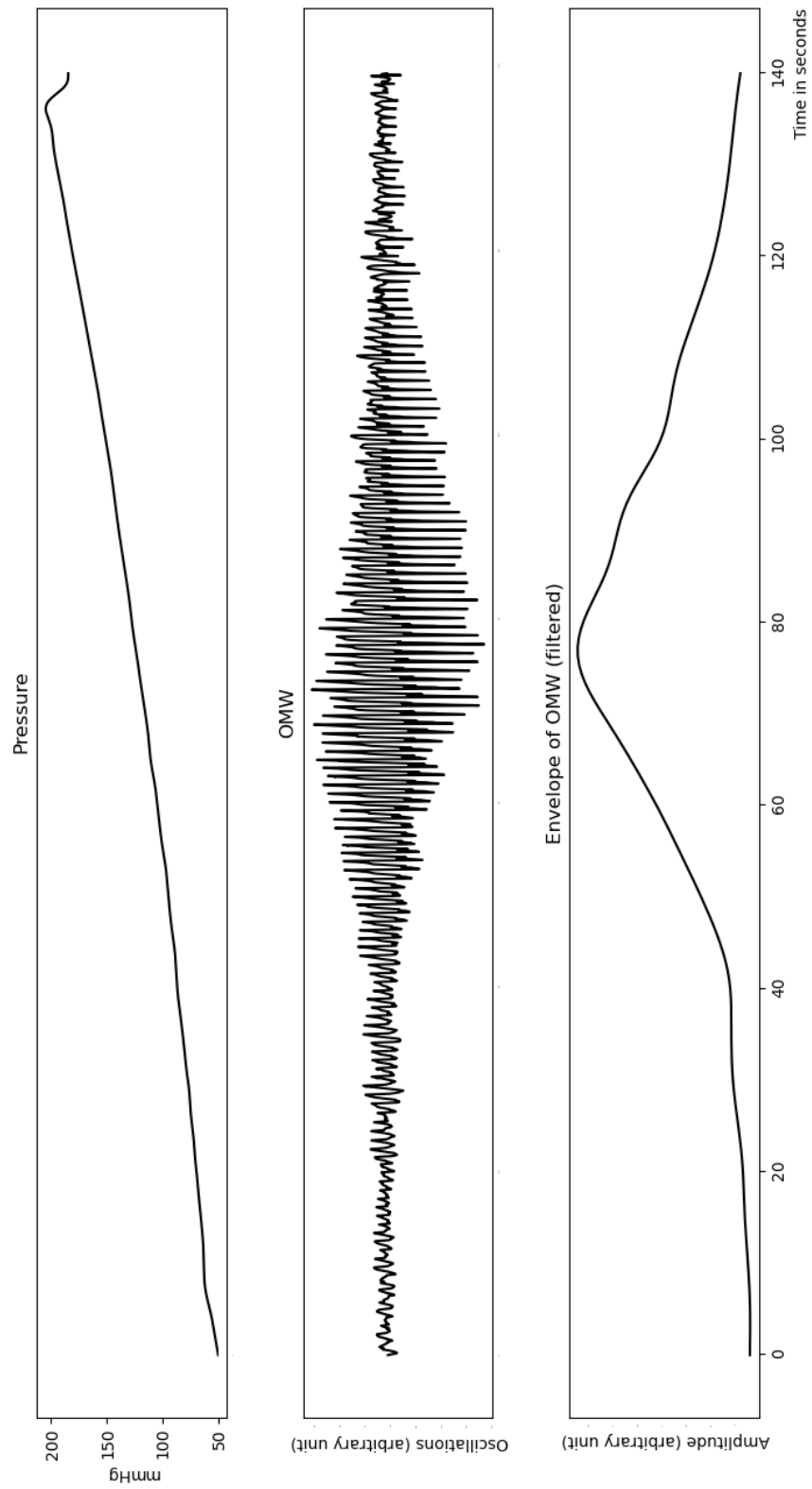


Figure 4.11.: Prototype V.2. Applied pressure, oscillations and oscillometric envelope as averaged point-line diagram; recorded on the left middle finger of test subject 1.

4.3.2. Boxplots

The boxplots in the figures 4.12 and 4.13 show an evaluation of the parameters MD and KB. To enable a representative dataset, no distinction is made between the index and middle finger data (no systematic differences between the different fingers but same test subject), but all values are displayed together. This combination of both datasets is deliberately chosen because, similar to a clinical trial, subgroup analyses can then be carried out in further steps. However, the comparability of CNAP2GO and CNAP can already be argued with this analysis and is presented in the chapter "Discussion". The measurement of the left index finger failed at test subject 5 due to an internal measurement error in the beat detection, thus only n=27 values are available.

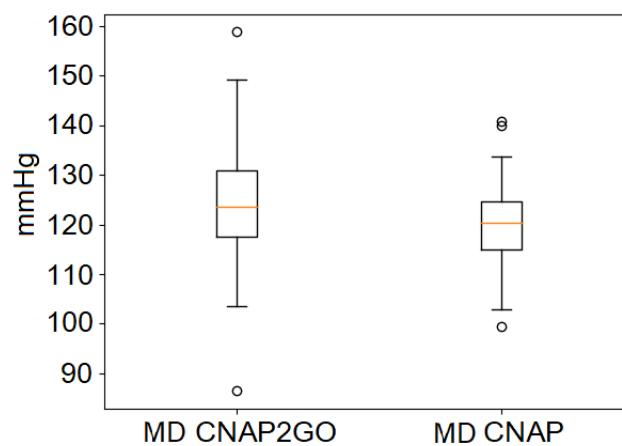


Figure 4.12.: Prototype V.2. Boxplot for MD in comparison: CNAP2GO and CNAP Classic.

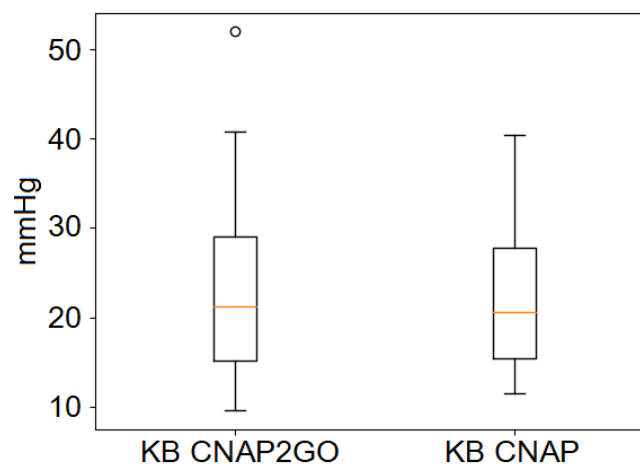


Figure 4.13.: Prototype V.2. Boxplot for KB in comparison: CNAP2GO and CNAP Classic.

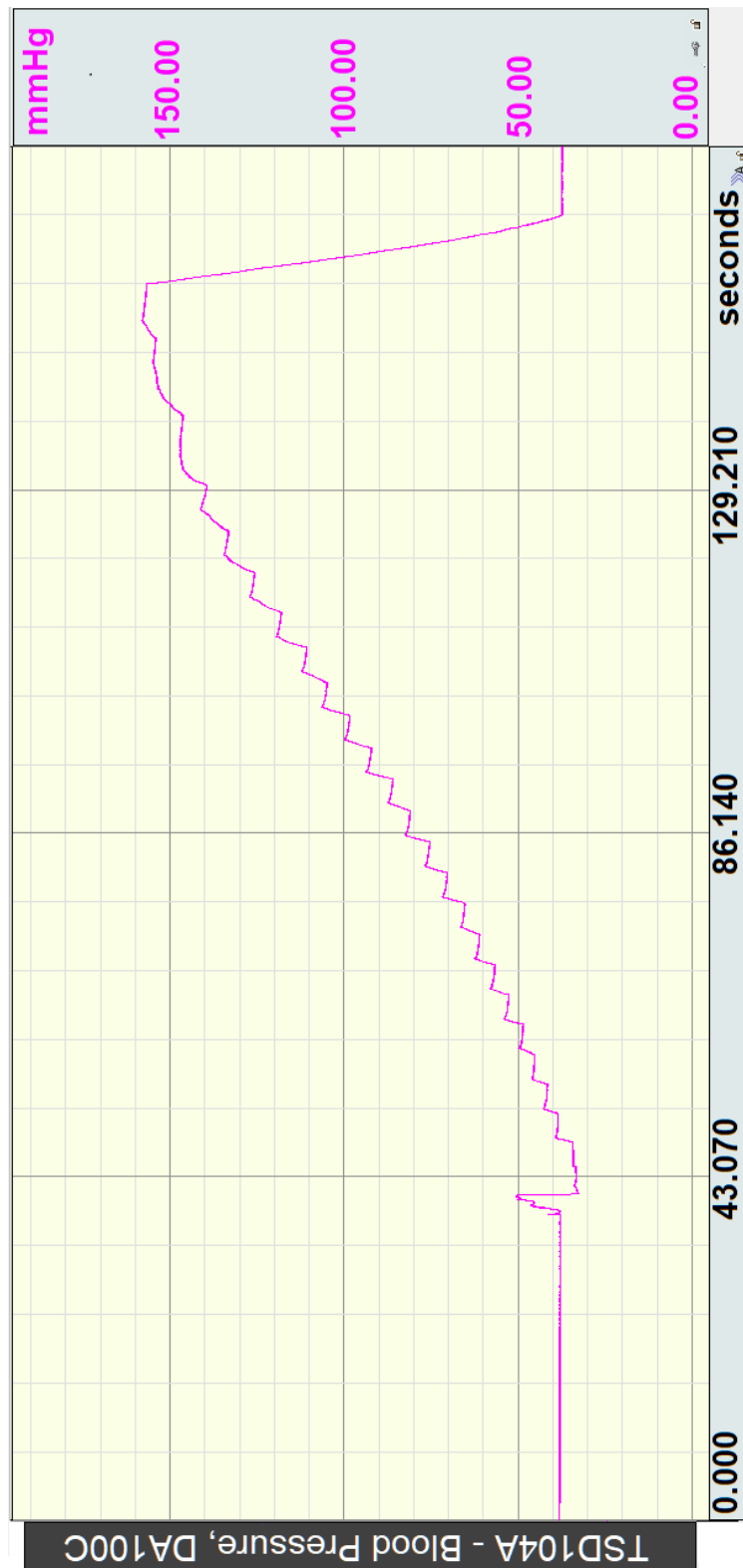
4.4. Prototype V.3

4.4.1. Results of first setup - V.3

Figures 4.14 and 4.15 show the pressure curves of the first setup of prototype V.3. The required step curves were generated by the step control of the PCB motor. In figure 4.14 the measurement using 15 x 100 steps (180° rotation of the motor) followed by a 3 second pause is shown. The achievable number of steps up to the stalling of the motor was 11 x 100 steps. For figure 4.15, a smaller step size of 30 x 50 steps (90° rotation of the motor) followed by 3 seconds pause was chosen. Here, the number of steps actually achieved up to stalling of the motor was 23 x 50 steps. The total number of steps was therefore 1150 steps, according to motor data (see appendix, 200 steps per revolution, M3 x 0.35 threaded spindle) this corresponds to a stroke of 2.01 mm. The calculated maximum achievable pressure p_e of 160 mmHg is almost reached in the first setup, whereas the relevant pressure difference is 120 mmHg.



Figure 4.14.: Prototype V.3. First setup. Control with 11 x 100 steps, between the 100 steps 3 seconds stop. Pressure increase of 38 to 158 mmHg



4.4.2. Results of second setup - V.3

The figures 4.16, 4.17 and 4.18 show the pressure curves of the second setup. In the first graph 4.16 on the human finger, 25 x 50 steps (90° rotation of the motor) were utilised for controlling the motor with 3 seconds pause between the 50 steps. After 25 steps the pressure in the cuff dropped slightly, as can be seen in the graph as red marker. Additionally, 4 x 50 steps could be added until stalling of the piezo motor, reaching a total number of steps 29 x 50. The measured pressure values are in the range of 45 to 78 mmHg. For the finger dummy made of PVC with a higher degree of hardness a control of 15 x 100 steps (180° rotation of the motor), 3 seconds pause was implemented, the pressure curve in 4.17 runs from 30 to 55 mmHg (until stalling of the motor). In figure 4.14 the pressure curve of the silicone finger dummy can be seen. A maximum iteration of 24 x 50 steps (90° rotation of the motor) with 3 seconds stop until stalling of the motor was possible. The pressure curve shows values from 25 to 50 mmHg.

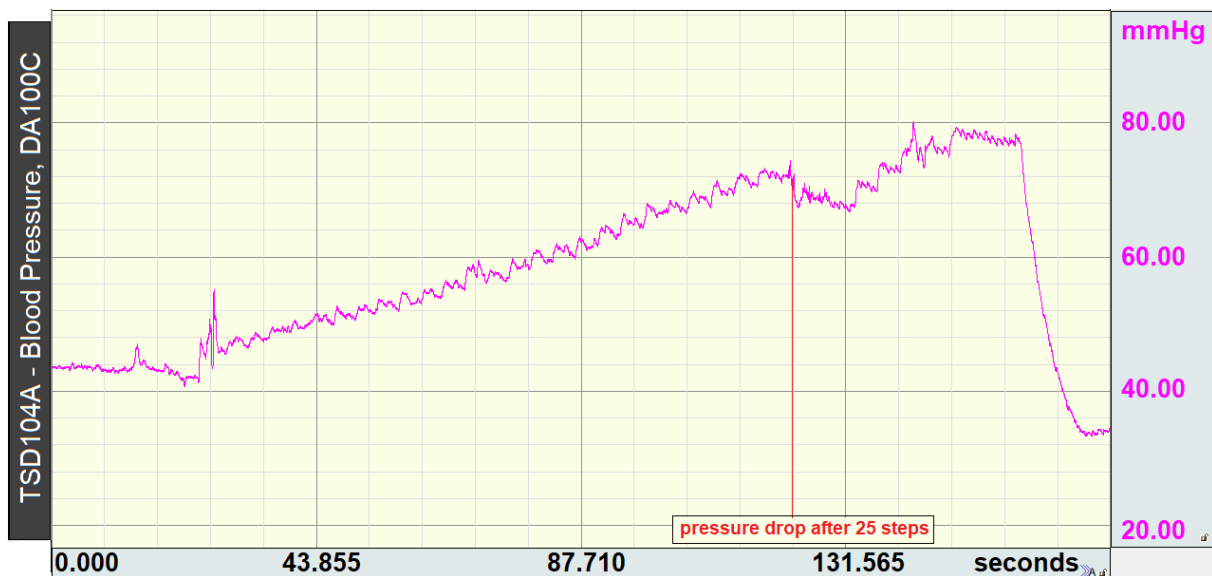


Figure 4.16.: Prototype V.3. Second setup. Control with 29 x 50 steps, between the 50 steps 3 seconds stop. Pressure increase on the human finger from 45 to 78 mmHg.

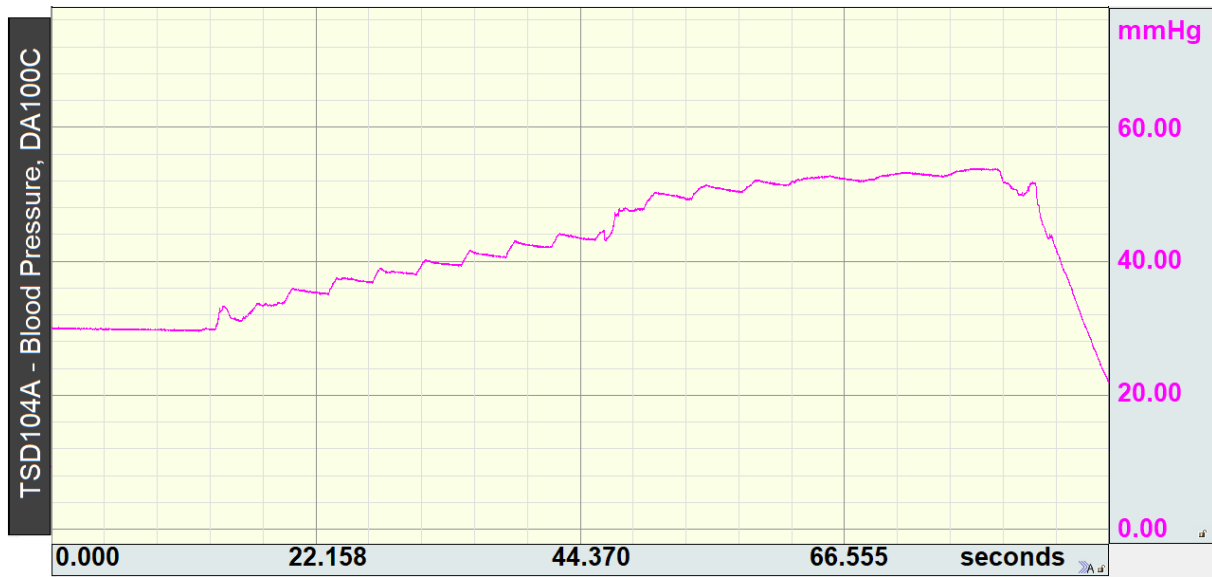


Figure 4.17.: Prototype V.3. Second setup. Control with 15 x 100 steps, between the 100 steps 3 seconds stop. Pressure increase on the finger dummy of PVC from 30 to 55 mmHg.

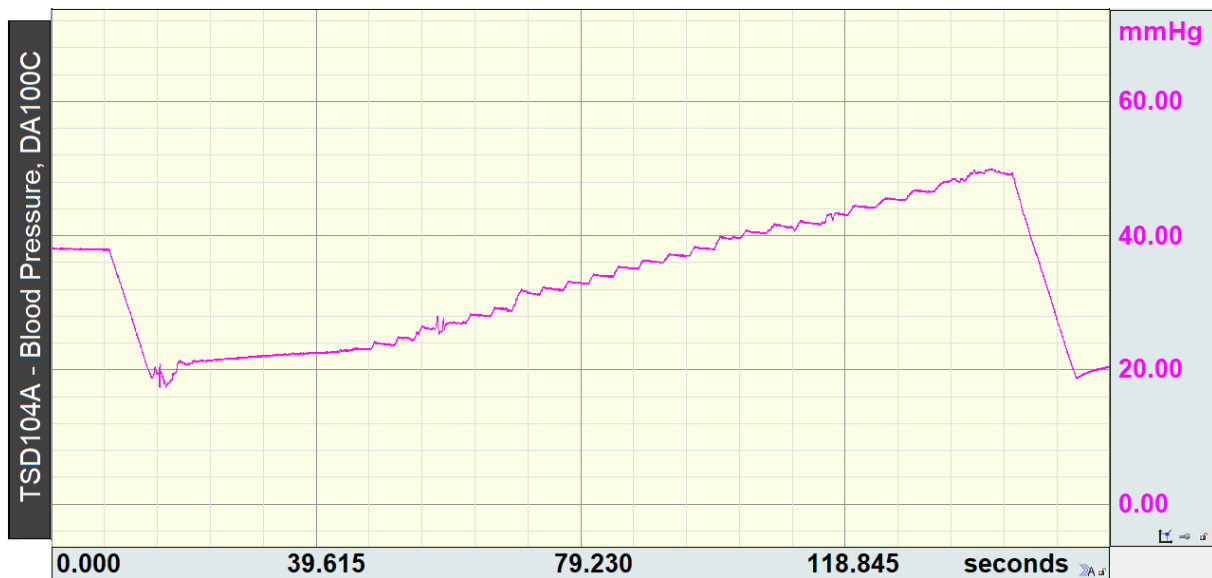


Figure 4.18.: Prototype V.3. Second setup. Control with 24 x 50 steps, between the 50 steps 3 seconds stop. Pressure increase on the finger dummy of silicone from 25 to 50 mmHg.

4.4.3. Results of third setup - V.3

The results of the third setup are shown in the following figures 4.19 and 4.20. Two different starting points were chosen. The first diagram starts at 30 mmHg and stops with stalling of the motor at approx. 80 mmHg. As control setting for the PCB motor, 30 x 50 steps with 3 seconds pause each, as in the previous setups, were used. The second diagram 4.20 starts at 60 mmHg and the maximum achievable pressure value is approx. 120 mmHg. Again, 30 x 50 steps with a 3 second pause each were necessary to create the desired step function. Additionally, further iterations (in 50 steps each) up to the power limit of the motor (motor stops rotating) were added to both variants, thus, the graphs show more than 30 steps. The motor current averaged over all steps was 365 mA, the motor voltage was set to 3.5 V.



Figure 4.19.: Prototype V.3. Third setup. Control with 30 x 50 steps (increase to 34 x 50 until motor stalling), between the 50 steps 3 seconds stop. Pressure increase from 30 to 80 mmHg.

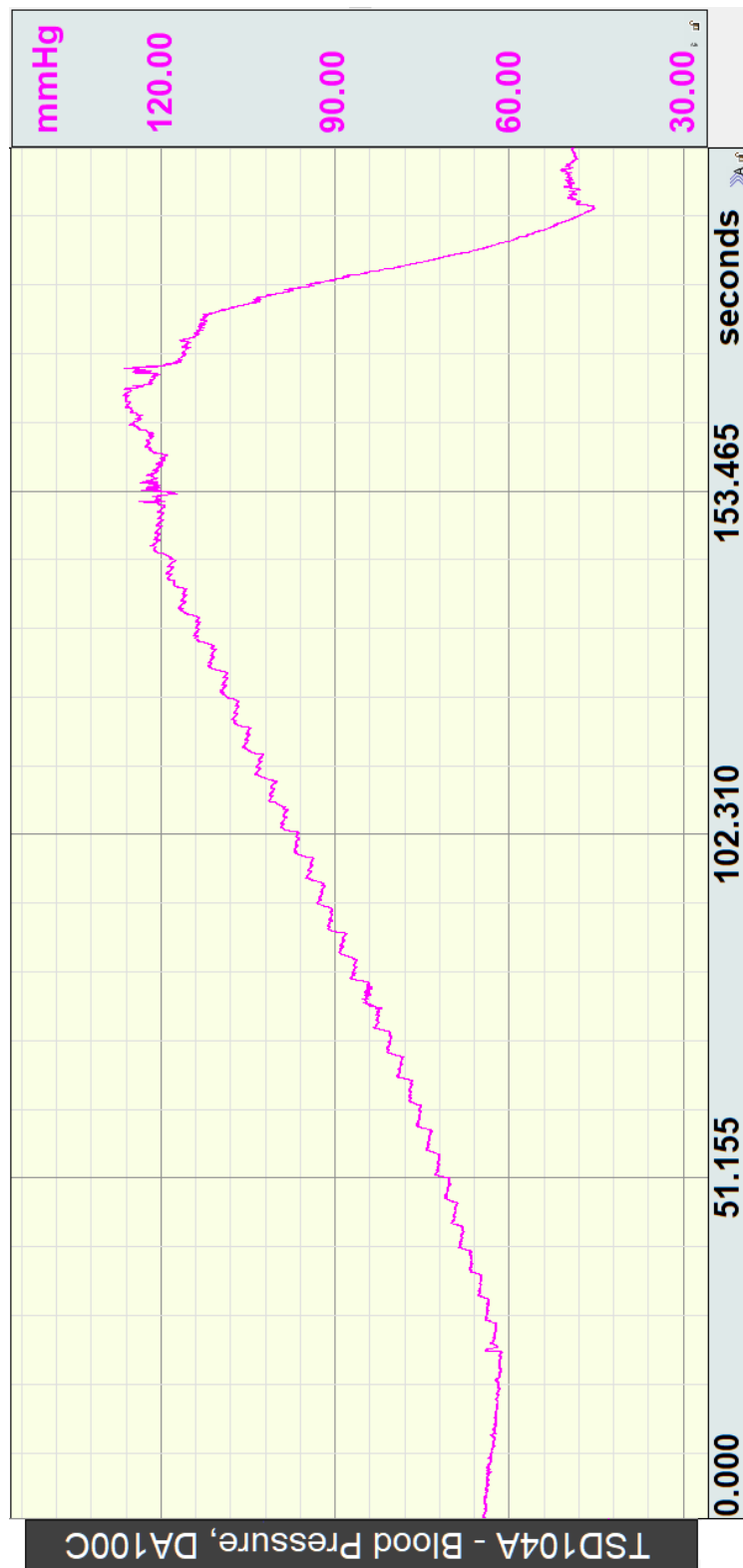


Figure 4.20.: Prototype V.3. Third setup. Control with 30 x 50 steps (increase to 32 x 50 steps until motor stalling), between the 50 steps 3 seconds stop. Pressure increase from 60 to 120 mmHg.

5. Discussion

In the following, the results are discussed in terms of feasibility of the CNAP2GO concept. First, the particular topic of the fluid component is addressed, followed by an extended explanation of the selected mathematical parameters as a criterion for comparison with the CNAP classic system. The main part of the discussion focusses on the three prototypes created - each in a general form (discussion of the setups, assumptions, etc.) and specific to the respective results. Finally, further considerations for future prototypes are given and the objectives achieved are described in the conclusion.

5.1. General discussion

5.1.1. Fluid component & basic controlling assumptions

Due to the miniaturisation and the project specifications for CNAP2GO, suitable fluids that are as incompressible as possible were researched in the first step to enable the application of pressure in the existing CNAP system. Distilled water combines, as already mentioned in the chapter "Preamble", important properties with regard to the feasibility and was used for all prototypes after consultation with experts. A difficulty when using fluid systems was the correct venting. Despite the prefilling of the entire connection system of each prototype, the cuff could only be filled without air to a limited extent. The residual air bubble was sucked out of the pressure system by negative pressure into the syringe in order to create the most ideal fluid system possible between the cuff and the pressure sensor system. Furthermore, the use of a degassed fluid (heating of the water above boiling temperature, cooling and fluid withdrawal from the same fluid container) was dispensed in order to be able to design the concepts more rapidly and adaptable with regard to the measurement setup. The problem of venting had a negative effect on the properties of the pressure fluid, since both dissolved (absorption process) and undissolved air (dispersion process) occur in the hydraulic system [16].

These negative effects are sufficiently suppressed by the design of the prototypes, because before start-up of the measurement, the air in the entire system was sucked ("vented") into the syringe by negative pressure and shortest possible hydraulic lines were used. The short lines as well as the low flow velocity of the fluid to increase pressure (see the calculation of the flow rate in the chapter "Methods") enable low flow resistance and thus low pressure loss in the system during pressure application. Furthermore, at these low flow speeds, the influence of cavitation phenomena, explosions or implosions in the micro range is negligible.

5.1.2. Metrological assumptions

For further explanation and argumentation from the chapter on "Metrological Parameterisation" the basic metrological assumptions are discussed here. The metrologically and control engineering relevant range of $\pm 10\%$ of the maximum light signal is ideally very narrow. This results in an accurate or inaccurate measuring system - in simple terms, the system resembles a sharp or blunt pencil, enabling accurate or inaccurate drawing. Figure 5.1 shows this phenomenon. The steep, slim curve enables precise measurement of the MAP, the wider, flatter curve with a larger plateau leads to an unprecise measurement. The essential parameter for the size of the plateau is the "Width of the Oscillometric Envelope (KB)".

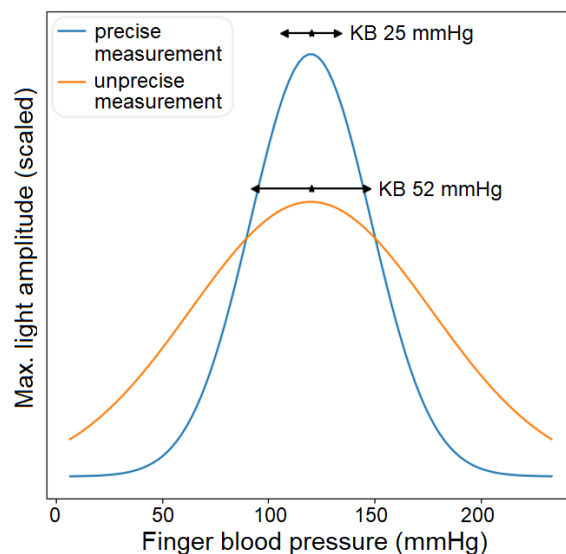


Figure 5.1.: Metrological assumptions. Schematic Illustration of the KB values of a precise and an unprecise measurement.

5.2. Prototype V.0

5.2.1. General discussion V.0

The prototype V.0 was designed as a first empirical experiment after a literature search to test the fluid technology approach. Before the expert meeting at Institute for Fluid Mechanics and Heat Transfer (ISW), tests were carried out with both distilled water and ultrasonic gel and attempts were made to reproduce the required pressure curves.

The use of ultrasound gel led to a metrological problem, thus, no data are shown in the results: The filling of the cuff compartments in the lower pressure regions was not uniformly. The entire system was filled with gel as much as possible. The geometry of the cuff (seams of the three compartments see Fig. 3.9), however, caused an unsteady distribution of the gel and as a consequence a discontinuous pressure distribution. It could not be guaranteed that the entire cuff was evenly filled. Venting of the system was not possible, the gel enclosed the residual air as many small air bubbles. Furthermore, a pressure increase was already measured by filling the pressure sensor due to the smaller diameter of the sensor. Pre-filling the entire connection system (lines from syringe to sensor and through sensor to cuff) caused offset errors in the range of 20 mmHg due to the sensitivity of the pressure sensor. Therefore, due to internal friction effects in the lines, the geometrical shape of the cuff and the viscosity of the gel, pressure could be increased at the sensor, but this pressure was not transmitted in the cuff. The increase of 5 mmHg per 3 seconds was difficult to adjust with the gel, because the pressures already increased more than 10 mmHg with the smallest rotation of the screw clamp. The associated reaction time of the system is one positive aspect.

Other hydraulic fluids mentioned - such as mineral oils - were excluded due to contamination of the pressure sensor and the cuff. Based on the previous observations, after consultation at the ISW, distilled water was chosen as the pressure medium for the following iterations.

5.2.2. Discussion of results V.0

The resulting pressure curves showed promising results and were the starting point for further development in prototype V.1 by combining the CNAP components. It should be mentioned that even with this rudimentary, rough mechanical setup V.0, the pressure curves with 5 mmHg steps were sufficiently well reproducible to continue this approach. In figure 4.2, an overshoot can be seen in the pressure range of 5 to 40 mmHg. This was necessary with the adjustment of the screw clamp to reproduce 5 mmHg steps, because in this aforementioned pressure range the cuff was not yet completely filled. Above pressure values of 40 mmHg, a proficient coupling of the cuff and the finger was achieved and the pressure steps became flatter. The sensitivity of the system and in particular the sensitivity of the sensor is clearly shown in figure 4.1, whereas above pressure values of 80 mmHg even the individual pulses (visible as small oscillations at every pressure level) can be detected.

5.3. Prototype V.1

5.3.1. General discussion V.1

As an extension of prototype V.0, the light signal was additionally recorded via the CNAP components. The slow control as well as the coarse mechanical setup with the screw clamp aimed for the measurement of plausible results and aimed to point out metrologically critical points of the construction. Thus, with regard to the prototype V.2, the main focus was on confirming the functionality and combinability with the CNAP system. The combination of the light measurement with the CNAP system worked perfectly when the CNAP cuff was carefully prepared. The reproducibility of the results - the reproducibility of equal step-like pressure increases by means of this manual, coarse mechanical screwing movement - could not be guaranteed.

5.3.2. Discussion of results V.1

The resulting curves (Fig. 4.3 and B.6) showed satisfactory results of the oscillometric envelope. The MD-values and KB-values from the metrological parameterisation were within the required tolerances. The additional graphs - shown in the appendix - depicted similar results, however, the second measurement of test subject 3 and the results of test subject 4 illustrate the metrological imprecision of this setup. Despite the careful measures taken to reduce movement (clamping of the cuff and the actuator unit "syringe"), artefacts occurred in the measurement curves. This was particularly the case when the test subject spoke, moved the inserted finger in the cuff or slightly changed the sitting position during the measurement.

By changing the orthostatics, the pressure coupling or the coupling of the light signal, this induced a biological artefact in the recorded light signal. The manual generation of the pressure curve required a high degree of concentration and was another critical point that significantly influenced the entire measuring process. The entire system had to be moved as smoothly as possible and the grip on the mechanical actuator was not allowed to be released at any pressure level in order to reproduce the step curve correctly. These pressure curves (Fig. B.3 - B.9) could not facilitate the correct measurement up to 200 mmHg, but only until 160 mmHg. However, due to the relevant controlling area, which is explained in the chapter "Methods", these curves could also be used for the CNAP2GO principle. The quality of the results was sufficiently performant to continue with concept V.2.

5.4. Prototype V.2

5.4.1. General discussion V.2

Prototype V.2 was created to ensure the thorough, reproducible measurement and optimisation of the measurement results. Theoretical performance assumptions and miniaturisation of the system were secondary factors in this step. The aim was a qualitative & quantitative improvement of the results and a statistically more descriptive measurement.

The use of the syringe pump was necessary for precise dosing and pressure increase, since the setup with the screw clamp did not provide a precision mechanical actuator for reproducible results. The theoretical flow rate (see table 3.3) was calculated up to 25 mmHg at 300 ml/h and up to 65 mmHg at 150 ml/h, but the syringe pump only provides a maximum flow rate of 99.9 ml/h. This limiting factor was accepted as the relevant range (see table 1.1) of 65 mmHg to 200 mmHg was optimally covered with a delivery rate of 45 ml/h.

Due to the mechanical function of the pump, the pressure curves generated were now continuous curves rather than step curves. The slow control of the CNAP2GO concept [15] aims at measuring the oscillometric envelope and the mean arterial pressure also with continuous pressure signals - the only disadvantage for the current concept is the more complicated evaluation in the post-processing of the data. The filters in the evaluation of the results were applied to suppress low-frequency interference from the oscillations (e.g. offset due to temporally fluctuating finger coupling) or high-frequency fluctuations in pressure (e.g. pulse signal at high pressures visible on the signal). The high order of the filters was needed to achieve the steepest possible drop at the cut-off frequency and thus the highest possible resolution or suppression in this range.

5.4.2. Discussion of results V.2

The resulting graphs, shown in the preceding chapter, indicated similar oscillometric envelopes in comparison to the simultaneously tested CNAP classic system. This was also depicted by the pulse signals - as can be seen in figures 4.6 and 4.10. Pressure values below the MAP resulted in "fatter" pulses with lower light amplitude, pressure values above the MAP lead to "spikier" pulses with lower light amplitude as well - thus, this is comparable to the in the "pre-print" (see [15]) and in the chapter "CNAP2GO & Volume Control Technique (VCT)" presented measuring principle. The V.2 concept is therefore comparable with the CNAP classic system.

The measurement results in the figures 4.12 and 4.13 showed that prototype V.2 possessed the same median, but larger boxes or a wider distribution of mean pressures in comparison to the CNAP classic system. The mechanics of the setup was a possible factor in the marginally poorer result of the prototype (see additional graphs of oscillometric envelopes in the appendix). The measurement data generated ought to be used as indicative or exemplary data for the comparability with CNAP classic system. However, the boxes for the KB values (= most important parameter) were almost identical. Resulting curves with MD-values as shown in figure B.30 are to be regarded as outliers and were caused by artefacts already discussed at prototype V.1 such as speaking of the test subject and movement artefacts of the measurement setup. The level of the mean pressures was metrologically uncritical, as calibration would have been necessary, for example, by measurement on the upper arm. The cuff used for the comparative measurement in the prototype V.2 already featured optimised materials - a softer but stiffer film - and geometry compared to the CNAP cuff currently available on the commercial market. All relevant parameters of the cuff (Prototype V.2 and comparison measurement CNAP) were at least 10 mmHg below the values of the CNAP cuffs currently available on the market.

Comparable scientific studies confirming the "proof of principle" of a novel approach for determination of vital parameters such as heart rate and blood pressure use a sample size of $N=1$ [29, 30, 31]. The measurement series of this work was carried out with a sample size of $N=7$ subjects at 4 measurement points each (28 measuring points in total), in order to achieve a statistically higher significance with regard to comparability with the CNAP system.

5.5. Prototype V.3

5.5.1. General discussion V.3

The theoretical considerations for prototype V.3 confirmed the usability of the selected piezo motor. The maximum achievable pressure p_e of 160 mmHg from the calculation in the chapter "Methods" sufficiently covered the core range of measurement from 40 - 160 mmHg (see table 1.1 - Grade 3 Hypertension). The control software made it possible to apply a step-shaped pressure curve, whereas the various measurement setups had a decisive influence on the course of these curves. The piezo motor was elected due to the advantage of the low weight and the available holding torque. Comparable stepper motors - also with hybrid technology (stepper motor has holding torque) - are heavier and unsuitable for miniaturisation as a "wearable device" due to their external geometry and power consumption (see NEMA8 motor; 12V - 0.6A per coil bipolar (Nanotec Electronic GmbH & Co. KG, Feldkirchen, Germany)). The alternative of a piezoline actuator is discussed using the N-310.10 NEXACT[®] OEM-miniature linear actuator (Physik Instrumente GmbH & Co. KG, Karlsruhe, Germany).

The following information was obtained directly from Physik Instrumente GmbH. These actuators are without stepping function, the movement of the rotor is generated by several piezo elements in the actuator. The internal friction conditions change the step size per control cycle. Therefore an exact control is necessary to implement a stepping function. The lifetime is designed for a distance of 5 km overall stroke, but due to the friction drive these actuators are not designed for continuous use in a 24 hour time cycle. These aspects and the - for a "consumer product" - high price without control (approx. 1400€), with control (1 Vp-p sin/cos differential) (approx. 2800€) or alternatively only with an open-loop driver and individually developed controller (approx. 2100€) are excluding factors for CNAP2GO.

5.5.2. Discussion of results V.3

The three measurement setups were designed in a way that first a preferably ideal one-dimensional force transmission system was tested, then the CNAP cuff was analysed for adaptability and finally, the CNAP2GO concept with single-fluid bladder was implemented.

During the third measurement setup, the required microstep time was recorded, the resulting real speed of the motor under load was calculated from this and is processed here as the subject of the discussion. It is important to note that all resulting curves were started from a pressure level of > 0 mmHg, as the system already generated a certain pressure increase with filling and coupling to the threaded spindle through the metallic pressure surface. The different controls of 50 or 100 microsteps were chosen for test purposes, whereby an increase of approx. 5 mmHg could be achieved with 50 microsteps in the first setup. For this reason, a pure 50 microstep control was chosen for the third setup to implement the CNAP2GO concept. Another finding from the measurement setups was that the pressure curves, depending on the offset (pressure level > 0), resulted in a variable pressure difference - and thus different maximum pressures - until the motor is stalled. The more rigid the entire setup was designed, the higher were the achievable pressure differences from start pressure to end pressure.

In the first setup (cf. chapter "Methods": "idealised mounting, 1D") the friction of the mechanical components (threaded spindle, contact surfaces) was acoustically perceptible already from 100 mmHg onwards due to the force development, despite the lubrication. The stroke of the threaded spindle was only 2.01 mm before the motor finally stalled. The maximum achievable pressure difference was 120 mmHg (start: 38 mmHg - end at full load: 158 mmHg). The theoretically achievable pressure difference Δ_{pT} is calculated for this setup. For the following measuring setups, it can be determined in the same way. Δ_{pT} is computed with presumed sufficient motor power and full stroke of 4 mm as:

$$\Delta_{pT} = \frac{4 \text{ mm}}{\frac{2.0125 \text{ mm}}{120 \text{ mmHg}}} = 238.5 \text{ mmHg} \quad (5.1)$$

After deducting the offset of 38 mmHg, 200 mmHg pressure would be achievable with this setup under ideal conditions - but the speed of the pressure slope decreases with increasing pressure levels. The reason for this phenomenon and the recalculation of the idealised, theoretical computation of the piezo motor is summarised in the following paragraphs after the third measurement setup.

The results of the second setup (cf. chapter "Methods": "full opening, 3D") show that there is hardly any distinction in the use of materials of different hardness as inserts for the cuff (human finger/silicone/PVC), the pressure differences are 33/25/25 mmHg with almost identical total steps 1450/1500/1200 (2.54/2.625/2.1 mm stroke). The theoretically achievable pressure differences Δp_T are thus 52/43/48 mmHg. It is important to note that the use of softer materials resulted in motor stalling at lower strokes. In this setup, too, friction effects were audible until overloading the motor, despite the lubrication. The adaptation of the cuff housing (opening of the upper side) had the negative effect: The mechanical energy of the motor was not only converted to generate pressure with friction loss. It was also converted into deformation energy by deformation of the cuff housing and deformation of the soft materials. The use of a circumferential cuff was also a factor to be criticised, as the pressure application was only one-dimensional from above, which meant that the homogeneous transmission of force around the whole finger could not be guaranteed.

In the third setup (cf. chapter "Methods": "fully embedded, 1D") a single-fluid bladder - as intended in the CNAP2GO concept - was used in combination with the CNAP classic housing. The maximum real achievable pressure difference Δp_{real} up to the upper power limit of the motor is 60 mmHg (start: 60 mmHg - end at overload: 120 mmHg), at a maximum real stroke H_{real} of 2.8 mm (32 x 50 steps; 0.35 mm per 200 steps; taken from figure 4.20). The theoretically achievable pressure difference Δp_T (calculation see above) is 86 mmHg. Although the cuff housing was only adapted minimally for the coupling of the threaded spindle to the metallic pressure surface and thus the mechanical integrity of the housing was maintained, the third setup did not achieve the calculated maximum pressure p_e (see tab. 3.7). In addition to the energy losses from the tribological considerations, deformation energy was applied at the housing and the cuff.

An important factor in this analysis of the piezo motor was the non-speed controllability of the motor - the set steps were achieved within a certain time depending on the load torque. The microstep time t_{step} was recorded in this setup, to analyse the performance of the motor. In the "worst-case" scenario - at maximum pressure difference - this was 0.027 seconds. This value is now used to calculate the actual speed of the motor v_{real} from t_{step} and number of steps per revolution in the "worst-case". At a constant set distance (50 steps) the increasing load reduces the speed of the motor. By reducing the speed of the motor, the step duration is extended. The recalculation of the key data of the prototype is explained in the following equations 5.2 - 5.5.

$$v_{\text{real}} = \frac{1}{t_{\text{step}} \cdot \text{steps per revolution}} \quad (5.2)$$

The real length difference ΔL_{real} per mmHg is computed from the actual stroke H_{real} and the actual pressure difference Δp_{real} :

$$\frac{\Delta L_{\text{real}}}{\text{mmHg}} = \frac{H_{\text{real}}}{\Delta p_{\text{real}}} \quad (5.3)$$

The time $t_{1\text{mmHg}}$, needed for 1 mmHg increase of pressure at maximum pressure difference results from the actual length difference ΔL_{real} per mmHg, the thread pitch P (corresponds to the distance in mm per revolution of the motor) and the real speed of the motor v_{real} :

$$t_{1\text{mmHg}} = \frac{\frac{\Delta L_{\text{real}}}{P} \text{ in } \%}{v_{\text{real}}} \quad (5.4)$$

At a maximum pressure difference of 60 mmHg, respectively maximum pressure of 120 mmHg, the rate of pressure change k_p for 50 steps is:

$$k_p = \frac{P}{\text{steps per revolution} \cdot \Delta L_{\text{real}} \cdot t_{\text{step}}} = \frac{1}{t_{1\text{mmHg}}} \quad (5.5)$$

Recomputation Prototype V.3

Measured

| Description | Value | Unit |
|---|-------|------|
| Microstep time t_{step} | 0.027 | s |
| Steps per revolution | 200 | |
| Thread pitch P | 0.35 | mm |
| Real stroke H_{real} | 2.8 | mm |
| Real pressure difference Δp_{real} | 60 | mmHg |

Computed

| Description | Value | Unit |
|--|-------|---------|
| Real speed of motor v_{real} | 0.19 | rev/s |
| Reale length difference ΔL_{real} | 0.047 | mm/mmHg |
| Reale time for 1 mmHg $t_{1\text{mmHg}}$ | 720 | ms |
| Pressure change rate at max. load k_p | 1.38 | mmHg/s |

Table 5.1.: Computation of the real values for the maximum pressure difference of prototype V.3

This calculation can be carried out analogously for the first and second setup. For the first setup, the time at maximum pressure difference is extended (see figure 4.15) for the penultimate 50 steps or the penultimate stroke to 3.5 seconds - the last stroke was aborted prematurely to avoid damaging the motor. For the second setup, the time required for 100 steps with the hard PVC finger dummy, for example, is extended to a maximum of 2 seconds (see figure 4.17). Therefore, the gradient k_p is below the required pressure change rate of 1.67 mmHg/s (5 mmHg / 3 seconds), which is essential for the CNAP2GO controller - the step time is too long to reproduce the desired behaviour.

Considering the CNAP2GO's controller and its controlling time, this ON-time (720 ms + $t_{\text{controller}}$) is additionally increased in the "worst-case". This ON-time is essential for the performance considerations of the system: With an assumed heart rate of 60 bpm and an average change ΔMAP per beat of 1 mmHg, the ON-time without controlling must be at least 43.2 seconds (0.72 x 60). This results in a duty cycle of 72% (ON-time / 60 s).

At a motor power consumption of 1.3W (0.365 A x 3.5 V) and a duty cycle of 72%, this results in an overall power consumption of 0.94 W. At higher heart rates the ON-time is no longer sufficient to achieve a resolution of 1 mmHg Δ MAP per beat.

Thus, at high pressures of 100 mmHg and above, the speed and power of the motor are not sufficient to achieve the required pressure of 200 mmHg at the desired control speed of at least 1.67 mmHg/s due to energy loss in friction and deformation. The calculated pressure difference from 0 to 160 mmHg is not achieved with any setup, the maximum is achieved with the first setup (38 to 158 mmHg \equiv 120 mmHg pressure difference). The idealised calculation assumes a force transmission system that is as one-dimensional as possible, the surfaces (finger surface, metallic pressure surface, cuff surface) are assumed to be of equal size, the bearing of the cuff (housing, fingers) is assumed to be non-deformable. In reality, the force transmission system behaves three-dimensionally, the marginally different surfaces and deformations have an influence on the force relations, because the pressure in the cuff acts as a scalar. According to the manufacturer, the motor can be loaded with a torque of 10 Nmm, the idealised calculated torque (see table 3.8) of 5.48 Nmm varies depending on the real force conditions and friction losses and thus leads to overloading of the motor.

The further considerations regarding miniaturisation of the system for a commercial product are the miniaturised, fine mechanical construction as well as the analysis and simulation of the piezo motor system using, for example, a Finite Element Method (FEM). For miniaturisation of the CNAP2GO concept, the combination of the technologies can be used as (printable) piezo step motor or piezoline actuator in conjunction with suitable MEMS sensor technology. The mechatronic actuating system consisting of mechanics and microelectronic control can then be operated with a low total weight compared to standard stepper motors [17]. As preparation for the FEM the force test of the motor against a load cell or 5 kg balance (not available at the time of measurement) is required. The FEM is used for the strength and deformation investigation of materials with different elasticity modules and considered friction conditions in the thread and on the coupling surfaces. The power consumption of the entire system - drive and control - must be dimensioned for a wearable device with a 24 hour battery life.

5.6. Conclusion

The stated aim of the "proof of principle" for CNAP2GO was achieved in this work. Iterative prototype development (Prototypes V.0, V.1 and V.2), as well as systematic improvements enabled the generation of consistent results, which were achieved through a series of measurements compared to the existing CNAP system. The evaluation using boxplots shows promising results of the CNAP2GO principle. The piezo motor used in prototype V.3 as an approach to miniaturising the overall system shows the limits of the concept. Due to various influences (friction, deformation of components, etc.) the requirements of the CNAP2GO approach cannot be met, further limitation by using this stepper motor is the absence of speed control.

Bibliography

- [1] Bundesanstalt Statistik Österreich: *Todesursachen 2018: Herz-Kreislauf-Erkrankungen und Krebs weiterhin am häufigsten; insgesamt sinkende Sterblichkeit*. 12.048-114/19. https://www.statistik.at/web_de/statistiken/menschen_und_gesellschaft/gesundheit/todesursachen/121158.html, (2018)
- [2] Eurostat - Europäische Kommission: *Todesursachenstatistiken - Datenauszug 2019*. https://ec.europa.eu/eurostat/statistics-explained/index.php?title=Causes_of_death_statistics/de, (2020)
- [3] Forouzanfar M. H., Liu P., *et al.*: Global Burden of Hypertension and Systolic Blood Pressure of at Least 110 to 115 mmHg, 1990-2015. *JAMA* 317: 165–182 (2017)
- [4] Weber T., Arbeiter K., *et al.*: Österreichischer Blutdruckkonsens 2019. *Wiener klinische Wochenschrift - The Central European Journal of Medicine* 131: 489–590. 10.1007/s00508-019-01565-0 (2019)
- [5] Williams B., Mancia G., *et al.*: 2018 ESC/ESH Guidelines for the management of arterial hypertension: The Task Force for the management of arterial hypertension of the European Society of Cardiology (ESC) and the European Society of Hypertension (ESH). *European Heart Journal* 39: 3021–3104 (2018)
- [6] Perl S., Zweiker D., *et al.*: May Measurement Month 2017: an analysis of bloodpressure screening results in Austria—Europe. *European Heart Journal Supplements* 21: D17–D20 (2019)
- [7] Association for the Advancement of Medical Instrumentation: Manual, electronic or automated sphygmomanometers ANSI/AAMI SP10-2002/A1. *American National Standard* (2003)
- [8] Scheer B., Perel A., *et al.*: Clinical Review: Complications and Risk Factors of Peripheral Arterial Catheters Used for Haemodynamic Monitoring in Anaesthesia and Intensive Care Medicine. *Critical Care* 6: 199–204 (2002)
- [9] Association for the Advancement of Medical Instrumentation: Non-invasive Sphygmomanometers—Part 2: Clinical Investigation of Automated Measurement Type ANSI/AAMI/ISO 81060-2. *American National Standard* (2013)

-
- [10] Wax D. B., Lin H.-M., *et al.*: Invasive and Concomitant Noninvasive Intraoperative Blood Pressure Monitoring: Observed Differences in Measurements and Associated Therapeutic Interventions. *Anesthesiology* 115: 973–978 (2011)
- [11] Peñáz J.: Photoelectric Measurement of blood pressure, volume and flow in the finger. *Digest of the 10th intl. conf. on med. & biol. eng.*: 104 (1973)
- [12] Fortin J., Marte W., *et al.*: Continuous non-invasive blood pressure monitoring using concentrically interlocking control loops. *Comp. Biol. Med.* 36: 941–957 (2006)
- [13] Fortin J., Fellner C., *et al.*: The importance of VERIFI (“Vasomotoric Elimination and Reconstructed Identification of the Initial set-point”) for the performance of the CNAP technology. *IFMBE Proceedings, EMBEC & NBC* 65: 663–666 (2017)
- [14] Fortin J., Fellner C., *et al.*: Verfahren und Vorrichtung zur Validierung eines Blutdruckmesssystems. *AT Patentanmeldung A 50469/2019*. Anmeldedatum: 22.05.2019, IPC: A61B 005/021, Patenterteilung: 18.06.2020 (2019)
- [15] Fortin J., Rogge D., *et al.*: A novel art of continuous non-invasive blood pressure measurement. *medRxiv*. under consideration in Nature Communications (2019)
- [16] Will D., Gebhardt N.: *Hydraulik*. Pirna – Großhain, Springer Verlag (2014)
- [17] Isermann R.: *Mechatronische Systeme*. Darmstadt, Springer Verlag (2008)
- [18] Miao F., Fu N., *et al.*: A Novel Continuous Blood Pressure Estimation Approach Based on Data Mining Techniques. *IEEE J. Biomed. Health. Inf.* 21: 1730–1740 (2017)
- [19] Ding X., Yan B. P., *et al.*: Pulse Transit Time Based Continuous Cuffless Blood Pressure Estimation: A New Extension and A Comprehensive Evaluation. *Sci. Rep.* 7 (2017)
- [20] Nabeel P. M., Jayaraj J., *et al.*: Single-source PPG-based local pulse wave velocity measurement: a potential cuffless blood pressure estimation technique. *Physiol. Meas.* 38: 2122–2140 (2017)
- [21] Nabeel P. M., Jayaraj J., *et al.*: Bi-Modal Arterial Compliance Probe for Calibration-Free Cuffless Blood Pressure Estimation. *IEEE Trans. Biomed. Eng.* 65: 2392–2404 (2018)

-
- [22] Huynh T. H., Jafari R., *et al.*: An Accurate Bioimpedance Measurement System for Blood Pressure Monitoring. *Sensors* 18 (2018)
- [23] Chandrasekhar A., Kim C.-S., *et al.*: Smartphone-based blood pressure monitoring via the oscillometric finger-pressing method. *Sci. Transl. Med.* 10 (2018)
- [24] Solà J., Vybornova A., *et al.*: *Aktiia Bracelet: Monitoring of Blood Pressure using Off-the-shelf Optical Sensors* In: IEEE Eng. Med. Biol. Conf. (2019)
- [25] Pellaton C., Vybornova A., *et al.*: Accuracy testing of a new optical device for noninvasive estimation of systolic and diastolic blood pressure compared to intra-arterial measurements. *Blood Pressure Monitoring* 25 (2019)
- [26] BIOPAC Systems Inc.: *User Manual: MP System Hardware Guide*. Graz, AT, (2017)
- [27] Wittel H., Muhs D., *et al.*: *Roloff/Matek Maschinenelemente.*: 260–262. Reutlingen – Braunschweig – Augsburg, Springer Verlag (2015)
- [28] Böge A., Böge W.: *Handbuch Maschinenbau.*: 674. Braunschweig – Wolfenbüttel, Springer Verlag (2014)
- [29] Hui X., Kan E. C.: Monitoring vital signs over multiplexed radio by near-field coherent sensing. *Nat. Electron.* 1: 74–78 (2018)
- [30] Park S., Heo S. W., *et al.*: Self-powered ultra-flexible electronics via nanograting-patterned organic photovoltaics. *Nature* 561: 516–521 (2018)
- [31] Wang C., Li X., *et al.*: Monitoring of the central blood pressure waveform via a conformal ultrasonic device. *Nat. Biomed. Eng.* 2: 687–695 (2018)
- [32] CNSystems Medizintechnik GmbH: *Operators Manual - CNAP Development Kit 3.0*. Goleta, USA, (2017)
- [33] BIOPAC Systems Inc.: *User Manual: AcqKnowledge 5 Software Guide*. Goleta, USA, (2019)

Appendix

Appendix A.

Additional Components

| Utilised Components & Software - Biopac | | |
|---|----------------|-----------------|
| Description | Type | SN / Build Date |
| Power supply for Biopac system | | |
| Biopac Databox (e.g. MP 160) | MP160 | 1803A-0001D1D |
| Biopac blood pressure transducer | TSD104A | 1706002495 |
| Biopac differential amplifier | DA100C | DA1802C0008233 |
| AcqKnowledge Software | Version: 5.0.2 | Dec. 14 2017 |

Table A.1.: Utilised components of the Biopac system

| Additional Components V.0 | | |
|--|-----------------|--|
| Description | Type | SN / Build Date |
| Syringe 25 ml | | |
| Various hoses and Luer-Lock connectors | | |
| Distilled water | Pressure medium | |
| CNAP double-finger cuff | "Epurex med 3" | 19.07.2016 / LaserID: AB000005-59954933 |
| Mechanical screw clamp | Actuator | |

Table A.2.: Additional components for prototype V.0

| Additional Components V.1 | | |
|---|-----------------------------------|--|
| Description | Type | SN / Build Date |
| Syringe 60 ml Various hoses and Luer-Lock connectors Distilled water CNAP double-finger cuff | Pressure medium „Epurex med 3” | 19.07.2016 / LaserID: AB000005-59954933 |
| CNS Development Kit (DevKit) | V1.0 | CNPE-1807-0036 |
| CNS cuff controller | V4.1 | 8372700081 |
| Mechanical screw clamps | | |
| Additional Software V.1 | | |
| Description | Type | SN / Build Date |
| CNS DevKit Firmware | | FW Version: 5.2.36 |
| CNS SerialGUI | PV:12, baud rate 921600 | Version: 5.2.37 |
| CNS TestInterpreter | TestInterpreterscript | Build: 9da387f |
| Spyder | Python Version: 3.7.6 | Version 3.3.6 |

Table A.3.: Additional components and software for prototype V.1

| Additional Components V.2 – Prototype CNAP2GO | | |
|---|-----------------------------------|---|
| Description | Type | SN / Build Date |
| Syringe 60 ml Various hoses and Luer-Lock connectors Distilled water CNAP double-finger cuff | Pressure medium ”Epurex med 3” | 19.07.2016, LaserID: AB000005-59954933 |
| CNS Development Kit (DevKit) | V1.0 | CNPE-1807-0036 |
| CNS cuff controller | V4.1 | 8372700081 |
| Syringe pump (50 ml; 0.1 to 99.9 ml/h) | Braun Perfusor se- cura FT | 09578 |
| Additional Software V.2 | | |
| Description | Type | SN / Build Date |
| CNS DevKit Firmware | | FW Version: 5.2.36 |
| CNS SerialGUI | PV:12, baud rate 921600 | Version: 5.2.37 |
| CNS TestInterpreter | TestInterpreter script | Build: 9da387f |
| Spyder | Python Version: 3.7.6 | Version 3.3.6 |

Table A.4.: Additional components and software for prototype V.2

| Additional Components V.2 – CNAP System | | |
|--|-------------|------------------------|
| Description | Type | SN / Build Date |
| CNAP double-finger cuff | | LaserID: 3741319169 |
| CNS Development Kit (DevKit) | V1.0 | CNPE-1807-0037 |
| CNS cuff controller | V4.1 | 8551480009 |

Table A.5.: Additional components for comparative measurement with CNAP classic system

| Additional components V.3 – Prototype CNAP2GO | | |
|---|--|-----------------|
| Description | Type | SN / Build Date |
| Syringe 60 ml Various hoses and Luer-Lock connectors Distilled water CNAP double-finger cuff Piezo motor (PCB Motors, Hillerød, Denmark) www.pcbmotor.com last accessed 20.07.2020 | Pressure medium ”Epurex med 3” 30 mm PCB motor Lead screw kit with 4mm stroke length | |

Table A.6.: Additional components for prototype V.3

| Piezomotor Characteristics | | |
|-------------------------------|--------------|-------|
| Description | Value | Unit |
| Idle speed v_{LL} | 1 | rev/s |
| Holding torque M_{LL} | 10 | Nmm |
| Current consumption I_{max} | 480 | mA |
| Input voltage U_{max} | 5 | V |
| Output power P_{omax} | 59 | mW |
| Dimensions WxHxD | 42 x 20 x 62 | mm |

Table A.7.: Key data of the piezo motor for prototype V.3

Appendix B.

Plots

B.1. Prototype V.0

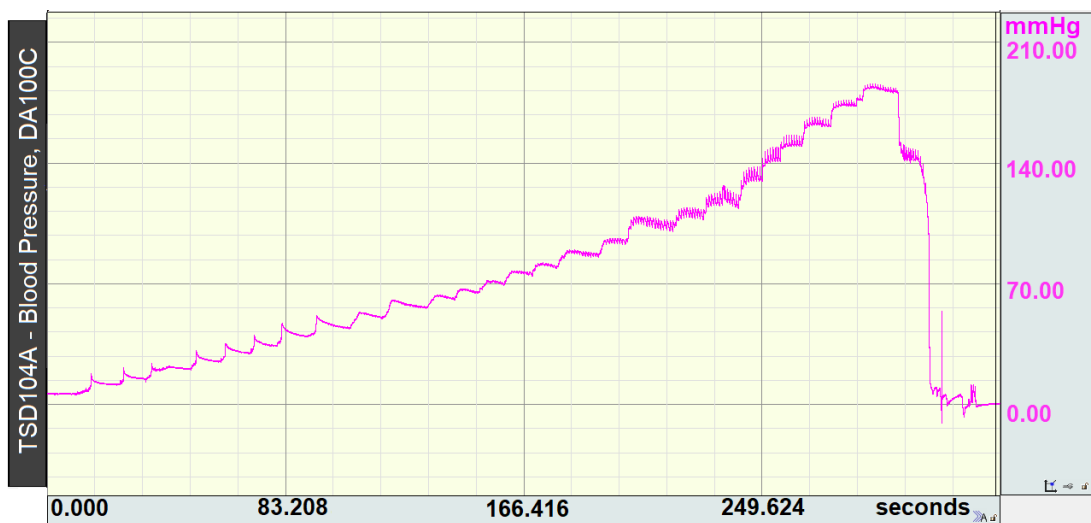


Figure B.1.: Prototype V.0. Pressure measurement on the middle finger of the test subject, $f_s = 100$ Hz

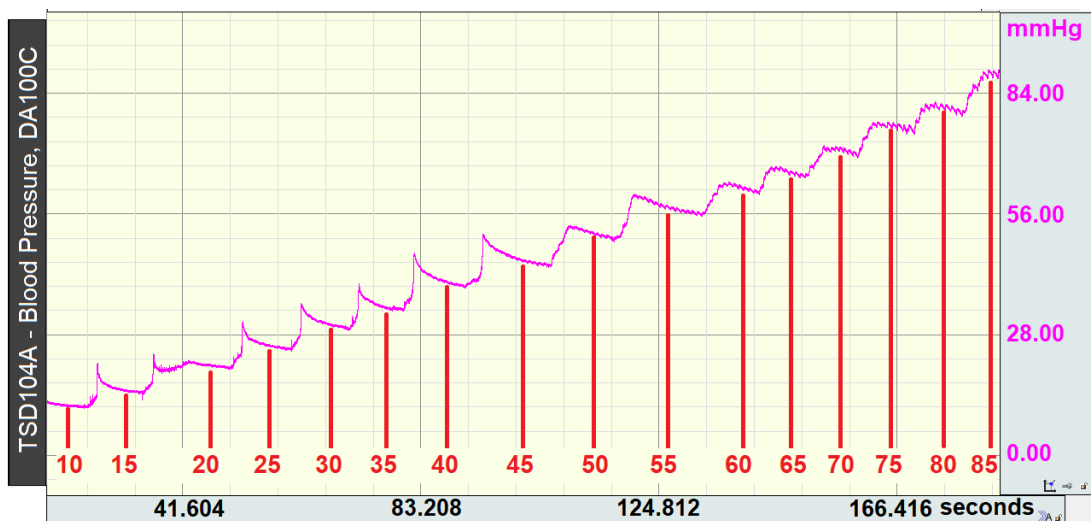


Figure B.2.: Prototype V.0. Exemplary range of 10 to 85 mmHg, 5 mmHg pressure steps per level, $f_s = 100$ Hz

B.2. Prototype V.1

B.2.1. Test Subject 1

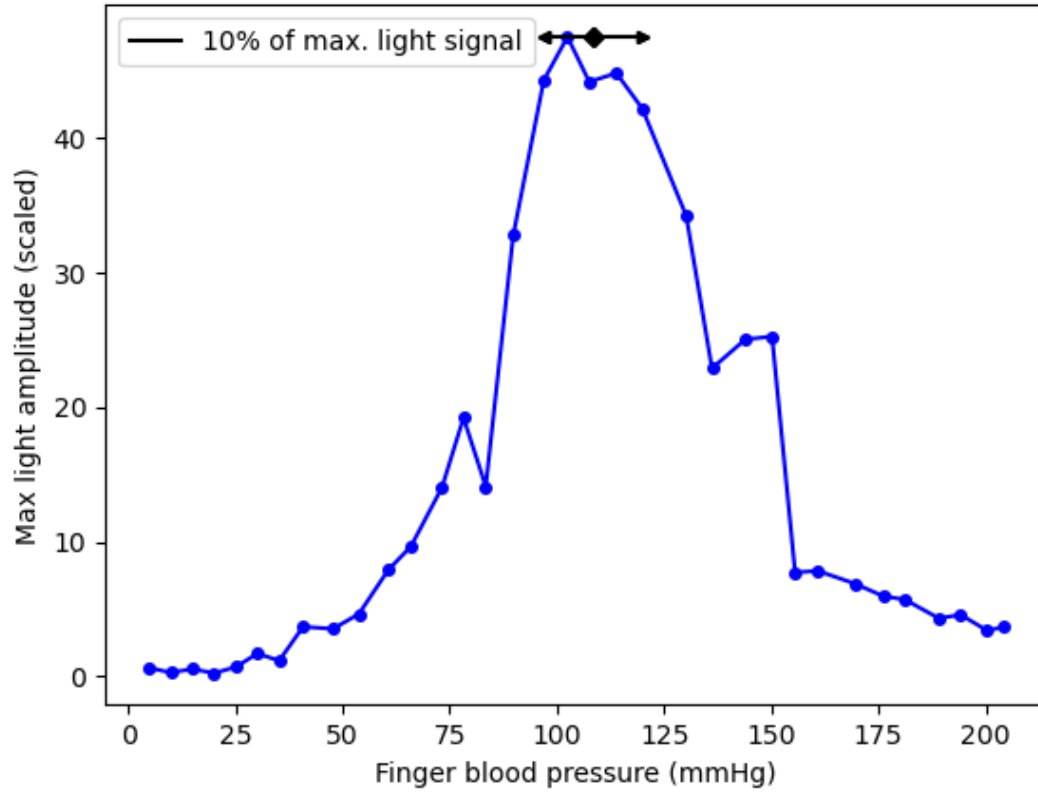


Figure B.3.: Prototype V.1. Oscillometric envelope as point-line diagram; recorded on the middle finger of test subject 1, $f_s = 100$ Hz

B.2.2. Test Subject 2

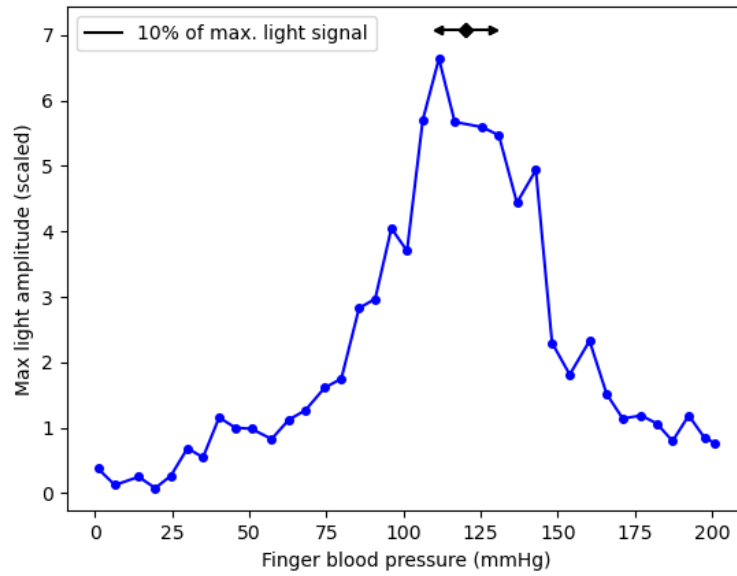


Figure B.4.: Prototype V.1. Oscillometric envelope as point-line diagram; recorded on the index finger of test subject 2, $f_s = 100$ Hz

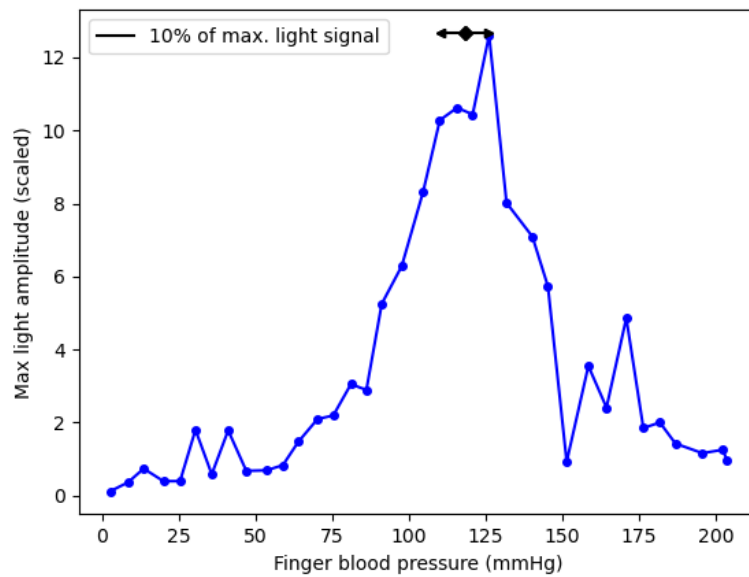


Figure B.5.: Prototype V.1. Oscillometric envelope as point-line diagram; recorded on the middle finger of test subject 2, $f_s = 100$ Hz

B.2.3. Test Subject 3

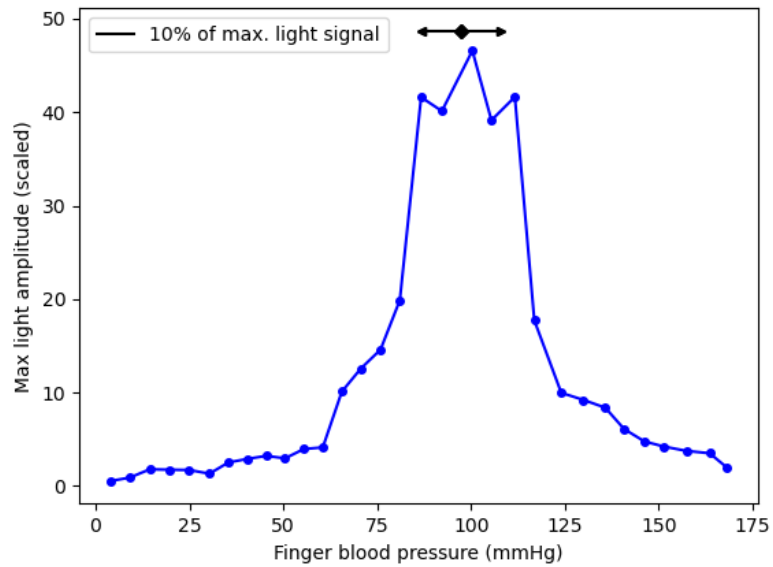


Figure B.6.: Prototype V.1. Oscillometric envelope as averaged point-line diagram; recorded on the index finger of test subject 3, $f_s = 100$ Hz

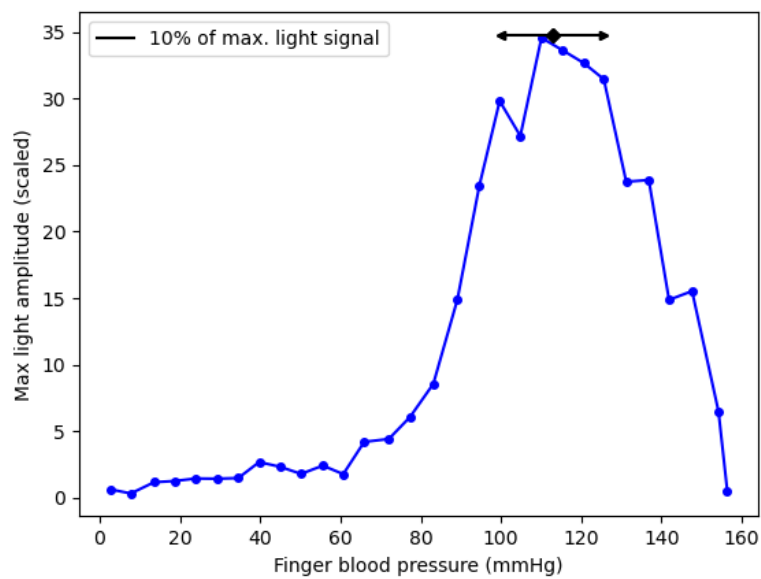


Figure B.7.: Prototype V.1. Oscillometric envelope as point-line diagram; recorded on the middle finger of test subject 3, $f_s = 100$ Hz

B.2.4. Test Subject 4

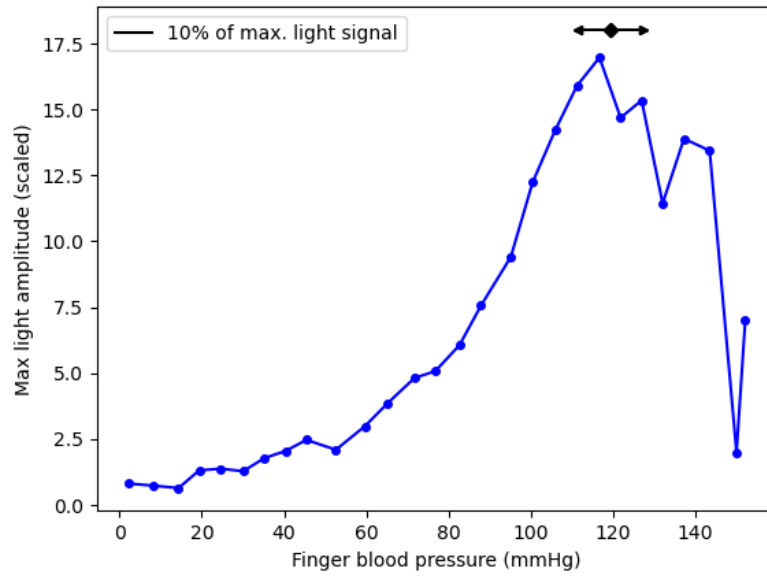


Figure B.8.: Prototype V.1. Oscillometric envelope as point-line diagram; recorded on the index finger of test subject 4, $f_s = 100$ Hz

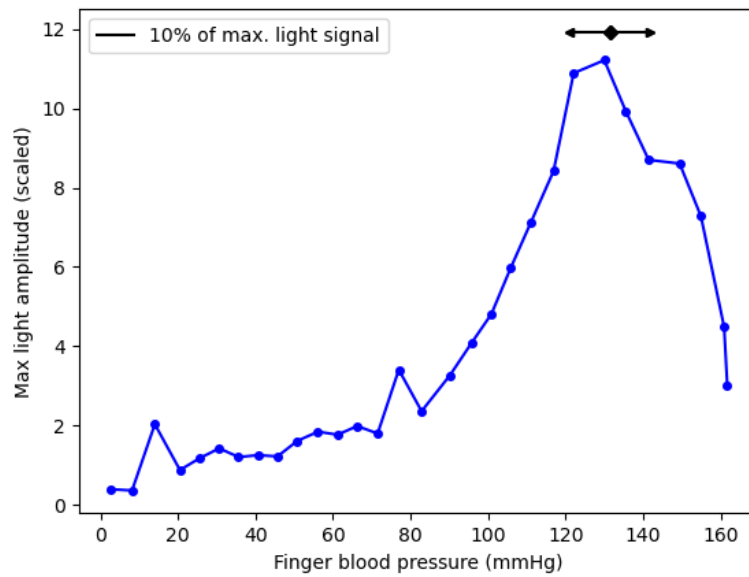
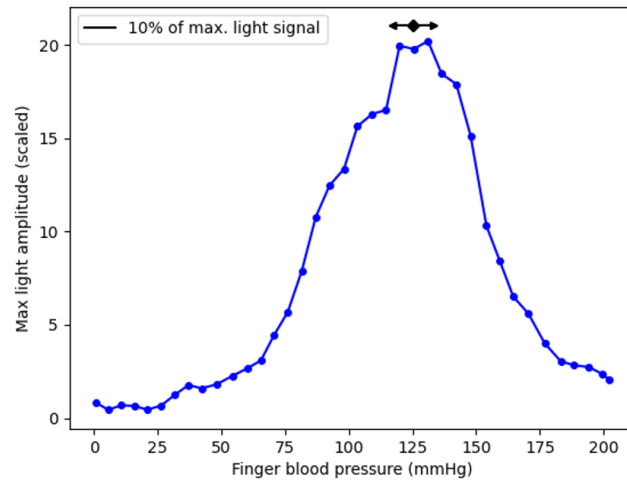


Figure B.9.: Prototype V.1. Oscillometric envelope as point-line diagram; recorded on the middle finger of test subject 4, $f_s = 100$ Hz

B.3. Prototype V.2

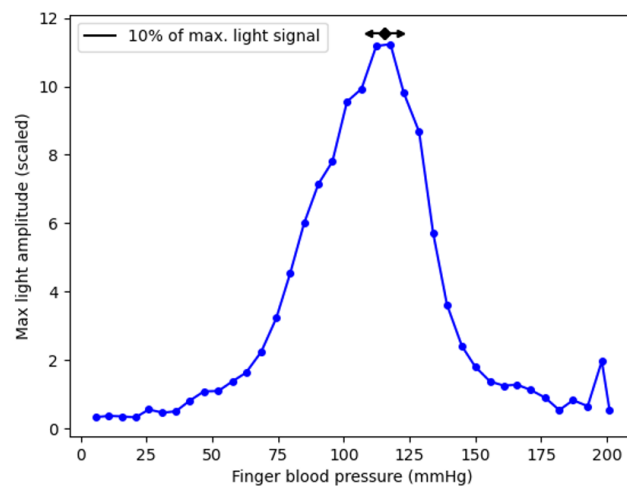
B.3.1. Test Subject 1

Index Finger (Left Hand: CNAP, Right Hand: Prototype V.2)



Prototype V.2 – right hand, index finger
 MD = 125.1 mmHg
 KB = 15.8 mmHg

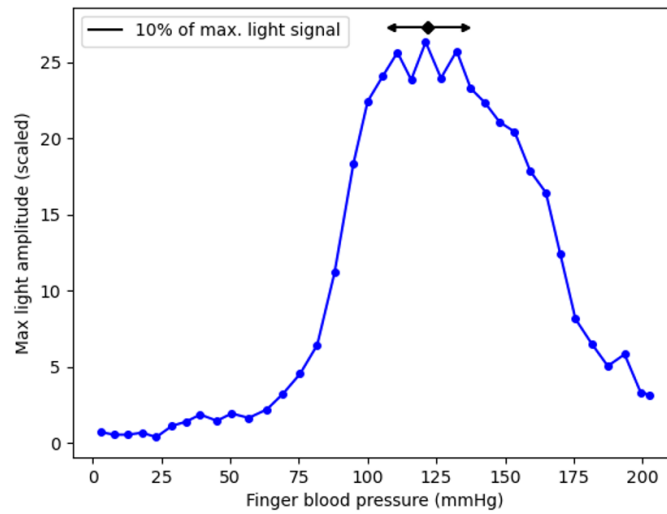
Figure B.10.: Prototype V.2. Oscillometric envelope as point-line diagram; recorded on the right index finger of test subject 1, $f_s = 10$ Hz



CNAP – left hand, index finger
 MD = 115.3 mmHg
 KB = 12.0 mmHg

Figure B.11.: CNAP. Oscillometric envelope as point-line diagram; recorded on the left index finger of test subject 1, $f_s = 10$ Hz

Index Finger (Right Hand: CNAP, Left Hand: Prototype V.2)

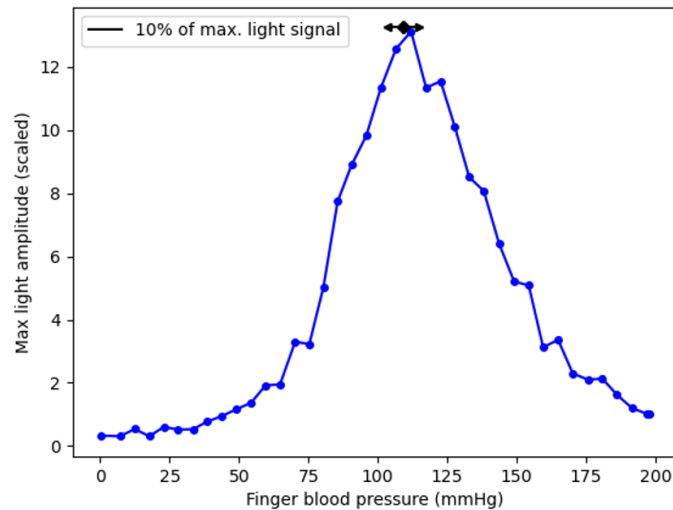


Prototype V.2 – left hand, index finger

MD= 121.98 mmHg

KB = 27.0 mmHg

Figure B.12.: Prototype V.2. Oscillometric envelope as point-line diagram; recorded on the left index finger of test subject 1, $f_s = 10$ Hz



CNAP – right hand, index finger

MD = 109.0 mmHg

KB = 11.4 mmHg

Figure B.13.: CNAP. Oscillometric envelope as point-line diagram; recorded on the right index finger of test subject 1, $f_s = 10$ Hz

B.3.2. Test Subject 2

Index Finger (Left Hand: CNAP, Right Hand: Prototype V.2)

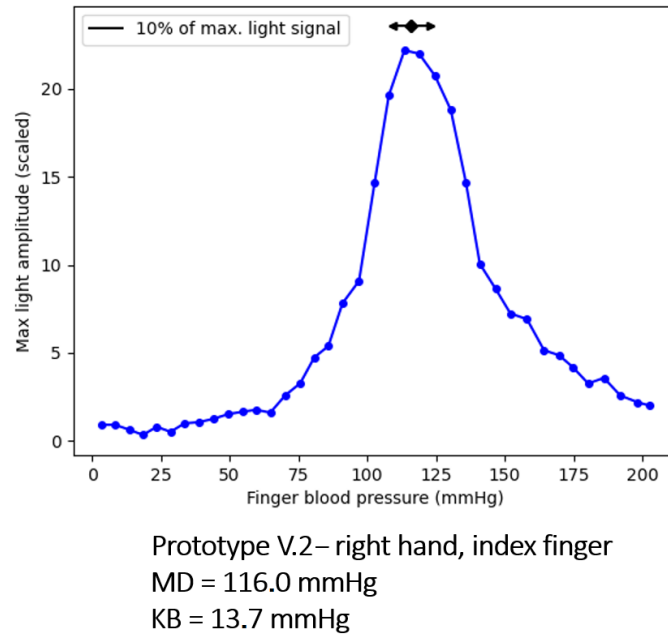


Figure B.14.: Prototype V.2. Oscillometric envelope as point-line diagram; recorded on the right index finger of test subject 2, $f_s = 10$ Hz

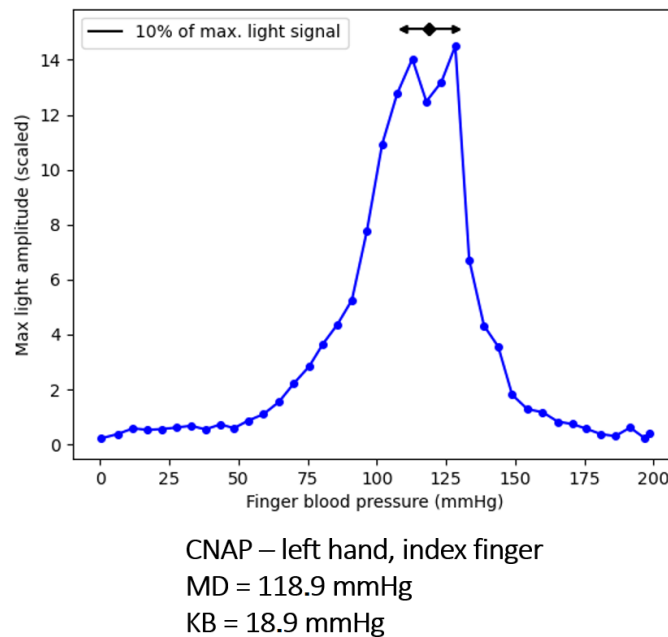
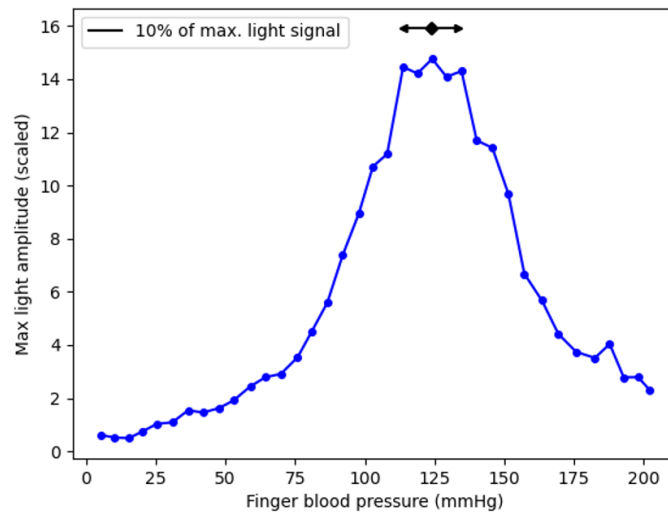


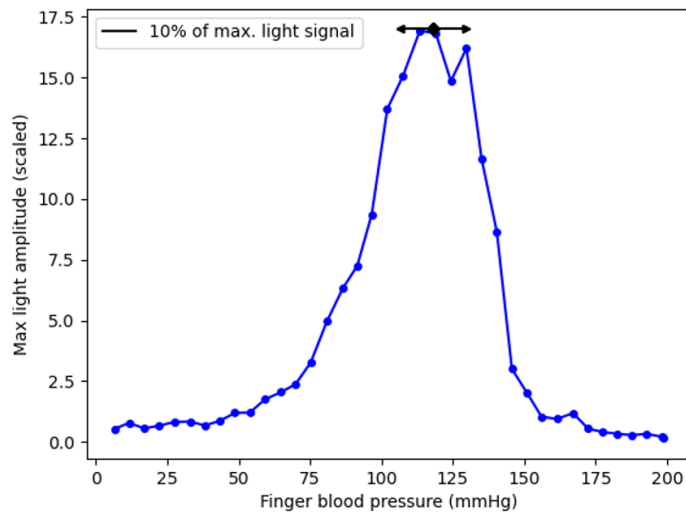
Figure B.15.: CNAP. Oscillometric envelope as point-line diagram; recorded on the left index finger of test subject 2, $f_s = 10$ Hz

Index Finger (Right Hand: CNAP, Left Hand: Prototype V.2)



Prototype V.2 – left hand, index finger
 MD = 123.6 mmHg
 KB = 19.8 mmHg

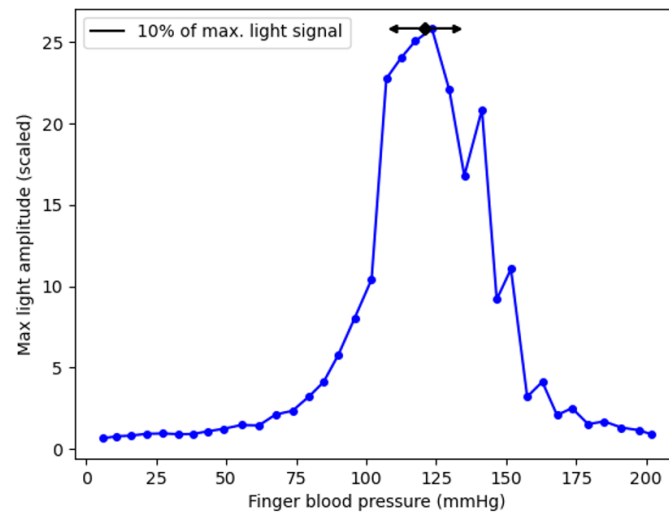
Figure B.16.: Prototype V.2. Oscillometric envelope as point-line diagram; recorded on the left index finger of test subject 2, $f_s = 10$ Hz



CNAP – right hand, index finger
 MD = 118.3 mmHg
 KB = 23.1 mmHg

Figure B.17.: CNAP. Oscillometric envelope as point-line diagram; recorded on the right index finger of test subject 2, $f_s = 10$ Hz

Middle Finger (Left Hand: CNAP, Right Hand: Prototype V.2)

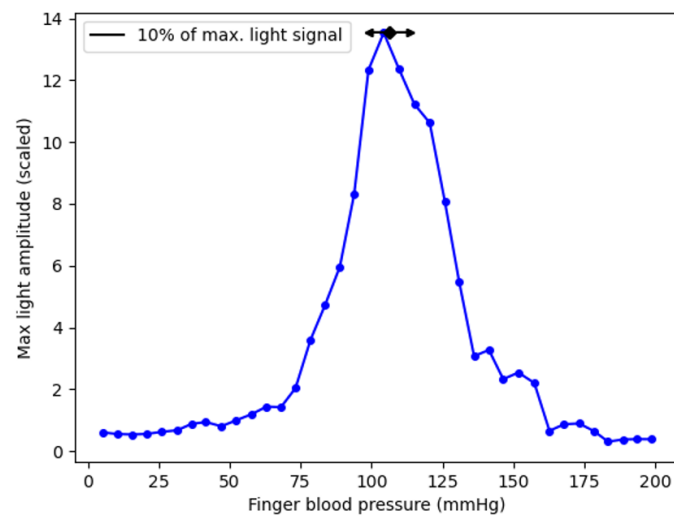


Prototype V.2 – right hand, middle finger

MD = 121.0 mmHg

KB = 22.7 mmHg

Figure B.18.: Prototype V.2. Oscillometric envelope as point-line diagram; recorded on the right middle finger of test subject 2, $f_s = 10$ Hz



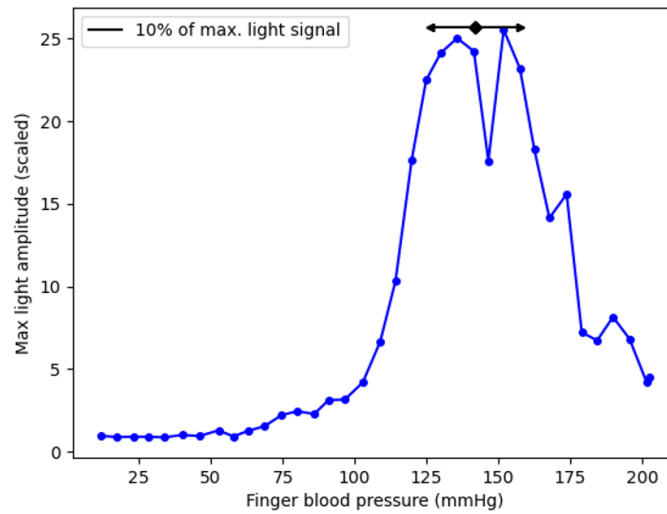
CNAP – left hand, middle finger

MD = 106.3 mmHg

KB = 14.8 mmHg

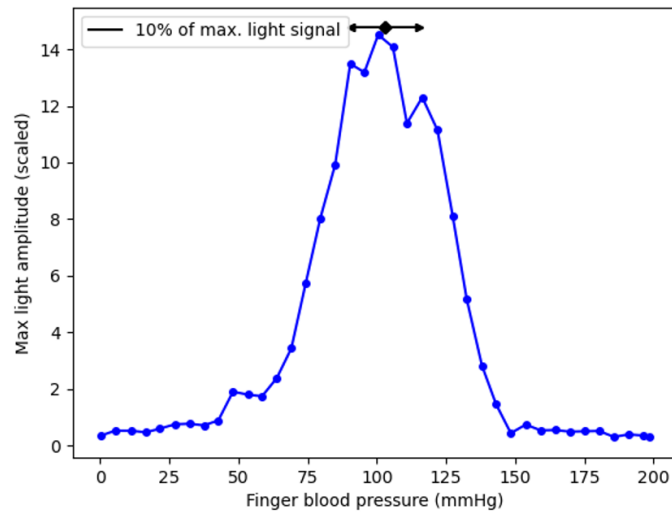
Figure B.19.: CNAP. Oscillometric envelope as point-line diagram; recorded on the left middle finger of test subject 2, $f_s = 10$ Hz

Middle Finger (Right Hand: CNAP, Left Hand: Prototype V.2)



Prototype V.2 – left hand, middle finger
 MD = 141.7 mmHg
 KB = 31.5 mmHg

Figure B.20.: Prototype V.2. Oscillometric envelope as point-line diagram; recorded on the left middle finger of test subject 2, $f_s = 10$ Hz

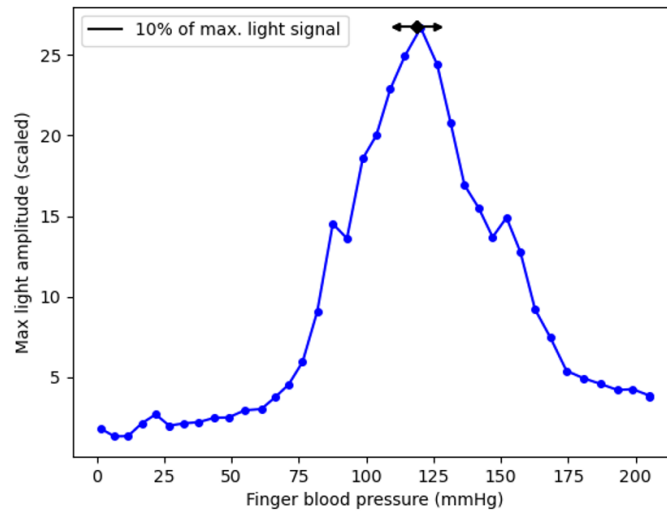


CNAP – right hand, middle finger
 MD = 102.8 mmHg
 KB = 24.8 mmHg

Figure B.21.: CNAP. Oscillometric envelope as point-line diagram; recorded on the right middle finger of test subject 2, $f_s = 10$ Hz

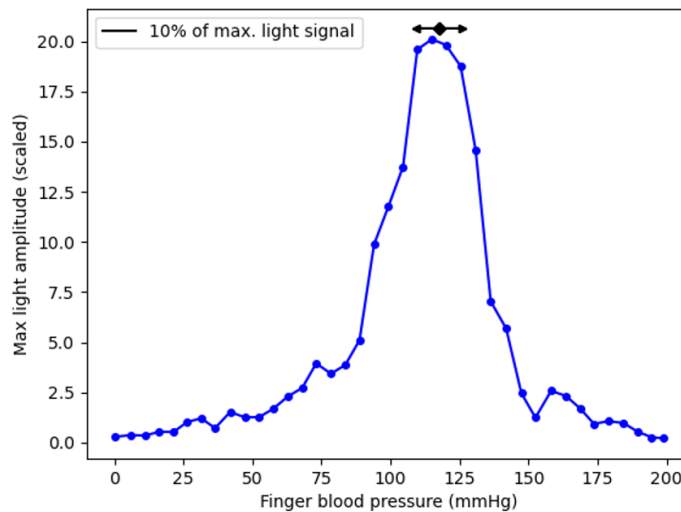
B.3.3. Test Subject 3

Index Finger (Left Hand: CNAP, Right Hand: Prototype V.2)



Prototype V.2 – right hand, index finger
 MD = 118.7 mmHg
 KB = 15.2 mmHg

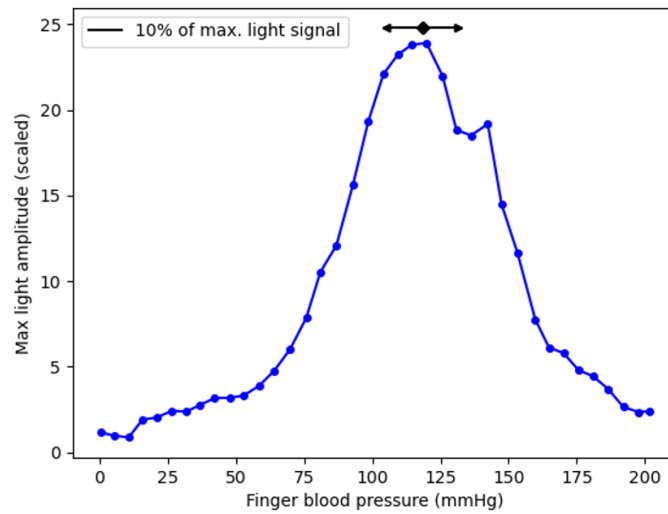
Figure B.22.: Prototype V.2. Oscillometric envelope as point-line diagram; recorded on the right index finger of test subject 3, $f_s = 10$ Hz



CNAP – left hand, index finger
 MD = 117.5 mmHg
 KB = 16.8 mmHg

Figure B.23.: CNAP. Oscillometric envelope as point-line diagram; recorded on the left index finger of test subject 3, $f_s = 10$ Hz

Index Finger (Right Hand: CNAP, Left Hand: Prototype V.2)

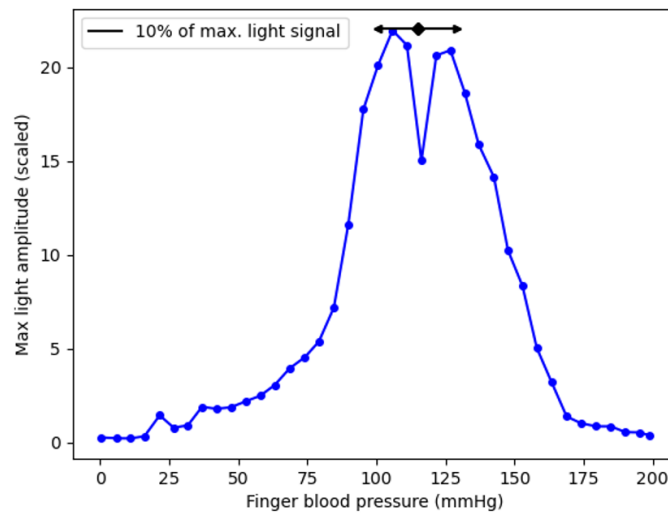


Prototype V.2 – left hand, index finger

MD = 118.3 mmHg

KB = 26.5 mmHg

Figure B.24.: Prototype V.2. Oscillometric envelope as point-line diagram; recorded on the left index finger of test subject 3, $f_s = 10$ Hz



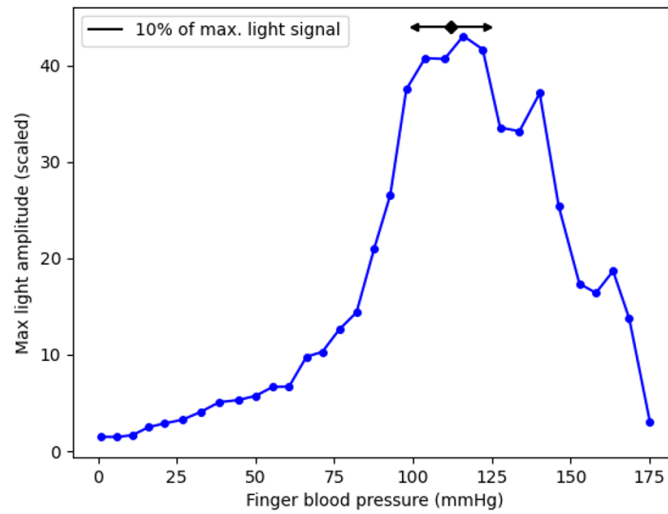
CNAP – right hand, index finger

MD = 114.8 mmHg

KB = 28.5 mmHg

Figure B.25.: CNAP. Oscillometric envelope as point-line diagram; recorded on the right index finger of test subject 3, $f_s = 10$ Hz

Middle Finger (Left Hand: CNAP, Right Hand: Prototype V.2)

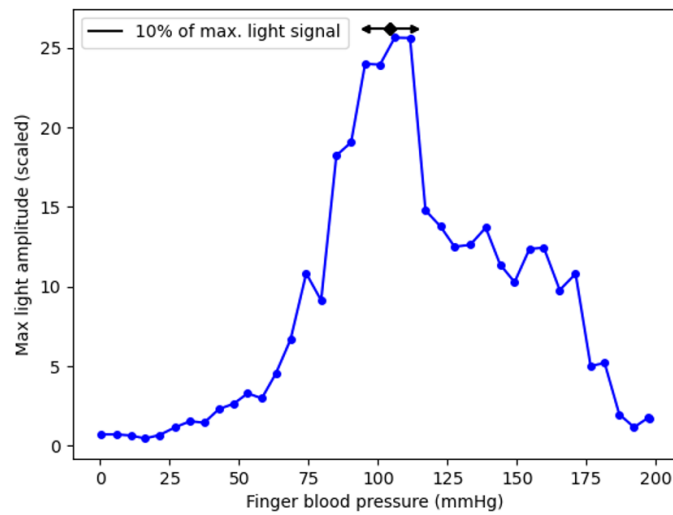


Prototype V.2 – right hand, middle finger

MD = 111.8 mmHg

KB = 23.3 mmHg

Figure B.26.: Prototype V.2. Oscillometric envelope as point-line diagram; recorded on the right middle finger of test subject 3, $f_s = 10$ Hz



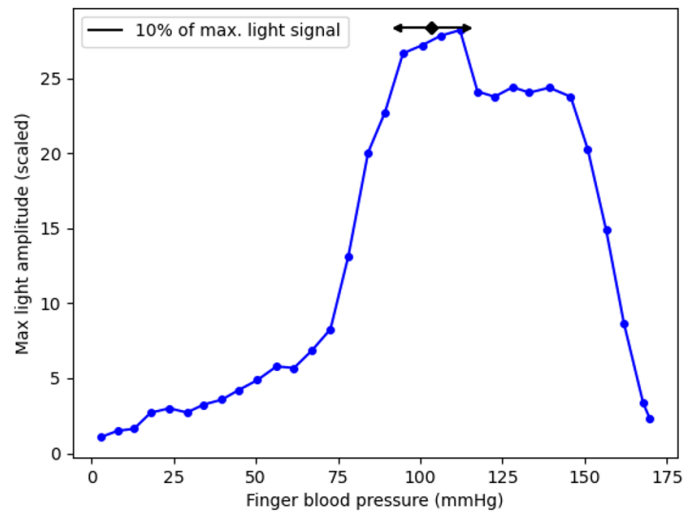
CNAP – left hand, middle finger

MD = 104.1 mmHg

KB = 17.5 mmHg

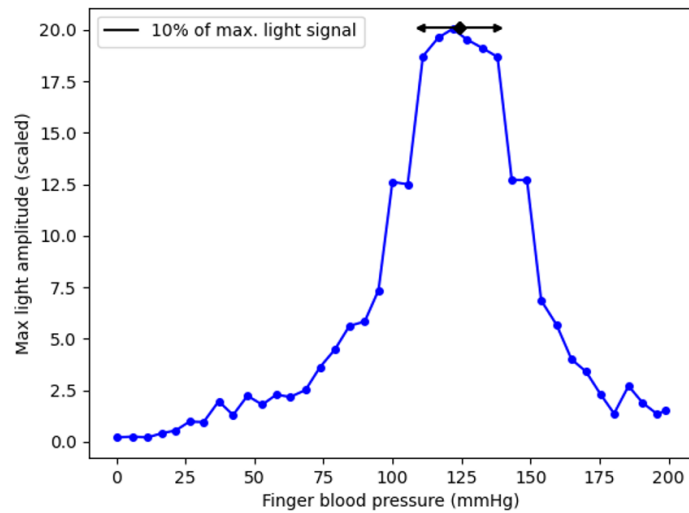
Figure B.27.: CNAP. Oscillometric envelope as point-line diagram; recorded on the left middle finger of test subject 3, $f_s = 10$ Hz

Middle Finger (Right Hand: CNAP, Left Hand: Prototype V.2)



Prototype V.2 – left hand, middle finger
 MD = 103.5 mmHg
 KB = 21.2 mmHg

Figure B.28.: Prototype V.2. Oscillometric envelope as point-line diagram; recorded on the left middle finger of test subject 3, $f_s = 10$ Hz

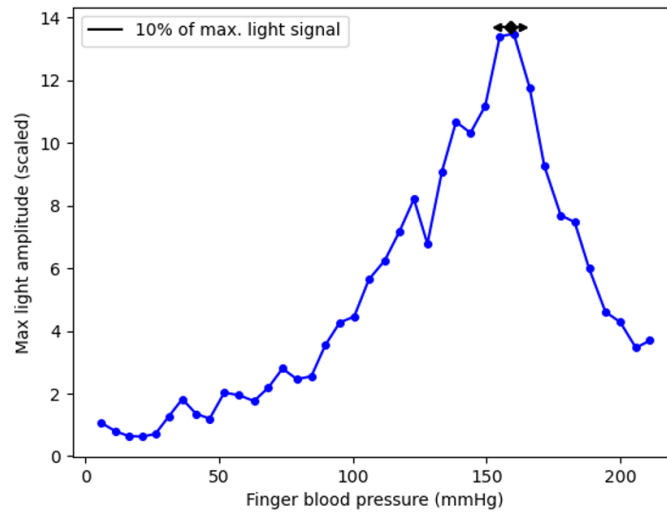


CNAP – right hand, middle finger
 MD = 124.1 mmHg
 KB = 27.7 mmHg

Figure B.29.: CNAP. Oscillometric envelope as point-line diagram; recorded on the right middle finger of test subject 3, $f_s = 10$ Hz

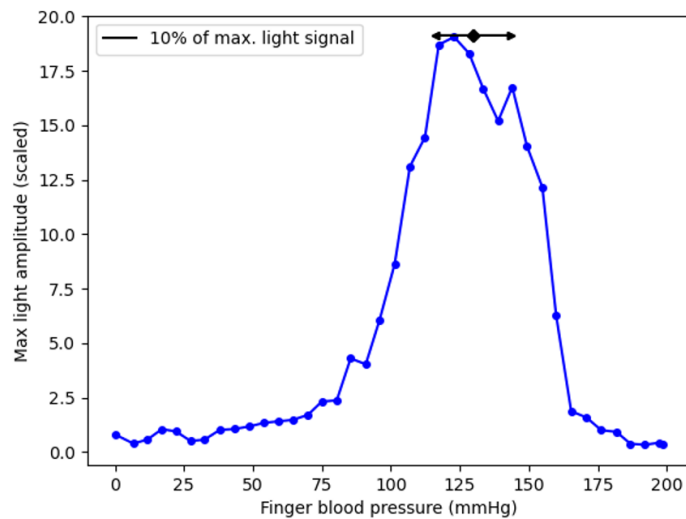
B.3.4. Test Subject 4

Index Finger (Left Hand: CNAP, Right Hand: Prototype V.2)



Prototype V.2 – right hand, index finger
 MD = 158.9 mmHg
 KB = 9.5 mmHg

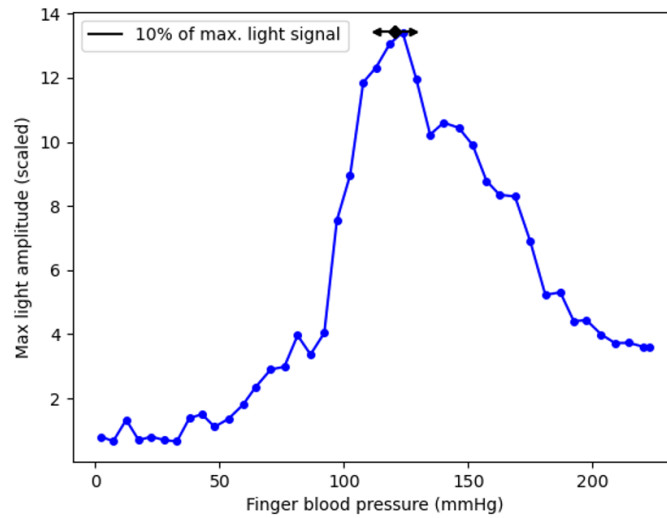
Figure B.30.: Prototype V.2. Oscillometric envelope as point-line diagram; recorded on the right index finger of test subject 4, $fs = 10$ Hz



CNAP – left hand, index finger
 MD = 129.8 mmHg
 KB = 27.7 mmHg

Figure B.31.: CNAP. Oscillometric envelope as point-line diagram; recorded on the left index finger of test subject 4, $fs = 10$ Hz

Index Finger (Right Hand: CNAP, Left Hand: Prototype V.2)

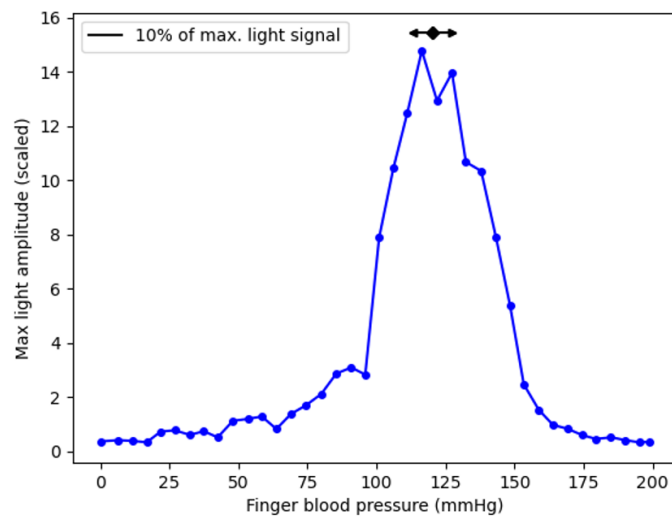


Prototype V.2 – left hand, index finger

MD = 120.5 mmHg

KB = 15.1 mmHg

Figure B.32.: Prototype V.2. Oscillometric envelope as point-line diagram; recorded on the left index finger of test subject 4, $f_s = 10$ Hz



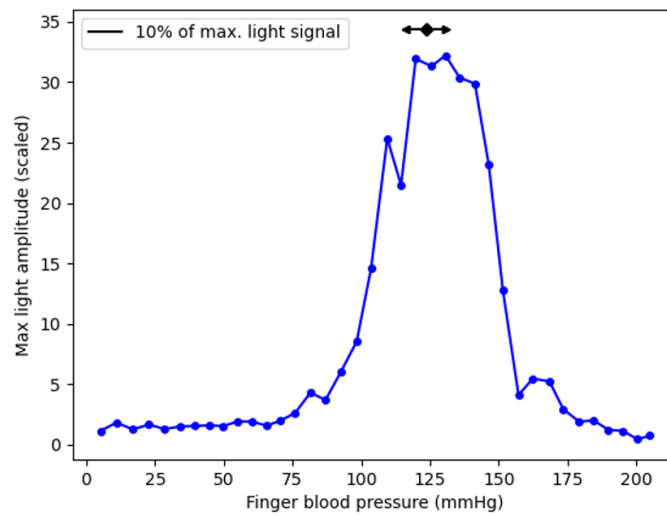
CNAP – right hand, index finger

MD = 120.3 mmHg

KB = 14.0 mmHg

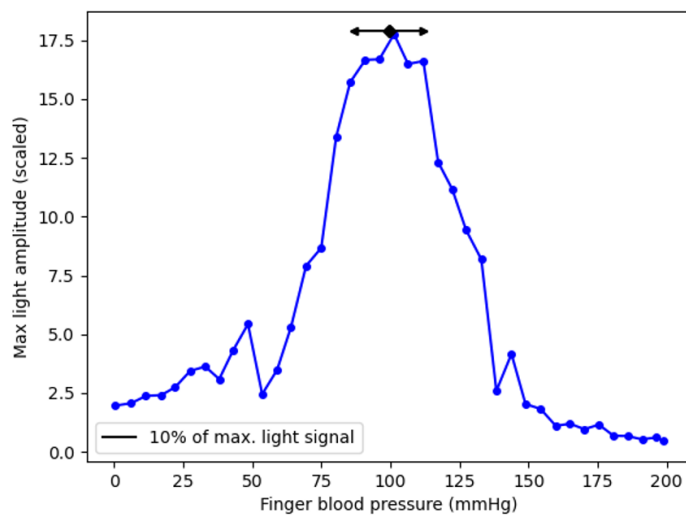
Figure B.33.: CNAP. Oscillometric envelope as point-line diagram; recorded on the right index finger of test subject 4, $f_s = 10$ Hz

Middle Finger (Left Hand: CNAP, Right Hand: Prototype V.2)



Prototype V.2 – right hand, middle finger
 MD= 123.5 mmHg
 KB = 14.3 mmHg

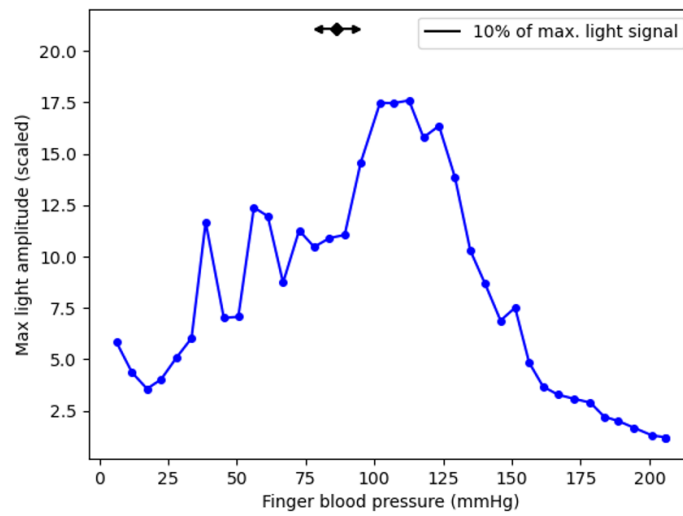
Figure B.34.: Prototype V.2. Oscillometric envelope as point-line diagram; recorded on the right middle finger of test subject 4, $f_s = 10$ Hz



CNAP – left hand, middle finger
 MD = 99.4 mmHg
 KB = 25.0 mmHg

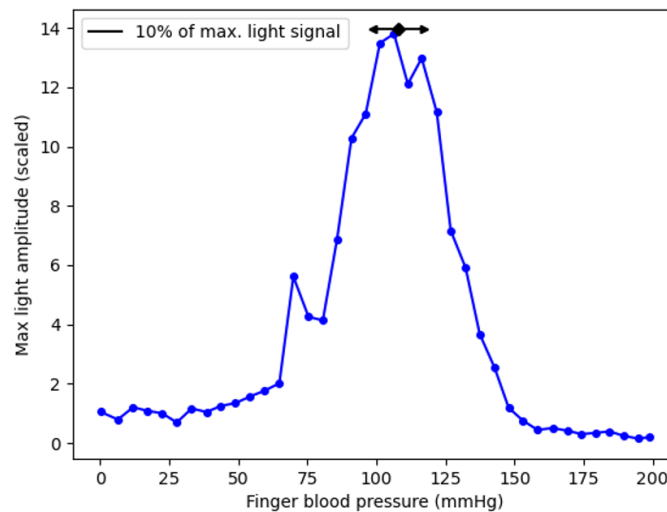
Figure B.35.: CNAP. Oscillometric envelope as point-line diagram; recorded on the left middle finger of test subject 4, $f_s = 10$ Hz

Middle Finger (Right Hand: CNAP, Left Hand: Prototype V.2)



Prototype V.2 – left hand, middle finger
 MD = 86.4 mmHg
 KB = 13.9 mmHg

Figure B.36.: Prototype V.2. Oscillometric envelope as point-line diagram; recorded on the left middle finger of test subject 4, $f_s = 10$ Hz



CNAP – right hand, middle finger
 MD = 107.8 mmHg
 KB = 18.8 mmHg

Figure B.37.: CNAP. Oscillometric envelope as point-line diagram; recorded on the right middle finger of test subject 4, $f_s = 10$ Hz

B.3.5. Test Subject 5

Index Finger (Left Hand: CNAP, Right Hand: Prototype V.2)

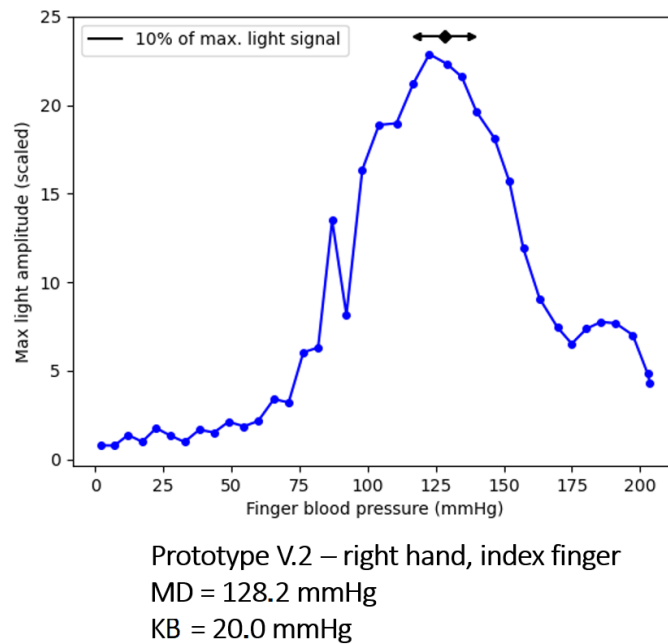


Figure B.38.: Prototype V.2. Oscillometric envelope as point-line diagram; recorded on the right index finger of test subject 5, $f_s = 10$ Hz

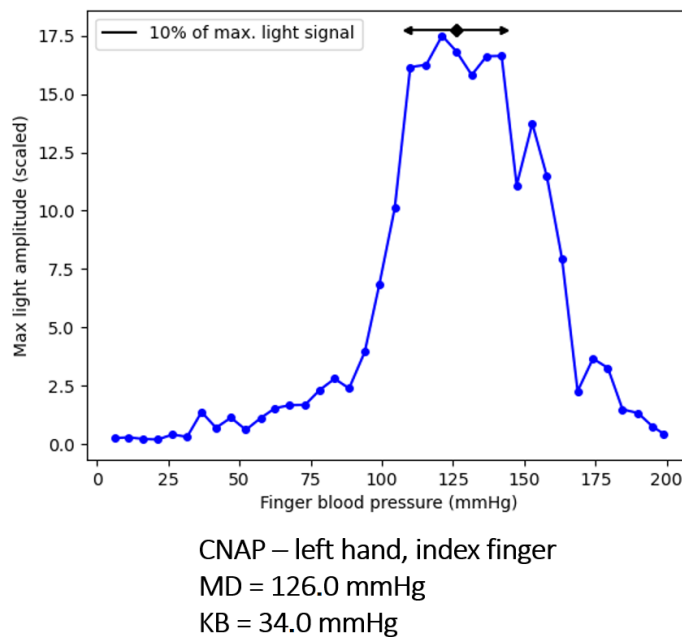
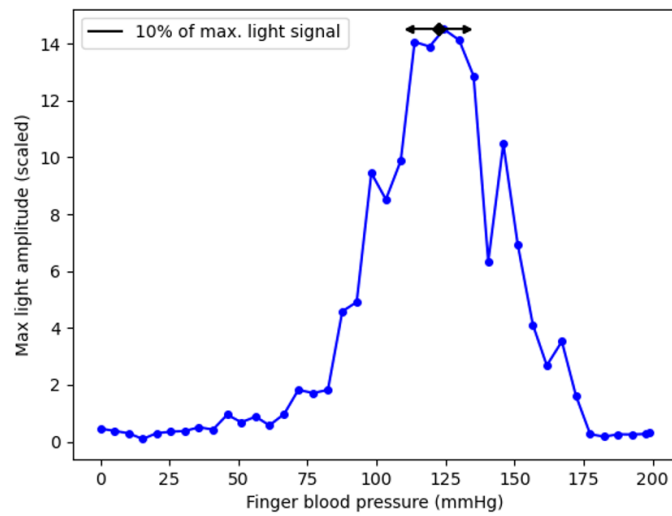


Figure B.39.: CNAP. Oscillometric envelope as point-line diagram; recorded on the left index finger of test subject 5, $f_s = 10$ Hz

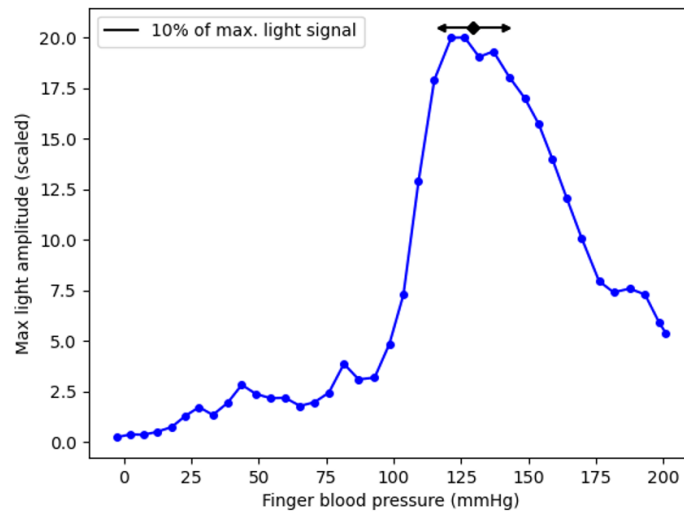
Index Finger (Right Hand: CNAP, Left Hand: Prototype V.2)



CNAP – right hand, index finger
MD = 122.3 mmHg
KB = 21.0 mmHg

Figure B.40.: CNAP. Oscillometric envelope as point-line diagram; recorded on the right index finger of test subject 5, $f_s = 10$ Hz

Middle Finger (Left Hand: CNAP, Right Hand: Prototype V.2)

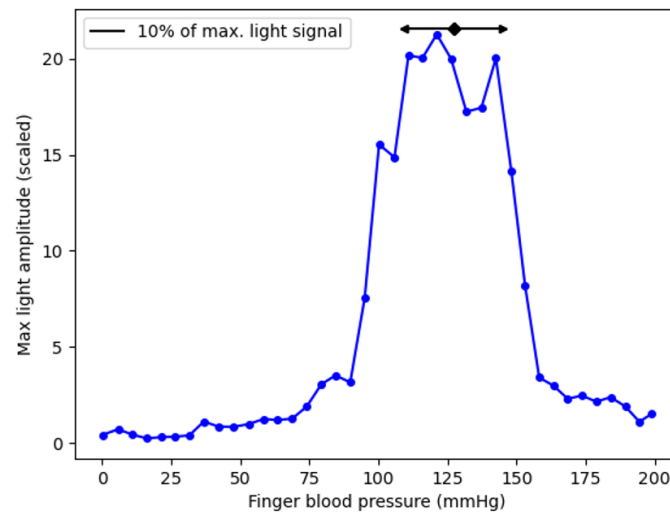


Prototype V.2 – right hand, middle finger

MD = 129.6 mmHg

KB = 24.1 mmHg

Figure B.41.: Prototype V.2. Oscillometric envelope as point-line diagram; recorded on the right middle finger of test subject 5, $f_s = 10$ Hz



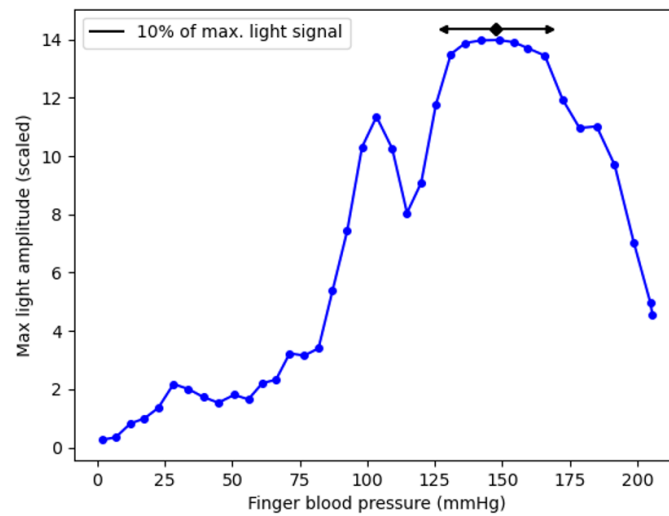
CNAP – left hand, middle finger

MD = 127.1 mmHg

KB = 35.7 mmHg

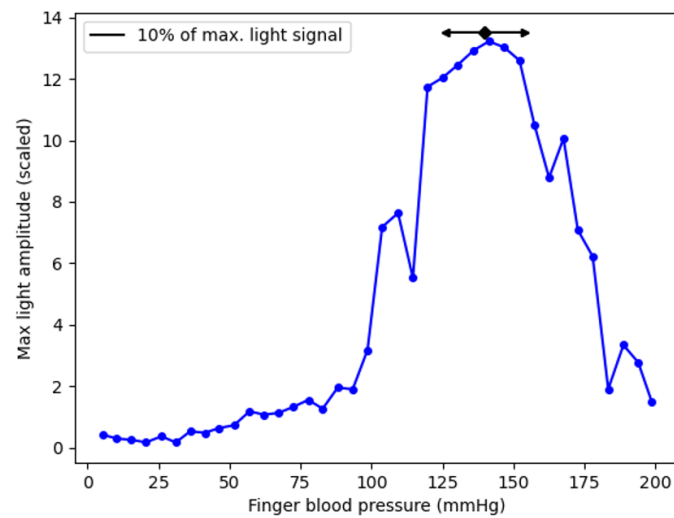
Figure B.42.: CNAP. Oscillometric envelope as point-line diagram; recorded on the left middle finger of test subject 5, $f_s = 10$ Hz

Middle Finger (Right Hand: CNAP, Left Hand: Prototype V.2)



Prototype V.2 – left hand, middle finger
 MD = 147.8 mmHg
 KB = 39.1 mmHg

Figure B.43.: Prototype V.2. Oscillometric envelope as point-line diagram; recorded on the left middle finger of test subject 5, $f_s = 10$ Hz



CNAP – right hand, middle finger
 MD = 139.9 mmHg
 KB = 27.8 mmHg

Figure B.44.: CNAP. Oscillometric envelope as point-line diagram; recorded on the right middle finger of test subject 5, $f_s = 10$ Hz

B.3.6. Test Subject 6

Index Finger (Left Hand: CNAP, Right Hand: Prototype V.2)

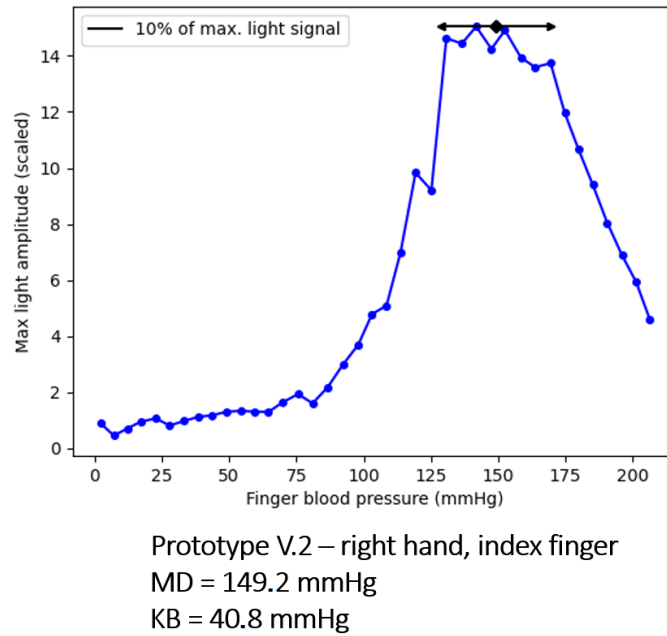


Figure B.45.: Prototype V.2. Oscillometric envelope as point-line diagram; recorded on the right index finger of test subject 6, $fs = 10$ Hz

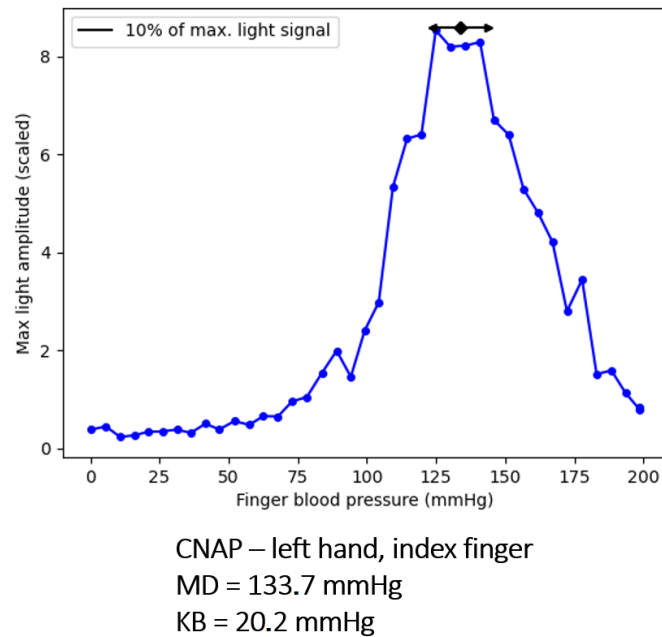
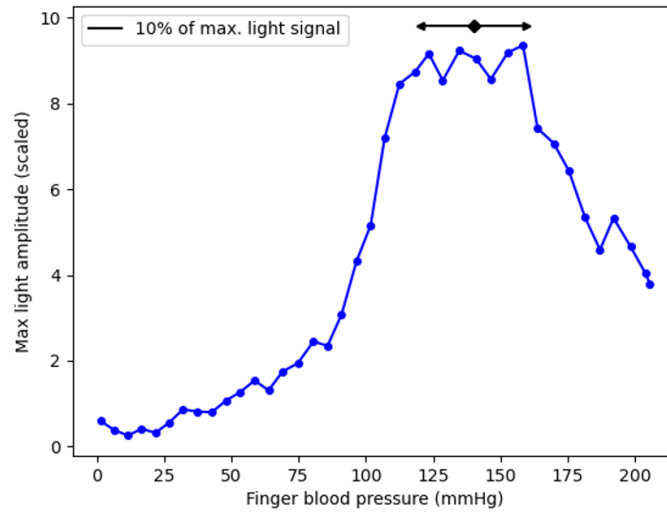


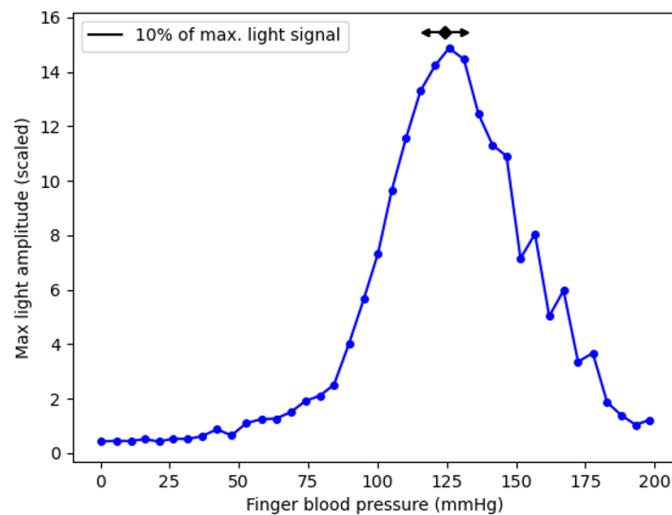
Figure B.46.: CNAP. Oscillometric envelope as point-line diagram; recorded on the left index finger of test subject 6, $fs = 10$ Hz

Index Finger (Right Hand: CNAP, Left Hand: Prototype V.2)



Prototype V.2 – left hand, index finger
 MD = 140.1 mmHg
 KB = 39.4 mmHg

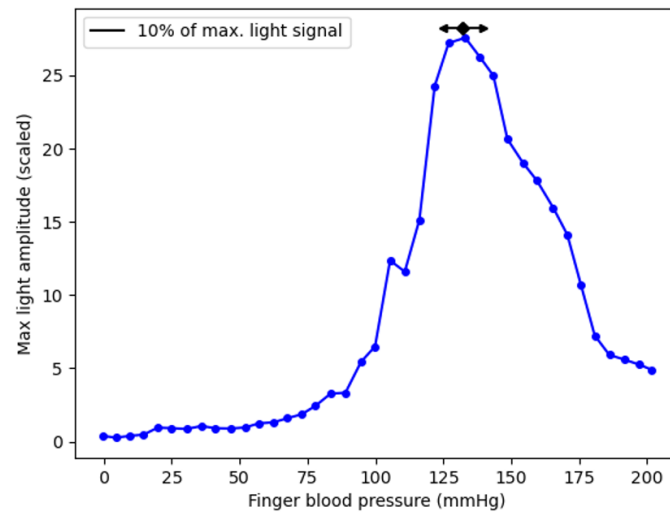
Figure B.47.: Prototype V.2. Oscillometric envelope as point-line diagram; recorded on the left index finger of test subject 6, $f_s = 10$ Hz



CNAP – right hand, index finger
 MD = 124.3 mmHg
 KB = 13.8 mmHg

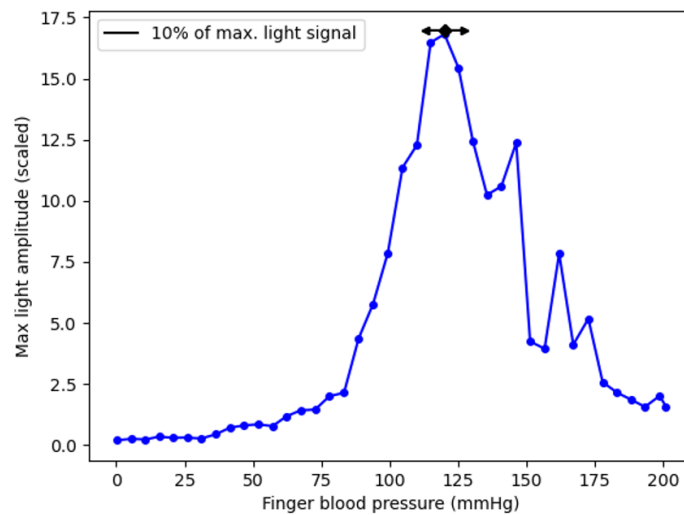
Figure B.48.: CNAP. Oscillometric envelope as point-line diagram; recorded on the right index finger of test subject 6, $f_s = 10$ Hz

Middle Finger (Left Hand: CNAP, Right Hand: Prototype V.2)



Prototype V.2 – right hand, middle finger
 MD = 132.2 mmHg
 KB = 14.6 mmHg

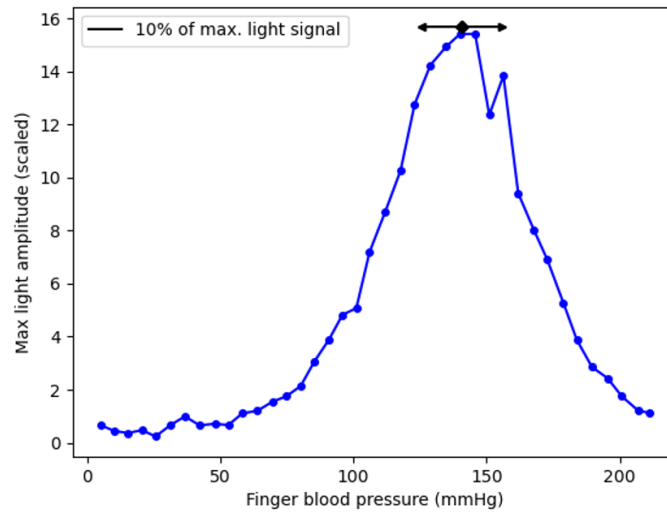
Figure B.49.: Prototype V.2. Oscillometric envelope as point-line diagram; recorded on the right middle finger of test subject 6, $f_s = 10$ Hz



CNAP – left hand, middle finger
 MD = 120.2 mmHg
 KB = 14.4 mmHg

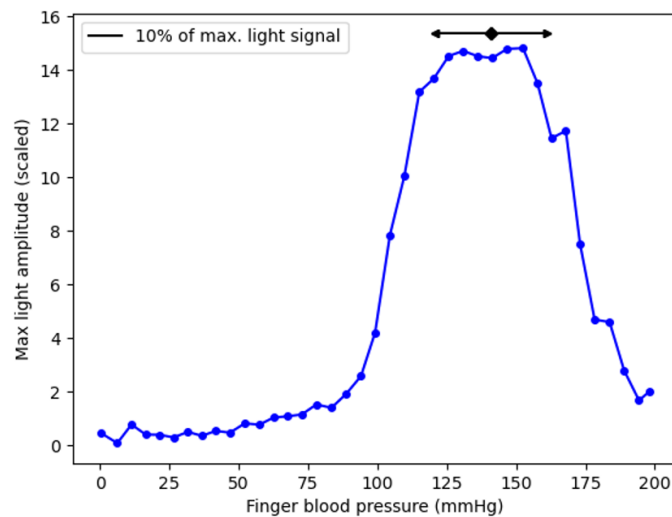
Figure B.50.: CNAP. Oscillometric envelope as point-line diagram; recorded on the left middle finger of test subject 6, $f_s = 10$ Hz

Middle Finger (Right Hand: CNAP, Left Hand: Prototype V.2)



Prototype V.2 – left hand, middle finger
 MD = 140.7 mmHg
 KB = 29.8 mmHg

Figure B.51.: Prototype V.2. Oscillometric envelope as point-line diagram; recorded on the left middle finger of test subject 6, $f_s = 10$ Hz

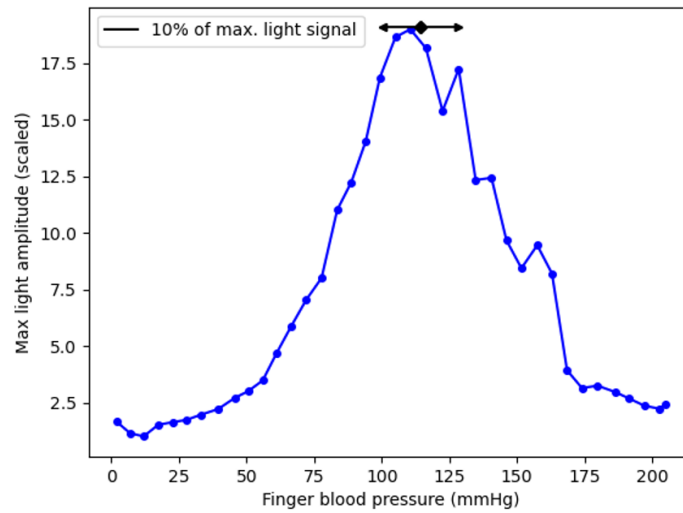


CNAP – right hand, middle finger
 MD= 140.9 mmHg
 KB = 40.4 mmHg

Figure B.52.: CNAP. Oscillometric envelope as point-line diagram; recorded on the right middle finger of test subject 6, $f_s = 10$ Hz

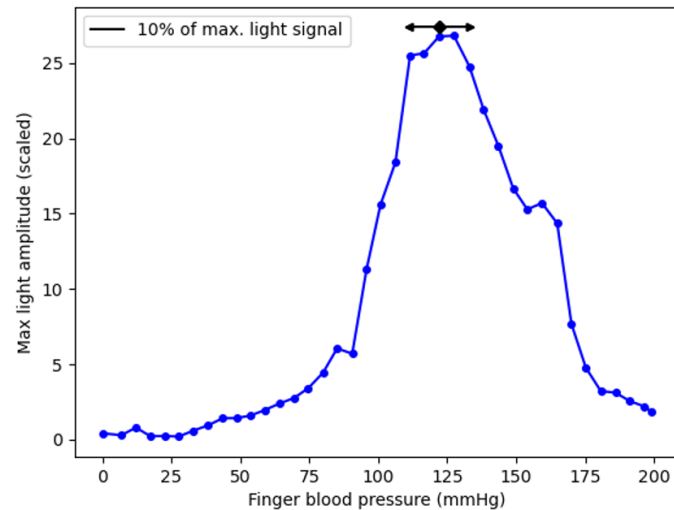
B.3.7. Test Subject 7

Index Finger (Left Hand: CNAP, Right Hand: Prototype V.2)



Prototype V.2 – right hand, index finger
 MD = 114.3 mmHg
 KB = 28.3 mmHg

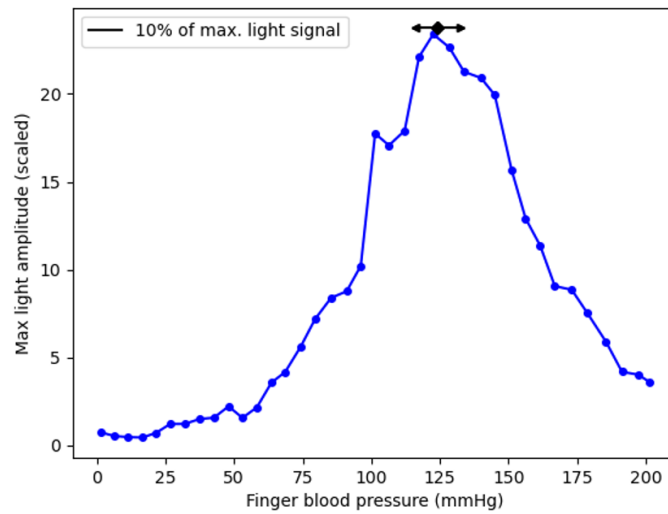
Figure B.53.: Prototype V.2. Oscillometric envelope as point-line diagram; recorded on the right index finger of test subject 7, $f_s = 10$ Hz



CNAP – left hand, index finger
 MD = 122.0 mmHg
 KB = 22.2 mmHg

Figure B.54.: CNAP. Oscillometric envelope as point-line diagram; recorded on the left index finger of test subject 7, $f_s = 10$ Hz

Index Finger (Right Hand: CNAP, Left Hand: Prototype V.2)

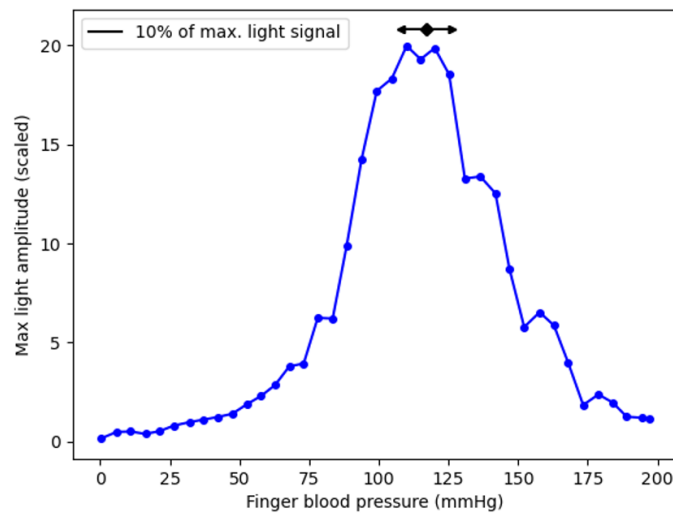


Prototype V.2 – left hand, index finger

MD = 124.3 mmHg

KB = 16.4 mmHg

Figure B.55.: Prototype V.2. Oscillometric envelope as point-line diagram; recorded on the left index finger of test subject 7, $f_s = 10$ Hz



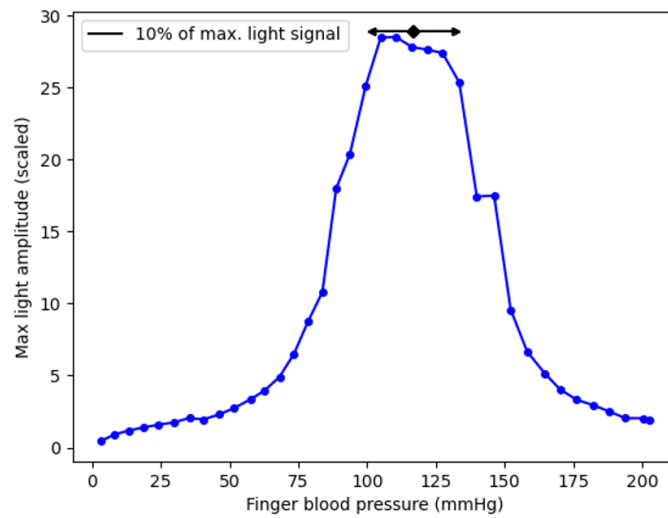
CNAP – right hand, index finger

MD = 117.0 mmHg

KB = 18.5 mmHg

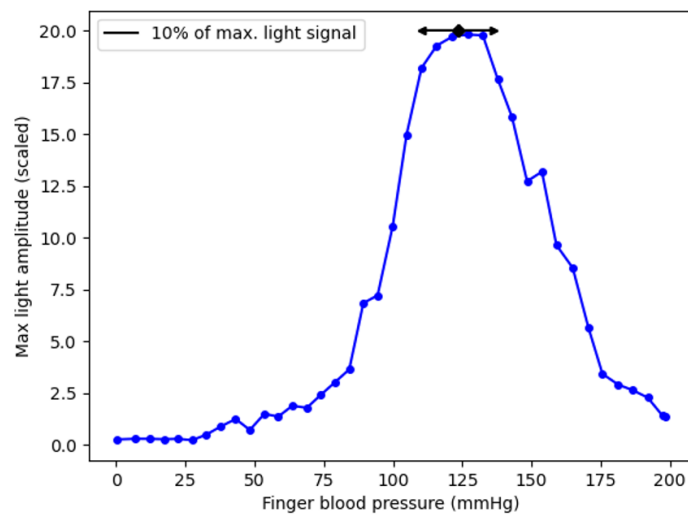
Figure B.56.: CNAP. Oscillometric envelope as point-line diagram; recorded on the right index finger of test subject 7, $f_s = 10$ Hz

Middle Finger (Left Hand: CNAP, Right Hand: Prototype V.2)



Prototype V.2 – right hand, middle finger
 MD = 116.8 mmHg
 KB = 30.4 mmHg

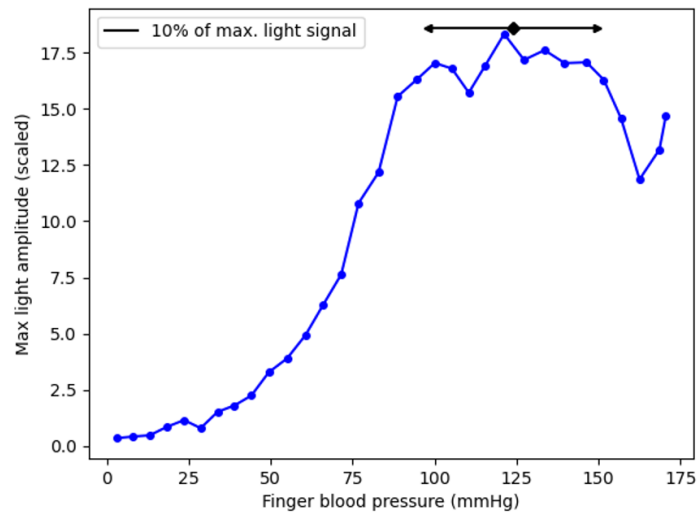
Figure B.57.: Prototype V.2. Oscillometric envelope as point-line diagram; recorded on the right middle finger of test subject 7, $f_s = 10$ Hz



CNAP – left hand, middle finger
 MD = 123.4 mmHg
 KB = 26.2 mmHg

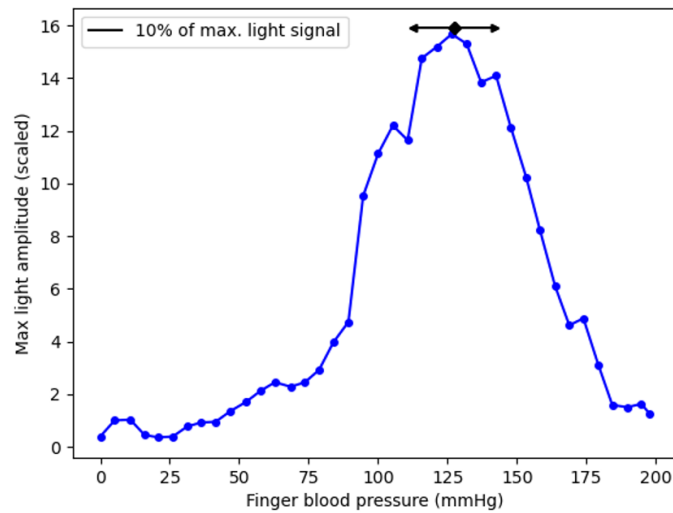
Figure B.58.: CNAP. Oscillometric envelope as point-line diagram; recorded on the left middle finger of test subject 7, $f_s = 10$ Hz

Middle Finger (Right Hand: CNAP, Left Hand: Prototype V.2)



Prototype V.2 – left hand, middle finger
 MD = 123.8 mmHg
 KB = 51.9 mmHg

Figure B.59.: Prototype V.2. Oscillometric envelope as point-line diagram; recorded on the left middle finger of test subject 7, $f_s = 10$ Hz



CNAP – right hand, middle finger
 MD = 127.3 mmHg
 KB = 29.2 mmHg

Figure B.60.: CNAP. Oscillometric envelope as point-line diagram; recorded on the right middle finger of test subject 7, $f_s = 10$ Hz

Appendix C.

Utilised Tools

C.1. CNAP Development Kit

The CNAP DevKit [32] was developed for research purposes and provides measurement of blood pressure (blood pressure wave form, beat-to-beat systolic/mean/diastolic pressure measurement), fluid reactivity (PPV and SVV) and haemodynamical parameters (CO, SVR). It serves as "first step" towards integration of the CNAP parameters in a patient monitor. The system consists of several components:

1. CNAP Development Kit
Main unit; responsible for measurement and data processing
2. CNAP double-finger sensor (cuff)
Finger cuffs in 3 sizes (S, M, L)
3. CNAP Controller
Connection interface between cuff and DevKit
4. CNAP Kabel
Signal line for light and pressure
5. Power supply

C.2. CNAP SerialGUI & CNS TestInterpreter

The software packages "SerialGUI" and "TestInterpreter" of CNSystems are used by the DevKit as software modules to perform test procedures, maintenance such as firmware updates and calibration. The TestInterpreter was developed for automated control of the SerialGUI. Furthermore, device information can be read out and important external data can be stored in the non-volatile memory area of the CNAP-module. A detailed description of launching and the various functions can also be found in the Operators Manual of the CNAP Development Kits [32].

C.3. Biopac Measurement System

The Biopac system (BIOPAC Systems, Inc., Goleta, CA) [26] consists of MP160 Box including the AcqKnowledge Software (ADC 64-bit system, data processing, real-time filtering, post-acquisition transformations, etc.), HLT 100C analog inputs, 3 x DA100C differential amplifiers, various sensors (TSD120 blood pressure cuff, TSD108 contact microphone, TSD104A blood pressure transducer) and mouthpieces with antibacterial filters. This equipment is primarily used for semi-automated intermittent blood pressure reference measurements and especially for auscultatory measurements with synchronous recording of Korotkoff's tones. The additional blood pressure sensor TSD104A is suitable for measuring a Vasalva manoeuvre (forced expiration against the closed mouth and nose opening) - this sensor was also utilised to measure the pressure signal in this thesis, as it was developed with high accuracy especially for pressures of liquids (animal blood). The sensor is connected as standard via a LuerLock system and measures arterial or venous blood pressure directly via flow. The supplied AcqKnowledge [33] software performs two functions: Data acquisition and data analysis. The acquisition settings determine the basic type of data to be acquired (e.g. time duration, sampling frequency, etc.), while the analysis functions allow the viewing, processing and transforming of data from the recorded signals.

Acknowledgements

At this point I would like to thank all the people who supported me in writing this Master's thesis.

An important contribution was made by my first supervisor, Ao.Univ.-Prof. Dipl.-Ing. Dr.techn. Scharfetter, who supported me with helpful suggestions and constructive criticism in the preparation of this work. For this I would like to thank him very much.

My sincere thanks also go to my second supervisor and head of CNSystems Medizintechnik GmbH, Dipl.-Ing. Dr. Jürgen Fortin, who gave me the opportunity to conduct this master's thesis. The exciting discussions and support on the technology always put me on the right track. Furthermore, I would like to thank Dr.rer.nat. Julian Grond, who assisted me during the research with his comprehensive professional knowledge and who was a decisive support in determining a suitable variant for my work from the variety of approaches. Special thanks also go to all employees of CNSystems - above all Hasib Haskic and Thomas Pust - who assisted with the technical implementation, agreed to carry out trial measurements and helped me with the daily work processes.

I would also like to thank the head of the Institute for Fluid Mechanics and Heat Transfer of the TU Graz, Univ.-Prof. Dr.-Ing. habil. Günter Brenn as well as Ass.Prof. Dipl.-Ing. Dr.techn. Walter Meile for technical expertise and extensive information.

Finally, I would like to thank my family, who made my studies possible through their support and strong emotional backing. In particular, I would also like to thank my brother and his partner for proofreading my master's thesis.

"Last, but not least" I would especially like to thank my girlfriend Bernadette for her tireless support, her open ear and her love.